From the
Institute of Parasitology
Faculty of Veterinary Medicine
Leipzig University

Calcium dependent protein kinase 1 in *Cryptosporidium parvum* (CpCDPK1): attempts to produce knockout parasites and functional studies

Inaugural-Dissertation
to obtain the degree of a
Doctor medicinae veterinariae (Dr. med. vet.)
from the Faculty of Veterinary Medicine
Leipzig University

Submitted by
Wanpeng Zheng
From Chengdu, China

Leipzig, 2020

With the permission of the Faculty of Veterinary Medicine, Leipzig University

Dean:	Prof. Dr. Dr. Thomas Vahlenkamp
Supervisor:	Prof. Dr. Arwid Daugschies
Reviewers:	Prof. Dr. Arwid Daugschies Institute of Parasitology Faculty of Veterinary Medicine Leipzig University
	Prof. Dr. Christina Strube Institute of Parasitology University of Veterinary Medicine Hannover, Foundation
Date of defense:	04.02.2020

Dedicated to my most staunch supporters – for my wife and my parents

Contents

1. Introduction

Cryptosporidium parvum is a protozoan parasite that causes diarrhoea in many host species worldwide. *C. parvum* invades the brush border of intestinal epithelial cells thus inducing maldigestion and malabsorption. In man, a lethal risk has been reported for immunocompromised hosts or young malnourished children. Calcium-dependent protein kinases (CDPKs) are believed to play critical roles in apicomplexan protozoa and appear to essentially contribute to accomplishment of the parasitic life-cycle. It has been demonstrated experimentally, that CDPK inhibitors ("bumped kinase inhibitors", BKI) hamper parasite development *in vitro* and reduce parasite reproduction in the natural host of *C. parvum* (LENDNER et al. 2015).

The main aim of the present study was to expand the knowledge about function of *C.parvum* CDPK1 in the invasion process. In order to assess the potential of this gene as target for anti-cryptosporidiosis drug development, two attempts to generate a CDPK1 knockout (CDPK1 KO) parasite strain were made. The first was restriction enzyme mediated integration (REMI). The KO plasmids were constructed and the electroporation pattern was established to generate CDPK1 KO *C. parvum*. The other attempt was to disrupt the CDPK1 gene via CRISPR/cas-9 mediated transfection. In this process, plasmids were constructed and transfected into freshly excysted *C. parvum* sporozoites followed by subsequent microscopic analysis after infection of host cells. In addition, I also attempted to establish an *in vitro* continuous culture for the parasite in order to propagate potential transgenic parasites, using the newly-described oesophageal squamous-cell carcinoma cell line, COLO-680N. For a potential propagation of the parasite *in vivo*, the RAGgcxIFN-gamma KO mouse strain was investigated. Also, we assessed the role of CDPK1 in Parasite development using the bumped-kinase inhibitor (BKI) K-1294. Overall this study hint at an essential role for CDPK1 in the development of *C. parvum* and further support the potential of this gene as a major target for anti-cryptosporidiosis drug development.

2. Literature Review

2.1 Biology

2.1.1 Systematics

Since it has been discovered in 1907, the genus *Cryptosporidium* is classified in the phylum *Apicomplexa*, class *Conoidasida*, order *Eucoccidioridahas* and family *Cryptosporidiidae* (TYZZER 1907). However, the taxonomic placement of *Cryptosporidium* became controversial. Convictive molecular phylogenetic evidences propose the genus to belong to the class of *Gregarinomorphea* as a subclass *Cryptogregaria* rather than to the *Coccidia* (CAVALIER-SMITH 2014). Like many other species in the genus, *C. parvum* is an intestinal protozoan parasite and may occur in a variety of vertebrates worldwide and is responsible for moderate to severe diarrhea and fatal disease in immunocompromised adult or neonatal hosts (MOSIER and OBERST 2000; ZAMBRANO et al. 2014). The main hosts are young calves at the age of 7-12 days that get infected through oral intake of oocysts (LENDNER and DAUGSCHIES 2014).

2.1.2 Life cycle

C. parvum has a complex life cycle which includes both sexual and asexual stages (Fig.1). The development starts when the infectious sporulated oocysts are ingested by a susceptible host. The oocyst measures approximately 5 µm × 4.5 µm and contains four sporozoites. After excystation of the sporozoites in the small intestine, invasion of mucosal epithelial cells takes place. The further development leads to the formation of trophozoites, followed by differentiation and asexual multiplication of merozoites, differentiation into sexual stages (gamonts), and finally, after fertilization, the formation of zygotes. These develop either into thin-walled oocysts that are probably responsible for autoinfection, or to the thick-walled oocysts that are excreted with the faeces into the environment (LENDNER and DAUGSCHIES 2014).

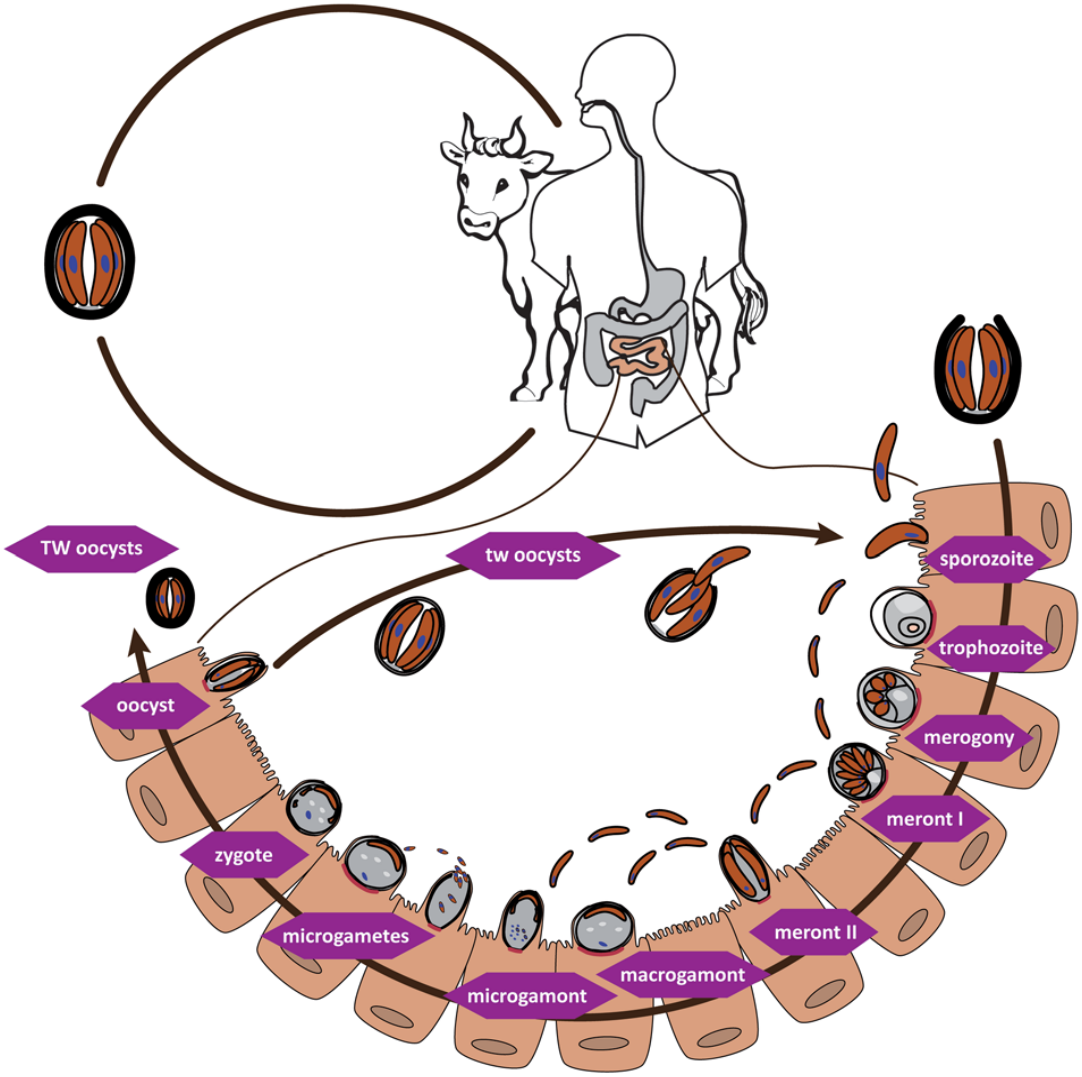

Fig.1 Life cycle of Cryptosporidium (Image adopted from Lendner and Daugschies (2014). TW: thick-walled oocyst. tw: thin-walled oocyst.

The life cycle of *Cryptosporidium* is peculiar. *Cryptosporidum* is completely enveloped by host cell membrane ("intracellular localization"), but Unlike other apicomplexan parasites, it does not penetrate the host cell membrane and thus does not invade the cytoplasm of the host cell (SIBLEY 2010; VALIGUROVA et al. 2007). Apical organelles (i.e., rhoptries, micronemes, and dense granules) are vesicular secretory organelles that are present in sporozoites and merozoites. These organelles have been demonstrated to be involved in the invasion process. Specifically rhoptries and micronemes have been implicated in host cell adhesion and entry. The discharge of these organelles triggers the following formation of a parasitophorous vacuole (PV).

Calcium is widely believed to be an important messenger participating in the complex mechanisms controlling the process of host cell invasion (CHEN et al. 2004).

Attachment is the initial step of invasion. Filamentous actin and other actin-associated proteins from the host cell accumulate at the host-parasite interface during attachment (ELLIOTT and CLARK 2000). This is followed by a short phase of active movement of the parasite on the surface of the host cell ("gliding motility"). The host's cell membrane then forms folds, enveloping the parasite gradually and eventually forming the PV. The PV is the particular niche where the parasite develops and appears to allow supply of essential nutrients from the host cells by forming a "feeder organelle" (CHEN et al. 2005; VALIGUROVA et al. 2008).

2.1.3 Tenacity of oocysts

The ovoid-shaped thick-walled oocysts of *C. parvum* are excreted with the faeces and are able to survive up to six months in the environment. The wall is a rigid protein rich layer that is covered by a lipid bilayer structure (LENDNER and DAUGSCHIES 2014). It provides mechanical resilience and resistance against physical or chemical attack (DELLING et al. 2016). The oocyst shows strong resistance to common water disinfectants like chlorine and monochloramine (KING and MONIS 2007). Although *C. parvum* tolerate a wide range of temperature under natural conditions, it is vulnerable in extreme environments which leads to desiccation and freezing (MORIARTY et al. 2005; ROBERTSON and GJERDE 2004). Over 90% of oocysts in water were proven not to be able to survive at -22 ℃ for 152 h and none could stay viable after 4 h desiccation at room temperature (RT) (ROBERTSON et al. 1992).

2.1.4 Excystation of oocysts and invasion of host cells

Exposure to stomach acid, bile salt and host gastrointestinal temperature triggers excystation (CHEN et al. 2004). The process is regulated by many factors. Due to low gastric pH the outer layer of the ingested oocyst is degraded. Increased temperature and the influx of bile salts promote the activation of the sporozoites. Intestinal enzymes cooperate with proteases of parasite origin to disrupt the oocyst wall. As a consequence, the sporozoites are released and the invasion of the epithelial brush

border is initiated (LENDNER and DAUGSCHIES 2014). Within a short period of 5 min after excystation invasion may be completed (FORNEY et al. 1999).

The invasion by sporozoites includes several sequential steps: (1) Attachment to host cells, (2) invagination of the host cell membrane at the binding site and (3) formation of a parasitophorous vacuole (PV). Glycoproteins on the epithelia apical membrane and sporozoite surface such as galactose-N-acetylgalactosamine (Gal/GalNAc)-specific lectins are involved in *C. parvum* sporozoite attachment to host cells (CHEN and LARUSSO 2000).

Gliding motililty is a phenomenon that is believed to be ubiquitously occurring in invasion of host cells by apicomplexan parasites (WETZEL et al. 2005). This type of movement does not depend on cilia or flagella, but relies on an actin-myosin motor beneath the parasite plasma membrane (SIBLEY 2004). Upon the binding of myosin to the inner membrane complex (IMC), the actin filaments are pushed backward resulting in the parasite moving ahead (LENDNER and DAUGSCHIES 2014). The gliding motility of *C. parvum* sporozoites is similar to that observed in other species of apicomplexa. Time lapse video showed that *C. parvum* can finish the invasion within 30 s which is faster than e.g. *Toxoplasma gondii* (WETZEL et al. 2005).

2.1.5 Formation of the PV

The PV represents a bubble-like structure induced by apicomplexan parasites invading the host cell. It is bordered by plasma membrane thereby offering a vacuolar space for the parasite to develop within the cell (LALIBERTÉ and CARRUTHERS 2008).

In the case of *C. parvum* infection, the host cell undergoes massive morphological changes after the attachment of a sporozoite. The cell forms protrusions along the surface of the parasite. Then, an electron-dense band gradually emerges at the attachment area between the parasite and host cell. After the parasite is fully covered, the feeder organelle is formed at the border between PV and host cell (UMEMIYA et al. 2005).

VALIGUROVA et al. (2008) suggest that "PV" is a misleading term to describe the unique structure that is created by *Cryptosporidium* spp. Because the PV indicates a vacuolar space with the boundary of membrane that isolates itself from the host cell (SCHOLTYSECK 1979). However, they found evidences that stood against this idea. Instead, they named it parasitophorous sac (PS) for the following reasons. (1) *Cryptosporidium* utilizes the membrane of the epithelial cells rather than its own plasma membrane to create this compartment. (2) A thin layer of host cell cytoplasma is found in the PS membrane fold. (3) incomplete fusion leads to openings in the PS membrane that are believed to connect the internal to the external environment of the parasite (UMEMIYA et al. 2005). (4) PS leaves a small gap between host cell and the parasite. (5) The PS is separated into modified and unmodified parts by an electron-dense band at the parasite-host interface (VALIGUROVA et al. 2008). However, despite these arguments PV is still the commonly used term to describe the intracellular location of the parasite.

2.1.6 Nutrient supply by the host

The mechanisms of how *Cryptosporidium* derives nutrients from the host cell remain unclear. The feeder organelle is believed to play the key role for nutrients intake during intracellular parasite development. It displays an extensively folded surface which dramatically increases the surface of the contact area between host cell and parasite (BOROWSKI et al. 2008; CAVALIER-SMITH 2014). In addition, transporters on the PV membrane are also essential, as 69 transporters have been detected on surface of freshly excysted sporozoites. They were demonstrated to serve functions of substrate acquisition including fatty acids, amino acids and nucleotides (THOMPSON et al. 2005; SANDERSON et al. 2008; YAMAGISHI et al. 2011).

The fatty acid beta-oxidation pathway does not seem to play the role of energy gaining in *C. parvum* since no genes related to Krebs cycle were found in the genome (ABRAHAMSEN et al. 2004). The main energy pathway appears to be glycolysis and the energy is probably stored in polysaccharides. The existence of enzymes associated with production and degradation of polysaccharides strongly supports this assumption (HARRIS et al. 1999; THOMPSON et al. 2005).

Fatty acid is believed to be generated by the type I fatty acid synthetase and a long-chain fatty acid enlongase-mediated system in *C. parvum* (ZHU 2004; FRITZLER et al. 2007). However, these two enzymes only endow the parasite with the ability of chain enlongation, not *de novo* biosynthesis of fatty acid. Therefore, it is very likely that *C. parvum* gains the basic substrate from the host cell. So far, no transporters but only three fatty acyl synthases have been demonstrated to potentially serve this function (ZHU et al. 2004; ZENG et al. 2006; ZENG and ZHU 2006).

Amino acids are also not *de novo* synthesized by *Cryptosporidium*, but acquired from the host as well. At least 11 transporters have been found on PV membrane associated to amino acid acquisition (ABRAHAMSEN et al. 2004). The parasite is able to convert several amino acids from one to another such as, serine to glycine and aspartate to asparagine (RIDER and ZHU 2010).

Polyamines are generated from arginine by *C. parvum* using a plant-like arginine decarboxylase rather than ornithine decarboxylase which is regularly seen in mammalian cells (KEITHLY et al. 1997).

2.2 Epidemiology

2.2.1 Human Cryptosporidiosis

It is widely known that *Cryptosporidium* infection can be lethally dangerous to individuals carrying human immunodeficiency virus (HIV) due to the deficiency of the immune system. Moreover, severe *Cryptosporidium* infection may also be associated to hepatitis B virus (HBV) infection in man (YANG et al. 2017) which probably is likewise associated to a compromised immune system (FERRARI 2015).

The predominating transmission of cryptosporidiosis to humans is by oocyst contaminated water or food. Besides, direct contact with infected hosts may also cause infection. The disease causes large economic losses in animal husbandry and threats to public hygiene worldwide. In 1993, a massive waterborne outbreak was reported in Milwaukee in which over 400,000 persons were infected. Such a massive transmission was ascribed to the contamination of public water supply (MACKENZIE et al. 1995) .

Throughout the world thousands of children younger than 5 years old die due to cryptosporidiosis annually. Most cases are reported from less developed countries in Africa and Asia. Malnutrition and undergrowth are associated to the infection and are commonly seen in these areas (MONDAL et al. 2009; MOLBAK et al. 1997).

Young livestock, especially calves, are frequently infected by *C. parvum* and are regarded an important infection source for humans (LENDNER and DAUGSCHIES 2014). Persons, particularly children, who live in close contact with young ruminants or drink surface water that is contaminated with ruminant faeces have a higher risk of infection (KOTLOFF et al. 2013; HELMY et al. 2015).

More than 15 species of *Cryptosporidium* are known to be potentially infectious to humans. *C. hominis* and *C. parvum* are the most frequently detected zoonotic species (CHECKLEY et al. 2015). *C. hominins* is found in humans ubiquitously, especially in developed countries, whereas the majority of human cases of infection in the Middle East and many developing regions are attributed to *C. parvum*. In Europe, however, both are observed (XIAO 2010). In Germany, human cryptosporidiosis is a rather rare disease with approximately 1000 documented cases annually since this disease became notifiable in 2002. It appears, however, rather probable that the number of not notified cases is much higher. In 2012, an almost 5 fold sudden increase of prevalence was reported for unknown reasons simultaneously in the Netherlands and the United Kingdom (FOURNET et al. 2013). In young animals and water bodies, *Cryptosporidium* is widely distributed form the north to the south of Germany with the zoonotic *C. parvum* generally dominating (KARANIS et al. 1998; BROGLIA et al. 2008; AJONINA et al. 2012).

2.2.2 Animal Cryptosporidiosis

Cryptosporidium is a ubiquitous parasite in domestic animals and wildlife. Ruminants are the most common hosts. In cattle, *C. parvum, C. bovis, C. andersoni, and C. ryanae* are recorded as the four most common species (XIAO and FENG 2008; XIAO 2010). Only *C. parvum* is considered pathogenic for young ruminants and to be of zoonotic impact while the other 3 species are rarely seen in humans (XIAO AND FENG 2008). In sheep, the prevalence of *Cryptosporidium* spp. ranges from < 5% up to > 70% upon distribution worldwide (ROBERTSON 2009). So far, at least eight species of the genus *Cryptosporidium* have been detected in sheeps globally, but only three species are claimed to be related to health problems, and they dominate diversely in different areas as follows; *C. parvum* in Europe, *C. xiaoi* in Australia, and *C. ubiquitum* in America and Asia (RYAN et al. 2014). *C. parvum, C. hominis*, *C. ubiquitum* and *C. xiaoi* have also been identified in goats (GEURDEN et al. 2008; DÍAZ et al. 2010; FAYER et al. 2010).

In pigs, *C. suis* and *C. scrofarum* have been reported to be the two most common species globally (YIN et al. 2011; NĚMEJC et al. 2013; YUI et al. 2014). Similar to the cases in calves, the infection appears to be age-related. That is to say, the parasite is more commonly detected in pre-weaned piglets than in adults (ZHANG et al. 2013; YUI et al. 2014). Dogs and cats have been found to host *C. canis*, *C. felis*, *C. parvum*, and *C. muris* (PALMER et al. 2008; LUCIO-FORSTER et al. 2010). *Cryptospordium* spp. were first identified in rabbits as a genotype that was later accepted as a separate species, *C. cuniculus*, in the Czech Republic (RYAN et al, 2003). It has both zoonotic and anthroponotic features and occurs in Europe and Africa (CHALMERS et al. 2009; MOLLOY et al. 2010). *C. meleagridis*, *C. baileyi*, *and C. galli* are recognized to be bird specific species of the genus *Cryptosporidium*. Except for *C. meleagridis*, which is regarded zoonotic, the other two species have no respective impact for humans (RYAN et al. 2014). Reptiles and amphibia, toads, snakes, lizards and tortoise are reported to host *C. fragile*, *C. serpentis*, *C. varanii* and *C. ducismarci*, respectively (JIRKU et al. 2008; XIAO et al. 2004; TRAVERSA 2010).

Compared to the species in terrestrial hosts, far less is known about cryptosporidia in aquatic animals. Seals and fishes have been reported to host *C. muris* and *C. molnari*, respectively (SANTÍN et al. 2005; RENGIFO-HERRERA et al. 2011; ALVAREZ-PELLITERO and SITJÀ-BOBADILLA 2002). Oocysts of *C. parvum* and *C. hominis* have been isolated from clams, mussels, cockles, and oysters (ABRAHAMSEN et al. 2004; STAGGS et al. 2015; TRAVERSA et al. 2004).

2.3 Detection and Diagnosis

Cryptosporidiosis should be suspected in hosts who undergo acute gastroenteritis or prolonged diarrhea. The diagnosis includes clinical consultation, fecal specimen sampling, microscopic testing and reporting (TAM et al, 2012).

Various methods have been developed to detect cryptosporidiosis in fecal samples. Microscopy of acid fast (AF)-modified Ziehl-Neelsen staining is one of the most commonly used methods. The oocysts are stained red against the blue background (STARK et al. 2009). The negative staining technique of Heine is another routine microscopy method to detect *Cryptosporidium* spp. which is easy and widely distributed with lower sensitivity than modified Ziehl-Neelsen staining (POTTERS and VAN ESBROECK 2010). However, microscopy is not very sensitive and may deliver false negative results, particularly in cases of low infection and sporadic shedding (CLAVEL et al. 1995).

Higher sensitivity is obtained by direct or indirect immunofluorescence assay (DFA / IFA). However, these methods are rather expensive and demand availability of a fluorescence microscope (CHALMERS et al. 2011).

Enzyme-linked immunosorbent assay (ELISA), enzyme immunoassay (EIA) and immunochromatography have been developed and commercial kits are available. The tests are easy to perform and do not need special laboratory equipment. However, the sensitivity varies a may range from 70% -100% (GARCIA and SHIMIZU. 1997; JOHNSTON et al. 2003; YOUN et al. 2009).

Molecular tests have also been used for detection of this parasite in faeces or/and water samples, such as polymerase chain reaction (PCR) and loop mediated isothermal amplification (LAMP) (KAUSHIK et al. 2008; PLUTZER and KARANIS 2009).

Recently, a study performed by MIRHASHEMI et al. (2015) compared the specificity and sensitivity of four detection methods (acid-fast staining, ELISA, DFA and PCR) in cattle, sheep and horse, respectively. The authors concluded that the optimal way is to combine DFA and PCR. PCR showed the highest sensitivity and specificity in

sheep and horse samples, whilst DFA was the best in cattle samples. Real-time PCR has been reported to show higher sensitivity than DFA and, as expected, was more accurate in terms of quantitative determination. Furthermore, quantitative PCR is also capable of revealing correlation between the diarrhea severity and oocyst excretion (OPERARIO et al. 2015). Particularly for examination of environmental probes PCR appears to be the most frequently applied method (STINEAR et al. 1996; HALLIER-SOULIER and GUILLOT 2000; HONG et al. 2014).

High sensitivity is not the only advantage of PCR. Its capability to distinguish *Cryptosporidium spp.*in clinical and environment samples is outstanding as well (CHALMERS and KATZER 2013). For sub-genotyping the 60-kDa glycoprotein (gp60) gene is the most widely used marker (ZAHEDI et al. 2016).

2.4 Treatment options

The lack of satisfactory treatment is a considerable concern that researchers are currently devoting themselves to. Numerous drugs have been tested and ended up in failure of cure. To date, only one FDA-approved drug, nitazoxanide (NTZ), is available for treatment of persons suffering from cryptosporidiosis. It is partially effective in children and immunocompetent hosts, but it is completely ineffective in AIDS patients (AMADI et al. 2009). Paromomycin, an aminoglycoside antibiotic, was reported several times to have the capability of inhibiting *Cryptosporidium* to a certain extent in man, animals and *in vitro* (TZIPORI et al. 1994a; GRIFFITHS et al. 1998a; CAI et al. 2005). So far, NTZ and paromomycin are the most widely used drugs in a large variety of livestock including ruminants, pigs, horses, house pets (cats and dogs) and birds (VIU et al. 2000; VAN ZEELAND et al. 2008; SCHNYDER et al. 2009; TZIPORI et al. 1994a; SCORZA AND Lappin 2007; ROBINSON et al. 2008).

Halofuginone has been reported to control *C. parvum in vitro* (NAJDROWSKI et al. 2007). More importantly, it is efficient in calves by effectively reducing oocyst shedding and diarrhea (BOROWSKI et al. 2008; JARVIE et al. 2005; JOACHIM et al. 2003; KEIDEL and DAUGSCHIES 2013; LEFAY et al. 2001). TROTZ-WILLIAMS

et al. (2011) confirmed the reduction of oocyst shedding. More importantly, they observed significant correlation between the diarrhea delay and the use of halofuginone.

It was suggested that decoquinate is able to prevent and control cryptosporidiosis in pre-weaned calves (HOBLET et al. 1989). In contrast, MOORE et al. (2003) stated that decoquinate has no effect on oocyst shedding or clinical signs in calves infected with *C. parvum*. Despite both halofuginone and decoquinate do not provide complete cure, the effectivity of halofuginone and decoquinate has been compared. The results showed that halofuginone performed better in reduction of oocysts excretion, while decoquinate improved the daily weight gain of calves (LALLEMAND et al. 2006).

Activated charcoal with wood vinegar liquid has been proposed to be effective in prevention and controlling of cryptosporidiosis in both calves and lambs, since it reduced oocysts excretion and diarrhea (WATARAI et al. 2008; PARAUD et al. 2011).

Combined uses of different drugs have been suggested to be more effective against cryptosporidia. In AIDS patients, treatment with paromomycin alone or in combination with azithromycin was proven protective against *Cryptosporidium* (MEAMAR et al. 2006). The combined use of norfloxacin and clopidol may help in prevention and treatment of cryptosporidiosis in chicken while this is not the case if they are used as single drugs (EL-SHAFEI et al. 2014).

Bovine hyperimmune colostrum and antibody containing egg yolk were found useful in mammals to various extents (NORD et al. 1990). Neonatal lambs receiving hyperimmune colostrum showed less mortality and stronger resistance (NACIRI et al. 1994). Oral bovine serum concentrate (BSC) relieves symptoms of cryptosporidiosis such as peak diarrhea volume, intestinal permeability, oocysts excretion and recovery of villous surface area in calves (HUNT et al. 2002). Oral application of serum-derived bovine immunoglobulin (SBI) controlled diarrhea caused by *Cryptosporidium* and *Norovirus* in organ transplant patients (GELFAND and CLEVELAND 2017).

Inhibiting the function of various enzymes of *Cryptosporidium* is a novel perspective for treatment. A cysteine protease inhibitor, K11777, eliminates *C. parvum* infection from cell lines *in vitro* and rescues mice from an otherwise lethal infection with the parasite (NDAO et al. 2013). A pyrazolopyrimidine-based compound, named BKI 1294, that acts as a calcium dependent protein kinase 1 (CDPK1) inhibitor, has been reported as a promising lead for the development of drugs for treatment of cryptosporidiosis. It was determined to possess significant curative effect against *Cryptosporidium* both *in vitro* and *in vivo* (CASTELLANOS-GONZALEZ et al. 2013; LENDNER et al. 2015).

The *Cryptosporidium* inosine 5'-monophosphate dehydrogenase (CpIMPDH) enzyme is critical for the parasite to survive in the host cell, as it provides the ability of purine salvage from the host. Eight CpIMPDH inhibitors have been investigated *in vitro*, and two compounds, named as P96 and P131, ended up as potential candidates supposed to control clinical infection (GORLA et al. 2014).

LOVE et al. (2017) screened 12 potential drugs including antibiotics and protein inhibitors by using a high-content imaging phenotypic assay to identify whether they have anticryptosporidial activity. As a result, only one out of twelve candidates was identified to have a potential as a drug for treatment of cryptosporidiosis. Unlike other candidates, clofazimine (CFZ), a FDA approved drug for treatment of leprosy, showed no toxicity-related undesirable effects to mammalian cells *in vitro*. The authors suggested that CFZ is worth to be studied as a potential new treatment of cryptosporidiosis in further investigation.

2.5 Hygiene

As the infection requires the direct contact with oocyst of the parasite, avoiding the exposure of the host to the pathogen is essential for any control measure.

A clean water source is of utmost importance. For humans, the water quality of tap water and swimming pools must be strictly monitored, because these two are the main routes of transmission of human cryptosporidiosis, and they could be contaminated by

surface water bodies (WIDERSTRÖM et al. 2014; JACOB et al. 2015). For animals, the environmental contamination is commonly the fundamental source of infection. Oocysts may be distributed in drinking water, feed, slurry, or on the surface of stables or skin of infected animals which may all possibly result in oral oocyst uptake by drinking, feeding or licking. Therefore, proper hygienic management is particularly important in husbandry (FAYER et al. 2004; KEIDEL and DAUGSCHIES 2013). SHAHIDUZZAMAN and DAUGSCHIES (2012) summarized following recommendations. (1) A duration of at least 7 days of quarantine needs to be applied when newly purchased animals arrive. (2) Coproscopy needs to be carried out for *Cryptosporidium* in animals that are under suspicion. (3) Stables and related equipment need to be properly cleaned and disinfected. (4) A suitable drug needs to be administrated in case of infection.

Many studies about inactivation of *Cryptosporidium* oocysts using various methods were published. Thermal treatment of oocysts for 20 min achieves complete inactivation at 56 ℃ or more (SHAHIDUZZAMAN et al. 2010). Exposure to UV light was also demonstrated to be effective (>99% inactivation) if applied for 30 min (CLANCY et al. 2004; DELLING et al. 2016). Over 98% inactivation of oocysts was observed with at least 2% concentration of cresol based disinfectants applied for 2 h while 6% sodium hypochlorite induced an inactivation rate of 92.7% (SHAHIDUZZAMAN et al. 2010). Formaldehyde and hydrogen peroxide were both reported to have anticryptosporidial activity (WEIR et al. 2002; CASTRO-HERMIDA et al. 2006). Neopredisan® 135-1 and Aldecoc® TGE, two commercial disinfectants appointed by the German Veterinary Society (DVG), are able to inactivate more than 99.5% of oocysts at a concentration of 2% and 4%, respectively (SHAHIDUZZAMAN et al. 2010). At the same contact time of 2 h 3% KENO™ COX, a amine based disinfectant, also has the ability to eliminate the infectivity of oocysts (NACIRI et al. 2011).

2.6 Vaccine

The mechanism of the interaction between the host immune system and *Cryptosporidium* remains unclear (PANTENBURG et al. 2008) and no efficient vaccines have been developed so far. Several antigens have been taken into account. However, limited protection and susceptibility of vaccinated animals to reinfection was reported (MEAD 2010; SHEORAN et al. 2012; PREIDIS et al. 2007). Vaccines containing irradiated or genetically modified cryptosporidia are likely to be the most promising paths to achieve effective protection (STRIEPEN 2013; MEAD 2014). Since the localization of the parasites in host is the intestinal mucosa, strengthening of the mucosal immune system seems to be the only option to induce sufficient protection by vaccines (MEAD 2014).

2.7 In vitro and vivo Models

In vitro completion of the life cycle of *C. parvum* was reported in an axenic system (HIJJAWI et al. 2004); however, another group failed to reproduce this observation (GIROUARD et al. 2006). In a recent study three life cycle stages (sporozoites, trophozoites and type I merozoites) of *C.parvum* were identified in an axenic culture by scanning electron microscopy (SEM) (YANG et al. 2015). In the same study, delayed and depressed expression of sporozoite surface antigen protein (cp15) and *Cryptosporidium* oocyst wall protein (COWP) was observed. The authors suggest that these phenomena may explain delayed development of new oocysts in axenic culture (YANG et al. 2015). In another study, *C. parvum* multiplied 2–3 fold after six days of cultivation on an aquatic biofilm and developed various stages including sporozoites, trophozoites, type I and II meronts (KOH et al. 2013).

Various cell culture types and animal models have been applied to study *C. parvum*. Abundant cell lines, such as the human ileocecal adenocarcinoma cell line (HCT-8), heterogeneous human epithelial colorectal adenocarcinoma cell line (Caco-2), Madin-Darby canine kidney cell line (MDCK), Madin-Darby bovine kidney cell line (MDBK) and a human, non-carcinoma, small intestinal epithelial cell line, named FHs

74 Int have been used (VARUGHESE et al. 2014). Immortalized cell lines are most commonly used, particularly HCT-8 (UPTON et al. 1994).

Cell lines have been studied for propagation of *C. parvum* as well as tools for investigation of the parasite's biology. It was observed that *C. parvum* could display its whole life cycle in a HCT-8 cell culture system, and no significant difference in *C. parvum* multiplication was seen between cell culture and axenic culture (PAZIEWSKA-HARRIS et al. 2016). COLO-680N cells have been recently described to be also suitable for *C. parvum* propagation as they produced sufficient infectious oocysts to infect subsequent cultures (MILLER et al. 2017).

Despite the evidence of successful *in vitro* propagation to date, none of the reported systems delivers enough oocysts to replace propagation *in vivo*. Of course, animal models are essential if clinical signs of infection and drug efficacy have to be recorded. Young ruminants such as suckling calves are very suitable for propagation of *C. parvum* since they excrete large amounts of oocysts (NYDAM et al. 2001). Piglets have been studied as well to test parasite pathogenicity and drug efficacy (ENEMARK et al. 2003; TZIPORI et al. 1994b).

Many experimental studies have been reported in laboratory rodent models, especially in mice. Suckling rats were used as the model to investigate the efficacy of probiotics against *C. parvum* (GUITARD et al. 2006). Suckling rats were also used to demonstrate the mechanism of amino acid malabsorption caused by *C. parvum* (TOPOUCHIAN et al. 2001 and 2003). Susceptibility of mice to *C. parvum* is increased in animals with reduced immunity. Thus various attempts to propagate *C. parvum* in immunodeficient mice have been reported, including neonatal mice, early weaned mice, malnourished mice and artificially immunocompromised mice (LACROIX et al. 2001; COSTA et al. 2011; COSTA et al. 2012). Interferon-gamma knock out (GKO) mice are highly sensitive to *C. parvum* and suitable as a model for drug screening (GRIFFITHS et al. 1998b). Dexamethasone-treated and thus immunosuppressed CF-1 mice are recognized as a better animal model than C57BL/6 mice in producing high numbers of *C. parvum* oocysts (WARE and VILLEGAS 2010).

2.8 Structure and function of Calcium-dependent protein kinases

Calcium-dependent protein kinases (CDPK) belong to a superfamily which consists of several types of the enzyme (CDPK 1 to CDPK12). Their activity is regulated by calcium and involves a set of intracellular cascade reactions (HARPER and HARMON 2005). CDPKs play critical roles in the calcium signaling pathway in plants, ciliates and apicomplexan parasites, they are not expressed in higher organisms and thus believed to be potential antiprotozoal drugs with no or minor side effects (HARPER and HARMON 2005).

Twelve subtypes of CDPK have been characterized in various organisms, so far. Though the various types of the superfamily differ more or less in structure and function, most of them share a similar structure with four domains: a variable N-terminal domain, a catalytic domain, a junction domain containing an autoinhibitory segment, and a calmodulin-like domain (Fig. 2) (HARMON et al. 2000). They have four EF-hands with the Ca^{2+} binding sites that promote the activation process in the calmodulin-like domain. As the activation demands the cooperation of the junction domain and the calmodulin-like domain, the two parts are collectively named as the CDPK activation domain (CAD). After binding with Ca^{2+}, a series of structural shifting is triggered including bending, folding and twisting, hence the message carried by Ca^{2+} accomplished transduction.

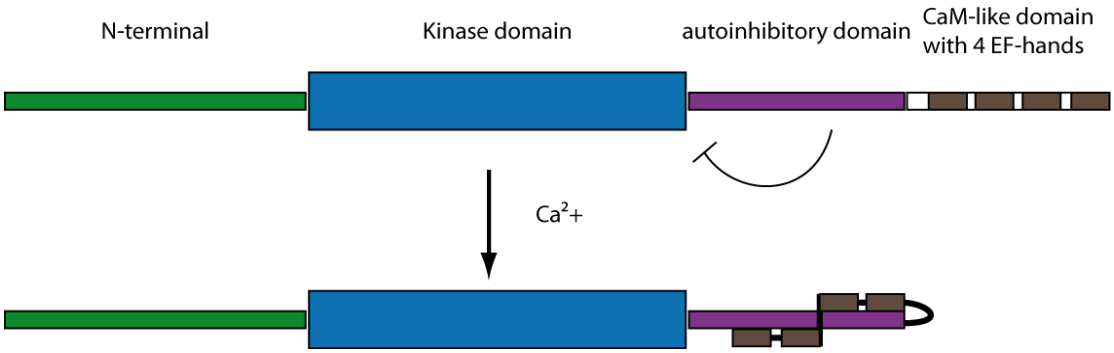

Figure 2. General structure of CDPK (HARMON et al. 2000). Two pairs of two EF-hands are triggered by Ca^{2+} binding to change conformation thus blocking the autoinhibitory domain. Thus the substrate binding site of the catalytic domain is made accessible to substrate binding and enzymatic activity is induced.

The abundant variety of CDPKs indicates physical inconsistencies among the subtypes of this family. Different CDPKs are found located at different cellular positions, including the cytosol, nucleus, plasma membrane (HARPER et al. 2004). Furthermore, they may show different response to different calcium ion forms (LEE et al. 1998). *In vitro* it was shown that the expression of CDPK in *C. parvum* (CpCDPK) is stage specific (ETZOLD et al. 2014). This superfamily of enzymes can control a large array of physiological processes precisely without any unexpected crosstalk (GEISLER and VENEMA 2011).

CDPKs have been extensively studied in other apicomplexans e.g. *Toxoplasma gondii* and *Plasmodium falciparum* (LIM et al. 2012; SUGI et al. 2010). In *T. gondii*, elevated intracellular calcium promotes multiple activities such as motility and invasion by stimulating the secretion of micronemes. On the contrary, decline of the Ca^{2+} concentration effectively inhibits cell invasion by the parasite (CARRUTHERS et al. 1999; CARRUTHERS and SIBLEY 1999). CDPKs transduce the information from the second messenger, intracellular Ca^{2+}, to the organelles and then trigger a set of processes that affect cellular features. For instance, CDPKs are reported to regulate cytoskeletal dynamics and motor complexes (BILLKER et al. 2009). In *Plasmodium*,

several studies suggest that invasion, motility, discharge of organelles and sexual differentiation are all regulated by the level of Ca^{2+} (BILLKER et al. 2004; ISHINO et al. 2006; VAID et al. 2008; ONO et al. 2008). It appears likely that this is related to CDPK, as well as discharge of micronemes during invasion supposed to occur in *Cryptosporidium* similarly to other apicomlexans (SHARMA and CHITNIS 2013).

3. Animals, materials and methods

3.1 Animals and materials

3.1.3 Mice

RAGgc (recombination activating genes common gamma chain) x IFN-gamma (interferon gamma) KO (knockout) mice

3.1.4 Cells

Table 1. Cells used in the study.

Cell lines for *in vitro* infection	HCT-8 cells
	COLO-680N cells
	MDBK cells
E. coli for cloning	XL1-Blue® competent cells (Stratagene, San Diego)

3.1.5 *C. parvum* oocysts

C. parvum oocysts (in house strain LE-08-Cp-08)

3.1.6 Reagents

Table 2. Reagents used in the study.

Reagents for cell culture and *in vitro* infection
PBS (phosphate buffered saline)
RPMI 1640 medium (Thermo Fisher Scientific, Waltham)
DMEM medium (Thermo Fisher Scientific, Waltham)
NaT(Sodium taurocholate hydrate) (Sigma-Aldrich, Hamburg)
G418 (Thermo Fisher Scientific, Waltham)
Reagents for molecular biology
Agarose (Roth®; Karlsruhe, Germany)
TBE (Tris-Borate-EDTA) (AppliChem, Darmstadt)

GeneRuler 100 bp Lader (Thermo Fisher Scientific, Waltham)
GeneRuler 1kb DNA Ladder (Thermo Fisher Scientific, Waltham)
Dream Taq buffer 10X with $MgCl_2$ (Thermo Fisher Scientific, Waltham)
DreamTaq DNA Polymerases (Thermo Fisher Scientific, Waltham)
dNTPs (Thermo Fisher Scientific, Waltham)
TaqMan® qPCR Master Mixes (Thermo Fisher Scientific, Waltham)
SOC (Thermo Fisher Scientific, Waltham)
LB-Agar (Lennox) (Carl Roth, Karlsruhe)
LB-Medium (Lennox) (Carl Roth, Karlsruhe)
FastDigest AatII (Thermo Fisher Scientific, Waltham)
FastDigest AvrII (XmaJI) (Thermo Fisher Scientific, Waltham)
FastDigest NdeI (Thermo Fisher Scientific, Waltham)
FastDigest NheI (Thermo Fisher Scientific, Waltham)
FastDigest MluI (Thermo Fisher Scientific, Waltham)
BbsI-HF (New England Biolabs® Inc, Ipswich)
T4 Polynucleotide Kinase (New England Biolabs® Inc, Ipswich)
CIP (New England Biolabs® Inc, Ipswich)
Reagents used in animal experiment
Metamizol (Ratiopharm, Ulm)
Glucose (Carl Roth, Karlsruhe)
Reagents for IFA
Glycine (Carl Roth, Karlsruhe)
PFA (Paraformaldehyde) (Sigma-Aldrich, Hamburg)
Triton X-100 (Carl Roth, Karlsruhe)
BSA (bovine serum albumin) (Carl Roth, Karlsruhe)
Antibodies and fluorescent dyes
Rat anti-Crypto (Waterborne, New Orleans)
Dylight™ 647 anti rat IgG (H&L) (Rockland, Limerick)
DyLight™ 488 anti-rat IgG (Rockland, Limerick)

DAPI (Thermo Fisher Scientific, Waltham)
Mouse anti-NPTII (Alpha Diagnostic International, San Antonio)
Crypto-a-glo (Waterbone, New Orleans)
Fluoromount-G (Thermo Fisher Scientific, Waltham)

3.1.7 Plasmids and oligonucleotides

3.1.7.1 Plasmids

Plasmids used in order to construct CDPK1 knock out plasmid via sub cloning are shown in Fig 3.

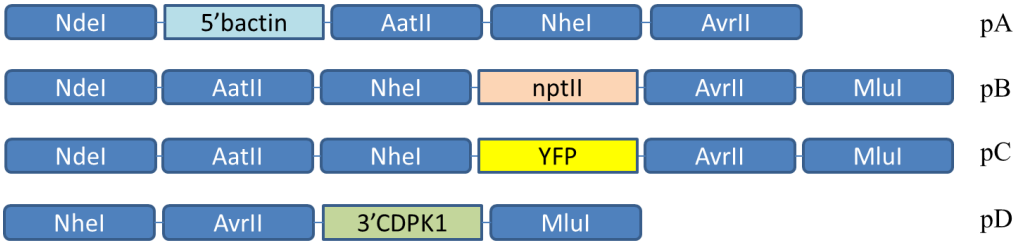

Figure 3. Plasmids (backbone vector pSC-A) for construction of *C. parvum* CDPK1 knock out plasmid. *The plasmids are denominated as pA, pB, pC and pD respectively as shown above.

Table 3. Plasmids supplied by researchers from other institutes.

Plasmid	Denomination	Provider
pCpact5'mcherryEtact3'	pmCherry	Anne-Kristin Teten (Institut für Zoologie, Technische Universität Dresden)
Aldo Cas9 Ribo + U6	p185	Boris Striepen (Pathobiology, University of Pennsylvania School of Veterinary Medicine)
Enoprom_Nluc_neo_enoutr	P71	
pCAG-mGFP-Actin	pGFP-Actin	Addgene

3.1.7.2 Primers and probes

Table 4. Primers used in the study

5UTR'_Cp CPDK1F	CGCCATATGGCGACTCGGAATTTATTTTTTCCTTCG
5UTR'_Cp CPDK1R	CGCGACGTCGCGTTATAACAAGCCTTAATTGTGAGT
hsp_70F	AACTTTAGCTCCAG TTGAGAAGTACTC
hsp_70R	CATGGCTCTTTACCGTTAAAGAATTCC
HSP_70_SNA	AATACGTGTAGAACCACCAACCAATACAACATC
CpCDPK1_181 F	GTTGGACTGGTATGTTTGTTCAGAG
CpCDPK1_181 R	AAACCTCTGAACAAACATACCAGTC
CpCDPK1_7 F	GTTGGAATACTGCAGTAGGGAATAC
CpCDPK1_7 R	AAACGTATTCCCTACTGCAGTATTC
gRNA screening primer	CTTTACTATTTATTCCGCTTCCACATGC
Seqp185 F	CTTTACTATTTATTCCGCTTCCACATGC
$CDPK_1koF$	ATTTTAGTTCAGGAATAATCCAAACAACTCACAATTAAGGCTTGTTATAATGGGGAAACTAAATATACTG
$CDPK_1koR$	TCAGAAGAATTCGTCAAGAAGACTACTCTCAAATAGTAGTGAACTCTATATATTTCAATTCTATTATTATTA

The under lined base pairs in primers represent for the overhangs compatible to restriction site Bbs I. Letters in red represent for the manually added base pairs when the corresponding gRNA does not start with "G".

3.1.8 Kits

GeneJET Gel Extraction Kit (Thermo Fisher Scientific, Waltham)

GeneJET PCR Purification Kit (Thermo Fisher Scientific, Waltham)

T4 DNA Ligase Kit (Thermo Fisher Scientific, Waltham)

GeneJET Plasmid Miniprep Kit (Thermo Fisher Scientific, Waltham)

GeneJET Plasmid Maxiprep Kit (Thermo Fisher Scientific, Waltham)

Qiagen Maxiprep kit (Qiagen, Hilden)

NucleoSpin® DNA Stool Kit (Macherey-Nagel GmbH & Co.KG, Düren)

3.1.9 Instruments and software

Mikro 200 (Hettich, Tuttlingen)

Centrifuge5810 R (Eppendorf, Hamburg)

Mini Incubator (Bode, Berlin)

Incubator BD 260 (Binder, Tuttlingen)

Incubator Hood TH 15 (Edmund Bühler, Bodelshausen)

Mx3000P qPCR System (Stratagene, San Diego)

Hera safe KS12 Class II Biological Safety Cabinet (Thermo Fisher Scientific, Waltham)

ECM 830 square wave electroporator (BTX, Holliston)

Gene Pulser Xcell™ (Bio-rad, Hercules)

TCS SP8 system (Leica, Wetzlar)

Fluorescent microscope DM IRB (Leica, Wetzlar)

FACS Aria™ III (Becton Dickinson, Heidelberg)

Bandelin sonopuls GM70 (Bandelin, Berlin)

FACSDiva™ V6.5 (Becton Dickinson, San Jose)

SPSS (IBM, New York)

Genenious (Biomatters, Auckland)

Imaris (Bitplane, Zurich)

ArgusX1 (Biostep, Burkhardtsdorf)

3.2 Methods

3.2.1 Preparation of reagents

PBS

10 x concentrate PBS stock was prepared by dissolving 1,4 M NaCl, 30 mM KCl, 40 mM Na2HPO4 and 20 mM KH2PO4 in ddH2O. Prior to use, 1 x PBS was prepared by diluting in ddH2O and pH was adjusted to 7.4.

Growth medium for HCT-8 and COLO-680N cells

RPMI 1640 medium (Thermo Fisher Scientific, Waltham) complemented with 10% FCS, 1% P/S, 1% Ampho B and 1% Napy.

Growth medium for MDBK cells

DMEM medium (Thermo Fisher Scientific, Waltham) complemented with 10% FCS, 1% P/S, 1% Ampho B.

Infection medium

Corresponding medium completed with 2% FCS, 1% P/S, 1% Ampho B and 1% Napy.

Excystation buffer

1.2 % NaT dissolved in growth medium and stored at 4℃ for maximum one week. Prior to use, dilute the stock with growth medium at the ratio of 1:3.

1.5% Agarose-Gel

375 g Agarose (Carl Roth; Karlsruhe) powder dissolved in 250 ml 1 x TBE buffer (AppliChem, Darmstadt), heated in microwave oven prior to use.

LB agar

35g LB-Agar (Lennox) powder (Carl Roth, Karlsruhe) was dissolved in 1 L ddH_2O and autoclaved, then split in to petri dish and stored at 4 ℃.

LB medium

20 g LB-Medium (Lennox) powder (Carl Roth, Karlsruhe) was dissolved in 1 L ddH2O and autoclaved. Stored at 4 ℃.

Incomplete cytomix buffer

10mM K_2HPO_4/KH_2PO_4, 120mM KCl, 0.15mM $CaCl_2$, 25mM HEPES, 2mM EGTA

and 5mM $MgCl_2$ dissolved in ddH_2O and pH was adjusted to 7.6.

Complete cytomix buffer

Incomplete cytomix buffer complemented with 2mM ATP and 5mM glutathione.

Fixation solution

20 g of PFA powder dissolved in 500 ml in pre-heated PBS.

Permeabilization solution

200 µl Triton X-100 dissolved in 100 ml PBS

Blocking buffer

Permeabilization solution completed with 2% BSA

3.2.2 *C. parvum* oocysts maintaince

C. parvum oocysts were stored in PBS at 4 ℃. The parasite strain is maintained by passage through calves approximately every 3 months. Calves are infected orally with *C. parvum* oocysts. Diarrheal stools were collected and washed by ether and centrifugation. Oocysts were isolated by saturated-salt solution flotation and stored in PBS.

3.2.3 PCR

3.2.3.1 Amplification of NdeI and AatII flanked 5'CDPK1

5UTR'_CpCPDK1 fragments with NdeI and AatII site at each end was amplified by using DNA isolated from freshly excysted sporozoites as template and forward primer 5UTR'_CpCPDK1F and reverse primer 5UTR'_CpCPDK1R. The PCR program was set as 95 ℃ for 5 min; 35 cycles of 95 ℃ for 30 s, 47 ℃ for 30s, 72 ℃ for 91 s; 72 ℃ for 5 min.

3.2.3.2 Annealing of gRNA

The forward primer was annealed with the reverse primer in a PCR tube with c polynucleotide kinase (PNK). Volumes of reagents used in the reaction are listed in Table 5.

Table 5. Composition of CpCDPK1 gRNA annealing.

Reagents	**Volume (µl)**
Forward Primer (100µM)	1
Reverse Primer (100µM)	1
T4 ligase buffer (10X)	1
PNK	0.5
ddH2O	6.5
Total	10

The annealing program starts with a 30 min pre-warm step at 37 ℃. Annealing: 1 round at 95 ℃ for 5 min. The step was repeated 14 times, with the temperature decreasing by 5 ℃ in each round. Hold at 4 ℃ overnight.

3.2.3.3 Amplification of repair cassette via Touchdown PCR (TD-PCR)

Involved reagents were used as listed in Table 6. TD-PCR was applied as follows: a) initial denaturation at 95 ℃ for 2 min; b) thermocycling: denaturation at 95 ℃ for 45 s for each cycle; annealing temperature was gradually decreasing (1 ℃ per cycle) from 65 ℃ to 56 ℃ during the first 10 cycles, and remained at 55 ℃ in the following 25 cycles with the consistent duration of 30 s; elongation at 72 ℃ for 112 s; c) final elongation at 72 ℃ for 10 min; hold at 4 ℃. PCR products were visualized by gel electrophoresis and those with the length of 1836 bp were selected for sequencing

Table 6. Reagents and TD PCR program for the amplification of repair cassette.

Reagents	Volume (µl)	Cycles	Temperature (℃)	Time (s)
ddH_2O	18	1	95	120
dNTPs	0.8	10	95	45
Template (p71)	2.5		65 to 56(-1/cycle)	30
Forward Primer ($CDPK_1koF$)	0.5		72	112
Reverse Primer ($CDPK_1koR$)	0.5	25	95	45
Taq Buffer 10X	2.5		55	30
Taq polymerase	0.2		72	112
Total	25	1	72	600

3.2.3.4 Colony PCR

Bacteria carrying plasmids were plated on LB agar and incubated overnight (see 3.2.8). Colonies were picked and incubated in 500 µl LB medium at 37 ℃ for 2-3h. Colony PCR was performed to verify the success of the ligation and transformation. Reagents involved were listed below (Table 7). Program runs as follows: initial denaturation at 95 ℃ for 5 min; denaturation at 95 ℃ for 30 s, annealing at 53 ℃ for 40 s, elongation at 72 ℃ for 1 min, repeat this cycle for 35 times; final elongation at 72 ℃ for 1 min. Finally, 10 µl of each PCR products were loaded on agarose-gel for electrophoresis. Positive colonies were saved for further cultivation and plasmid extraction.

Table 7. Reagents of colony PCR.

Reagents	**Volume(µl)**
Taq Buffer 10X	2.5
dNTPs	0.8
Primer T3	0.5
Primer T7	0.5
Taq polymerase	0.2
Template (bacterium solution)	2.5
ddH_2O	18

3.2.3.5 Real-time PCR for *C. parvum* hsp70

C. parvum heat shock protein 70 (hsp70) was selected as the reference gene. For each reaction 5 µl of template was used according to table 8 to quantify the hsp70 copy number in the template. DNA extracted from faeces was added into the 20 µl reaction system along with *C. parvum* hsp70 primers and Taqman probe. The qPCR program was designed as follows: denaturation: 95 ℃ for 15min; alignment: 40 cycles at 95 ℃ for 15 s; elongation: 60 ℃ for 1 min.

Table 8. Composition of qPCR reagents for Cp_hsp70 gene.

Reagents	**Volume per reaction (µl)**
Template	5
PCR Master Mix 2X	10
ddH2O	3.88
Cp_hsp 70 forward primer	0.24
Cp_hsp 70 revers primer	0.72
Cp_hsp 70 Taqman probe	0.16
Total	20

3.2.4 Restriction enzyme digestion

3.2.4.1 Restriction enzyme digestion of pA - pD

Plasmids were cut by specific pairs of restriction enzymes at a temperature for catalysis of 37 ℃ and varying temperatures of 65 ℃ to 85 ℃ for inactivation. Duration of incubation was 10 to 60 min for catalysis and 5 min for inactivation (Table 8). The reaction system included 1 µg plasmid, 1 µl restriction enzyme and 2 µl 10X FastDigest Buffer according to the manufacture's instruction. Double distilled water (ddH2O) was added up to a total volume of 20 µl.

Table 9. Temperatures and duration of incubation with restriction enzymes for catalysis and inactivation.

Catalysis			Inactivation	
Name	Temperature(℃)	Duration(min)	Temperature(℃)	Duration(min)
AatII	37	20	85	5
NdeI	37	60	65	5
NheI	37	15	65	5
MluI	37	15	80	5
AvrII*	37	10		

***AvrII cannot be heat inactivated.**

3.2.4.2 Enzyme digestion and dephosphorylation of p185

The plasmid Aldo Cas9 Ribo + U6 was digested by BbsI at 37 ℃ for 1 h or longer, until it was fully cut (<16 h). The reaction system included 1 µg plasmid, 1 µl restriction enzyme and 2 µl Cut Smart Buffer. Calf intestinal phosphatase (CIP, New England Biolabs® Inc, Ipswich) was used to dephosphorylate the plasmid at 37 ℃ for 30 min (Table 10). Then the plasmid was purified again and diluted to 50 ng/µl.

Table 10. Reagents used for Plasmid dephosphorylation.

DNA	1 µg
CutSmart® Buffer (10X)	1 µl
CIP	1 unit
ddH2O	Up to 20 µl

3.2.5 Agarose gel electrophoresis

Agarose gel electrophoresis was used to separate DNA fragments. DNA samples were loaded in the wells of 1.5 % agarose gel. Electrophoresis was carried out under the voltage of 200 V for 30 min in 1 x TBE. GeneRuler 1kb DNA Ladder® (Thermo Fisher Scientific, Waltham) or GeneRuler 100 bp DNA Ladder® (Thermo Fisher Scientific, Waltham) were used as reference. Afterwards, the gel was sunk in 0.01% EB solution for 30 min. The gel was imaged under UV light by ArgusX1 (Biostep, Burkhardtsdorf).

3.2.6 Gel purification

The target fragments were extracted from the gel by using GeneJET Gel Extraction Kit (Thermo Fisher Scientific, Waltham). After weighing the gel slice, 1:1 (buffer volume: gel weight) binding buffer was added into the tube and the tube was incubated at 50 – 60 ℃ for 10 min. Then up to 800 µl of gel solution was transferred into the GeneJET purification column along with 100 µl binding buffer and centrifuged at 12,000 rpm for 1 min in Mikro 200 (Hettich, Tuttlingen). Flow-through was discarded and 700 µl wash buffer was added to the column. Centrifugation at 12,000 rpm for 1 min was applied and flow-through was again discarded. The dry columns were spun at 12,000 rpm centrifugation to remove residues on the membrane. DNA was eluted by centrifugation at 12,000 rpm for 1 min in 50 µl elution buffer supplied with the kit, then collected in 1.5ml Eppendorf tubes and stored at -20 ℃ until further use.

3.2.7 Ligation

3.2.7.1 Ligation of CDPK1 KO plasmids

By applying T4 ligation, different purified DNA fragments were inserted into the mutual pSC-A vector. For example, after 5'UTR_bAct is cut down from pA, it could be inserted in pB that is pre-cut by enzymes AatII and NdeI with T4 ligation. The other fragments could be also inserted into the same plasmid by performing the same method.

T4 ligase kit was purchased from Thermo Fisher Scientific (Waltham). The reaction demanded 20-100 ng vector DNA, DNA fragment in an amount of 1-5 times of vector DNA, 2 µl buffer, 1 µl T4 ligase and nuclease-free water up to the total volume of 20 µl. After being incubated at 22 ℃ for 10 min, the ligation mixture was ready for transformation.

3.2.7.2 Ligation of gRNA and p185

T4 ligation was applied with different setups to optimize the dilution of insert with the highest of 1 and the lowest of 1/500 (Table 11). Controls were also included. Aim of treatment 1 was for controlling uncut plasmid and 2 for plasmid self-ligation. All setups were incubated at 4 ℃ overnight.

Table 11. Reagents used in gRNA-plasmid ligation setups.

Groups / Reagents	1	2	3	4	5
	Volume (µl)				
Cas9 Plasmid (50 ng)	1	1	1	1	1
Annealed guides			1		
Annealed guides diluted 1:200				1	
Annealed guides diluted 1:500					1
T4 DNA Ligase Buffer	1	1	1	1	1
T4 DNA Ligase Enzyme		0.5	0.5	0.5	0.5
Water	8	7.5	6.5	6.5	6.5
Total Volume	10	10	10	10	10

3.2.8 Transformation

The XL1-Blue® competent cells (Stratagene, San Diego) were stored at -80 ℃. For transformation, 50 µl competent cells were thawed on ice. During the process, 0.9 µl of β-mercaptoethanol was added into the tube and was gently mixed every 2 min until the cell suspension was completely thawed. After 10 min incubation, 0.1-25 ng ligation products were added and the tube further incubated on ice for another 30 min. Then, the tube was heat-pulsed in a 42 ℃ water bath for 45 seconds. Before mixed with 500 µl pre-heated super optimal broth with catabolite repression (SOC) medium, the tube was placed on iced and cooled down for 2 min. After 1 h shaking at 200 rpm at 37 ℃, 20 µl of the bacteria suspension was spread on a lysogeny broth (LB) agar plate and incubated at 37 ℃ overnight.

3.2.9 Plasmid extraction

Bacteria was cultivated in 5 ml LB medium in a shaking incubator Incubator Hood TH 15 (Edmund Bühler, Bodelshausen) at 37 ℃, 200 rpm overnight. After cultivation, the bacterium was collected in 1.5 ml Eppendorf tube and centrifuged at 8000 rpm for 2 min. Discard the supernatant and refill the tube with bacterium. The step was

repeated until all cells were pelleted. The pellet was resuspended in the 250 µl Resuspension Solution by vortexing. Next, 250 µl Lysis Solution was added in the tube and the tube was inverted gently 4 - 6 times. 350 µl Neutralization Solution was added and mixed by immediately gentle inverting for 4-6 times. The mixture was centrifuged at 12,000 x g for 5 min to pellet the cell debris and chromosomal DNA. The supernatant was transferred to a Thermo Scientific GeneJET Spin Column and centrifuged at 12,000 x g for 1 min. 500 µl Wash Solution was added to the column and centrifuged at 12,000 x g for 1 min. The flow-through was discarded and the wash step was repeated once. Another centrifugation at 12,000 x g for 1 min followed to dry the column. GeneJET Spin Column was transferred into a 1.5 ml Eppendorf tube with 50 µl Elution Buffer at the center of its membrane. After 2 min incubation at RT, a centrifugation at 12,000 x g for 2 min was performed to elute the plasmid DNA. Plasmid was stored at - 20 ℃.

3.2.10 *C. parvum* oocysts excystation

C. parvum oocysts were pelleted from PBS by centrifugation at 12,000 rpm for 4 min and then re-suspended in sodium hypochlorite (NaOCl). The oocysts were incubated on ice for 5 min and washed three times with cold PBS by centrifugation at 12,000 rpm for 4 min. After washing, the oocysts were incubated in 0.8% sodium taurocholate (NaT)/infection medium at 15 ℃ for 10 min, then, incubated at 37 ℃ for 1.5 h. Next, excysted sporozites were pelleted at 14,000 rpm for 8 min and filtered with ReliaPrep Filter 5 µm (Ahlstrom, Helsinki).

3.2.11 *C. parvum* infection

3.2.11.1 In vitro infection

4×10^6 excystated sporozoites were seeded into 24-well plates containing cells at the confluency at 70% - 80%. Throughout infection, growth medium was replaced by infection medium.

3.2.11.2 *C. parvum* infection in mice

C. parvum oocysts were stored at 4 ℃ in PBS. Propagation and purification was performed 1 week before animal experimentation. A novel strain, RAGgc × IFN-gamma KO mice were purchased (Dr. Christoph Hölscher, Leibniz-Center for Medicine and Biosciences, Borstel). The mice were maintained in the animal facility of Max-Planck Institute for Evolutionary Anthropology, Leipzig. Twenty one 6-week-old female RAGgc × IFN-gamma KO mice were randomly separated into 3 groups. Groups 2 to 4 were orally gavaged with 500 oocysts, 1000 oocysts, or 5000 oocysts of *C. parvum* per mouse, respectively. An additional six BALB/c WT mice were inoculated with 5000 oocysts as control group (G1).

3.2.12 Transfection

3.2.12.1 Electroporation for MDBK transfection

The plasmid pCAG-mGFP-Actin (obtained from Addgene, Cambridge, USA) was used for MDBK cell transfection. Electroporation was performed with the ECM 830 squarewave electroporator (BTX, Holliston). All electroporations were performed with incomplete cytomix buffer and complete cytomix buffer. Before electroporation, the cuvettes were washed with 70% ethanol and dried in the working bench. After MDBK cells were grown to 80% confluence they were detached by trypsinization and centrifuged at 1000 rpm for 10 min. The supernatant was discarded and the pellet was resuspended in incomplete cytomix buffer. Centrifugation was repeated once and the resulting cell pellet was resuspended in complete cytomix buffer. 5×10^6 cells and a minimum of 55 µg BamHI linearized pCAG-mGFP-Actin plasmids were gently mixed in a cuvette. PBS was added up to a total volume of 500 µl. The cuvettes were electronically pulsed in the safety chamber. A range of voltages, pulse durations and interval lengths were tested to determine the optimal electroporation conditions. Before being seeded on the 24-well plate, cells were incubated at RT for 15 min in the working bench. Thereafter, the electroporated cells were incubated at 37 ℃, 5% CO_2 overnight.

3.2.12.2 Electroporation for *C. parvum* transfection

The mcherry reporter plasmid pCpact5'mcherryEtact3'(pmcherry), kindly provided by Anne-Kristin Teten (Institut für Zoologie, Technische Universität Dresden), was used for electroporation. Electroporation conditions were optimized for ECM 830 square wave electroporator (BTX, Holliston) and Gene Pulser Xcell™ (Bio-rad, Hercules). For this purpose 5×10^6 *C. parvum* oocysts or the same number of sporozoites were suspended in 500 µl incomplete cytomix buffer. The suspension was centrifuged at 200 x g for 5 min. The pellet was resuspened in a transfection cuvette in 800 µl complete cytomix buffer. 100 µg of plasmid was linearized before electroporation through incubation with 2 µl SapI (New England Biolabs® Inc, Ipswich) at 37 ℃ for 2 h and added to the suspension. The electroporation conditions varied in wave form, voltage and pulse duration. Dozens of combinations were applied to search the optimal conditions as shown in table 12.

Table 12. Range of eletroporation conditions for *C.parvum* transfection

Parameters	Voltage (V)	Pulse duration (μs)	Pulse times	Wave Form
Minimum	1000	100	1	Square wave (for oocysts and sporozoites)
Maximum	3000	1000	10	Decay wave (for sporozoites only)

3.2.12.3 CpCDPK1 knock out through Cell penetrating peptide (CPP) - octaarginine mediated transfection

Plasmid p185 and the amplified repair cassette with CpCDPK1 flanks were incubated with CPP, specifically octaarginine, at the molar ratio of 1:400 at 37 ℃ for 1 h separately (Table 13). Then both compounds were mixed with freshly excysted sporozoites and incubated at 37 ℃ for another 1 h. At last, the sporozoites were seeded to COLO - 680 N or HCT - 8 cells at the confluency of 80%. Infected cells were cultivated at 37 ℃ for 2 weeks in growth medium DMEM with paromomycin (6 mg/ml). Medium was changed once a week. Passage was performed every 2 weeks.

Table 13. Reagents used for CPP-DNA compound.

	p185	Repair cassette
Reagents	Volume (μl)	Volume (μl)
DNA	5 μg (volume varies to concentration of DNA)	5 μg (volume varies to concentration of DNA)
Octaarginine	2.5	13.7
Polyethylenimine (PEI)	2.5	2.5
Growth medium DMEM	up to 1000	up to 1000

3.2.13 Geneticin screening for GFP-MDBK cells

Fluorescent microscopy (DM IRB, Leica, Wetzlar) was applied every 24 h after electroporation to check the transfection efficiency. Filter FITC was selected to detect the GFP signal. MDBK cells which expressed GFP were picked under the 40× objective lens and seeded into new plates for growth of transfected cells. Fluorescence-activated cell sorting (FACS) was applied when monolayers reached confluence of 80%. FACS Aria™ III (Becton Dickinson, Heidelberg) was used for the cell sorting. Single cells strained through a 40 µm mesh were analyzed by the software FACSDiva™ V6.5 (Becton Dickinson, San Jose). The GFP signal was excited by the 488 nm laser and detected with the 530/30 Filter. The pulse geometry gates that measure the forward and side scatter light signals in area (FSC-A/SSC-A) were used for gating cells, doublets of cells in the flow were eliminated by FSC-A, FSC-H (forward scatter light signal in height). At last the GFP expression was analyzed (GFP/FSC-A). Low and high expressing cells were gated and the cells in these gates were physically sorted into tubes containing DMEM medium pre-cooled to 4 ℃. Sorted cells with intense signal were seeded back on the culture plate and incubated in complete DMEM at 37 ℃.

After 24 h of incubation the aminoglycoside antibiotic G418 (500 µg/ml, Thermo Fisher Scientific, Waltham) was introduced into cultures of transfected MDBK cells. Cultures were checked daily under fluorescent microscope (40×/0.5, FITC). Growth medium and G418 were replaced every 72 h over the culturing period of 2 weeks. Cells that continuously displayed the green fluorescent signal were harvested and stored in liquid nitrogen until further use.

3.2.14 Indirect immunofluorescent assay (IFA)

The IFA was performed to visualize *C. parvum*. Infected monolayers were fixed in fixation solution for 20 min at RT. The slide was incubated in permeabilization solution for 20 min at RT to increase permeability of cell membranes. Thereafter blocking buffer was applied for 1 h. Primary and secondary antibodies were applied to

the monolayer stepwise for 1 h at RT. Specific antibodies and dilutions in blocking buffer used for different experiments are listed in Table 14. 4',6-diamidino-2-phenylindole (DAPI) solution with the concentration of 0.1 µg/ml was added for a 4 min staining at RT. Monolayers were washed 3 times with 0.2 % Triton/PBS between each step. The specimens were mounted on glass slides with the help of Fluoromount-G™ (Thermo Fisher Scientific, Waltham).

Table 14. Antibodies and their dilutions used in IFA

	Primary antibody	Secondary antibody
WT infection	Rat anti-Crypto (1:3000)	Dylight™ 647 anti rat IgG
Infection after *C. parvum* transfection	Rat anti-Crypto (1:3000)	Dylight™ 488 anti rat IgG (H&L) (1:3000)
	Mouse anti-human neomycin phosphotransferase (1:1000)	Alex Fluor™ 647 anti-mouse IgG (1:1000)

Confocal laser scanning microscopy (CLSM) was applied by TCS SP8 system (Leica, Wetzlar) to detect fluorescent signals and to capture images. The object lens for all fluorescent signals was a glycerol lens with 63 times of magnification and 1.3 of numerical aperture. Argon laser was applied consistently at the intensity of 20 %. The photo-multiplier tube (PMT) was used as detector for DAPI and green fluorescent signals and HyD for the red fluorescent signals.

3.2.15 Animal feeding and body conditioning score (BCS) monitoring

The mice were observed and weighed every day over the investigational period. Body condition was recorded daily considering weight, fur, posture, body temperature and responsiveness towards external stimulation. The body condition scores were rated

according to table 15. Mice scored **‘4’** were regarded intolerably suffering and were humanely sacrificed. Drinking water with metamizol (250mg/100ml) was replaced every day and accessible *ad libitum*. Glucose (20%) was added to drinking water to stimulate water consumption. The dose of metamizol was increased to 500 mg/100 ml when at least one mouse in a group was rated **‘3’**.

Table 15. Body conditioning score of mice.

Scoring	**Body conditions**
4 >>> euthanasia	**emaciated** - bones are generally not or hardly covered by visible musculature - the back vertebrae are clearly discernible - 20 % or more weight loss - apathia - no or almost no reaction to touch - body temperature below 34 ℃ - inability to rise - strong gastrointestinal cramps (buckling, recognizable bowel movement)
3	**underweight** - segmentation of the vertebral column visible - pelvic bones easily palpable - weight loss of about 10 % - the mouse separates from mates , eats less, humps its back
2	shaggy coat
1	**normal weight** - spine and pelvic bones covered by muscle, barely visible and difficult to palpate - smooth fur - normal behavior

3.2.16 Faecal sample collection

Feces were collected daily from day 0 to day 4 p.i. and then every second day until day 21 p.i.. Mice were kept group wise in cages, however, for feces collection individuals were separated over 2 h following weighing. Faeces samples were stored in 1.5 ml plastic tubes at -20 ℃ until further use.

3.2.17 DNA extraction and oocysts per gram (OPG) determination of fecal samples

DNA was extracted from 100 mg of feces collected from each mouse through NucleoSpin® DNA Stool Kit (Macherey-Nagel GmbH & Co.KG, Düren) according to the manufacturers' protocol. Feces were mixed with 1 ml ST1 lysis buffer in NucleoSpin® Bead Tubes which were pre-filled with ceramic beads. Then the feces underwent ultra-sonication for 8 min (Amplitude: 60 %, Puls: 0.5 ms, Bandelin sonopuls GM70, Berlin). After extraction, DNA was eluted in 50 µl molecular grade water and stored at -20 ℃.

Real-time PCR was performed to detect the Cp_hsp 70 gene copies in the faecal samples. As 5 µl of the total volume of 50 µl of DNA extracted from 100 mg of faeces were used as template for qPCR, and 1 oocyst contains 4 sporozoites = 4 genomes, the numbers of oocysts per gram (OPG) of faeces were calculated from the number of Cp_hsp 70 gene copies according to the following formula:

$$\mathbf{OPG} = \mathbf{n} \times \frac{\mathbf{50}}{\mathbf{5}} \div \mathbf{4} \times \frac{\mathbf{1000}}{\mathbf{100}} = \mathbf{25} \times \mathbf{n}$$

n= Cp_hsp70 gene copies

50/5: ratio total DNA volume/volume used as template

4: number of genomes per oocyst

1000/100: ratio one gram of feces to weight of taken feces

3.2.18 Statistical analysis

SPSS 22.0 (IBM, New York, USA) was used for statistical analysis. One sample Kolmogorov-Smirnov test was performed to test for normal distribution of data. Since data did not follow a normal distribution, nonparametric tests, Wilcoxon signed-rank test (for paired samples) and Mann-Whitney U test (for independent samples) were performed to evaluate whether intra- and inter-group data differed significantly at $P < 0.05$.

4. Results

4.1 CDPK1 knockout by REMI

At first, the attempt was made to generate mutation in *C. parvum* by REMI. In principle, the presence of restriction enzyme leads to random cleavages in sporozoites's genome and the linearization of plasmid. After the translocation of the plasmid by electroporation, the compatible cohesive ends in both the parasite's genome and linearized plasmids can ligate. This allows the integration of the plasmid into the genome through homologue recombination, and thereby the CDPK1 KO mutants can be generated and survive in the following drug screening.

4.1.1 Construction of Knockout plasmid

To construct CDPK1 knockout plasmid, the plasmids pA - pD were specifically cleaved by restriction enzymes. The cut-down fragments were inserted into the same plasmid stepwise as shown in Fig. 4.

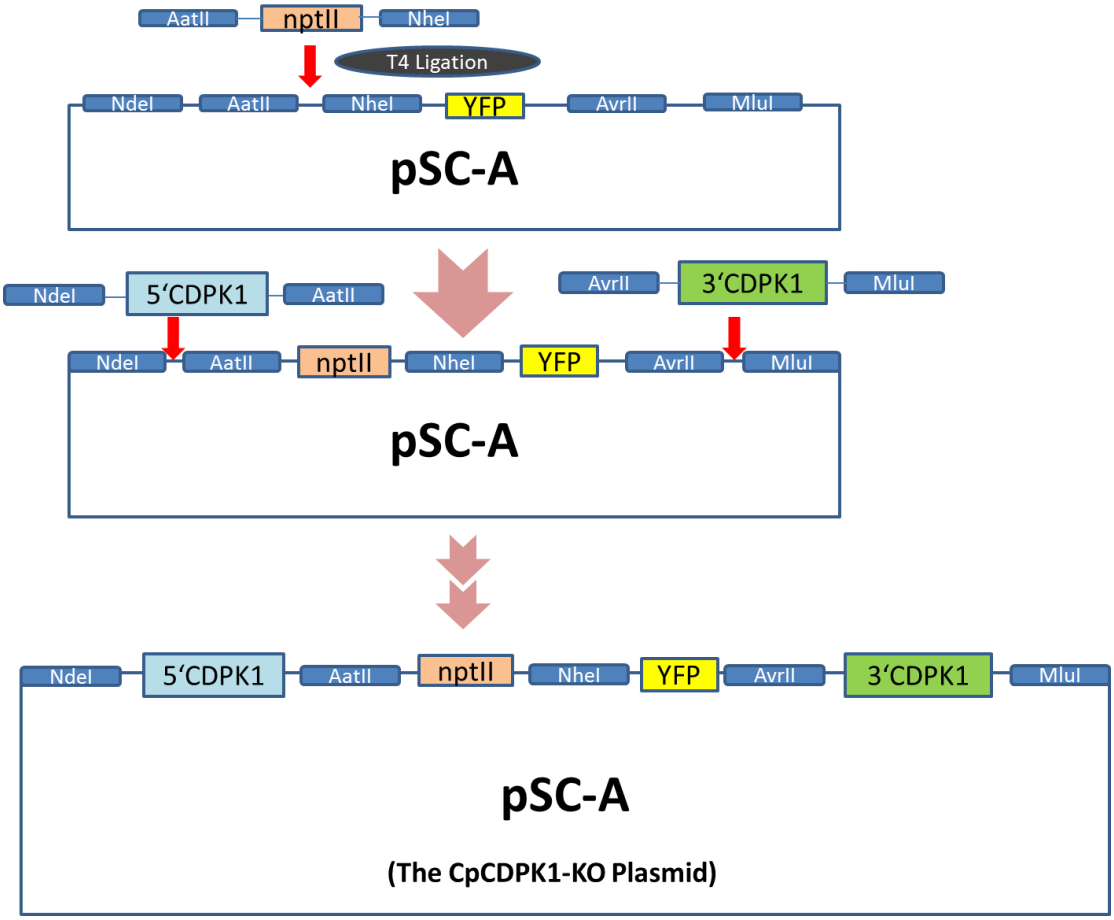

Figure 4. Schematic presentation of construction of *Cp*CDPK1 gene knockout plasmid. Target fragments were cut from the stored plasmids (pA-pD) and inserted into another plasmid through T4 ligation and transformation. Different fragments were inserted sequentially to achieve the knockout plasmid. In this example nptII with restriction enzyme overhang was nicked and pSC-A-YFP plasmid was cut with the same double restriction enzyme. Through T4 ligation and XL1-blue transformation, the pSC-A-nptII-YFP was constructed. Following this procedure fragments such as 5'CDPK1, 5'bAct or 3'CDPK1 were also inserted to obtain the final plasmid.

A plasmid (pSC-A-5'UTR_bAct-nptII-YFP-3'CpCDPK1) with 4 external inserts and pSC-A backbone was generated. Each insert was verified by enzyme digestion and analyzed on agarose gel. The plasmid showed positive bands on gel after cleavage by restriction enzymes (Fig. 5). The sizes of various fragments were as follows, 5'UTR_bActin: 924 bp; nptII: 796 bp; YFP: 822 bp; 3'UTR_CDPK$_1$: 1491 bp. The

sequencing results confirmed the correctness of the construct with identities of 100% of all fragments.

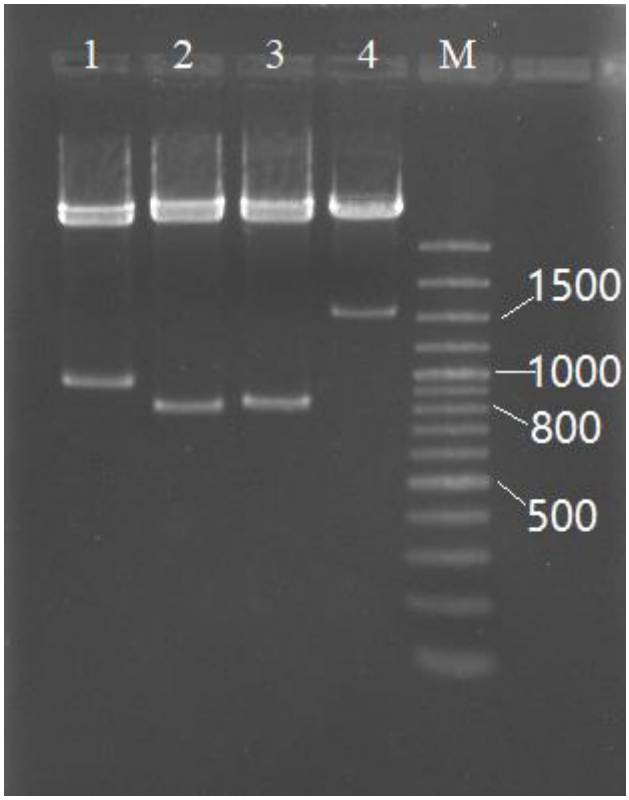

Figure 5. Plasmid pSC-A-5'UTR_bAct-nptII-YFP-3'CpCDPK1 analyzed by enzyme digestion and gel electrophoresis. Agarose concentration: 1.5%. Lane 1-4 represent the products of cutting by different pairs of restriction enzymes. 1: NdeI and AatII; 2:AatII and NheI; 3: NheI and AvrII; 4: AvrII and MluI. Lane M is for marker.

The 5'UTR_CpCDPK1 was amplified and used to replace the 5' UTR_bAct (Fig. 6). Finally, plasmid pSC-A-5'UTR_CpCDPK1-nptII-YFP-3'UTR_CpCDPK1 was constructed. With the generated construct bearing identical 5' and 3' regions with the CpCDPK1 gene locus, homologous recombination could now be performed in order to replace the original gene with the construct. This was achieved by transfecting the generated construct into the parasite. The successful integration of the construct will silence CpCDPK1 and enable the expression of the nptII-YFP reporter.

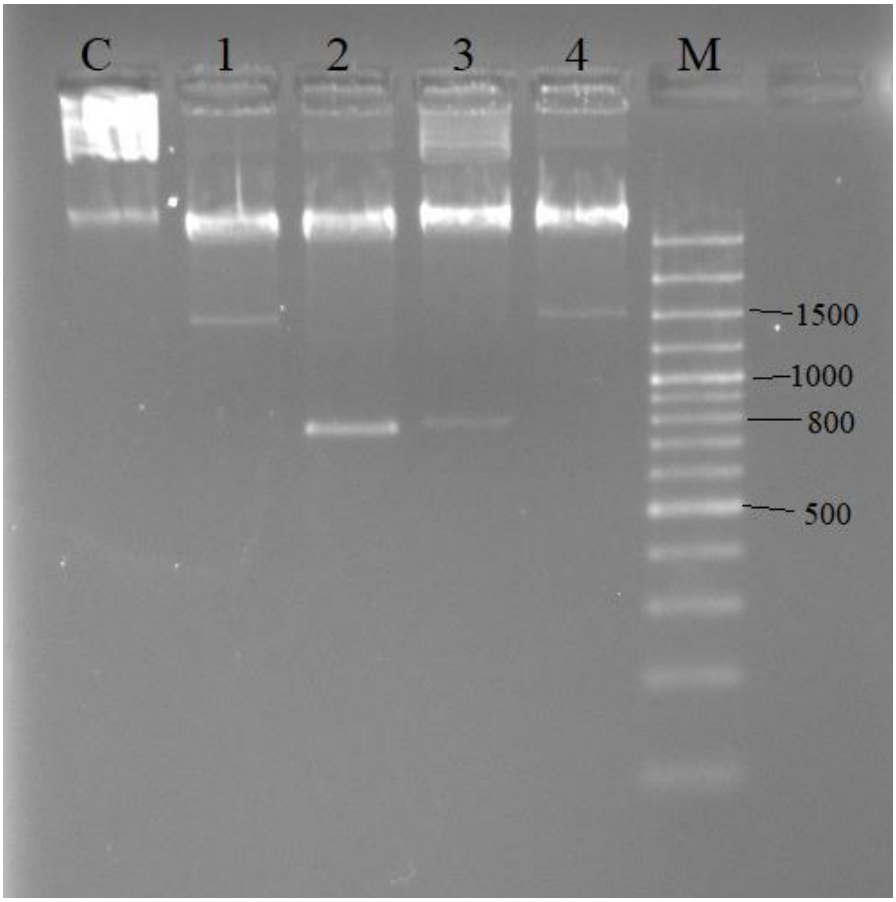

Figure 6. Plasmid pSC-A-5'UTR_CpCDPK1-nptII-YFP-3'UTR_CpCDPK1 analyzed by enzyme digestion and gel electrophoresis. Agarose concentration: 1.5%. Lane 1-4 represent the products of cutting by different pairs of restriction enzymes. 1: NdeI and AatII; 2: AatII and NheI; 3: NheI and AvrII; 4: AvrII and MluI. Lane M is for marker and C for uncut plasmid as control.

4.1.2 Electroporation protocol and *in vitro* analysis

In order to determine the optimal condition for electroporation, the reporter plasmid pCpact5'mcherryEtact3' was used. Transfection was found effective with the voltage range of 2500 - 3000 v and the pulse duration of 0.8 - 1 ms by Gene Pulser Xcell™ (Bio-rad, Hercules) (Fig. 7). Positively transfected parasites at intracellular stages were detected in MDBK cell culture after 48 h p.i. by IFA. However, when using ECM 830 square wave electroporator (BTX, Holliston), no transfected parasites were detected.

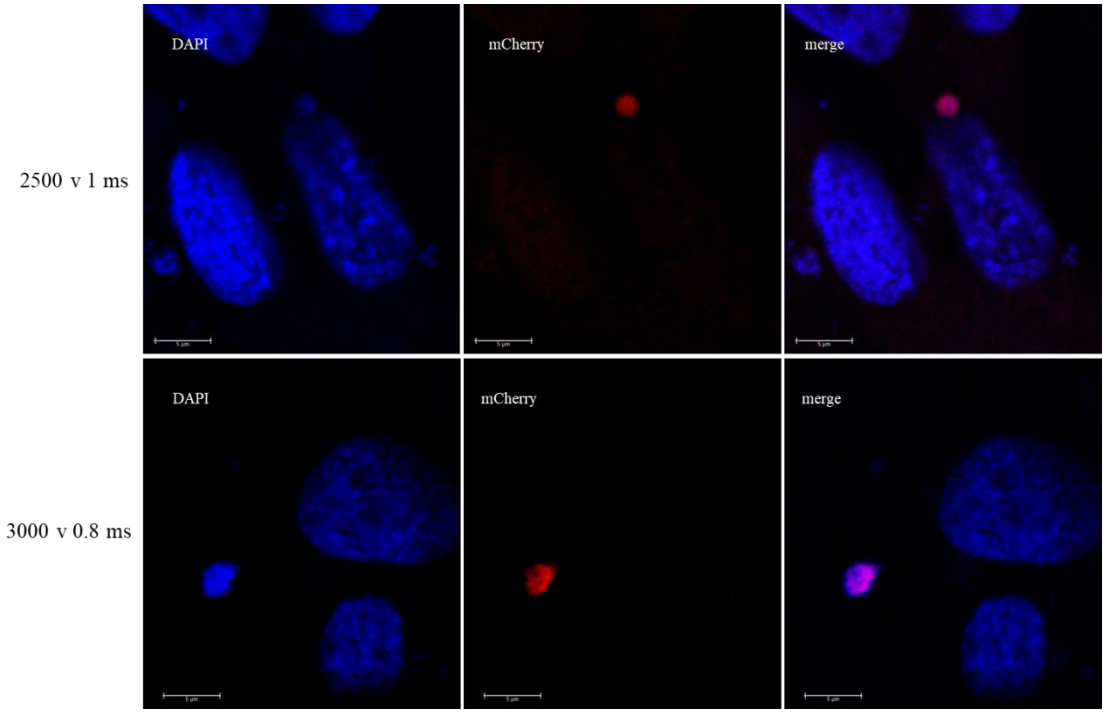

Figure 7. IFA of *C. parvum* electroporated with actin-mCherry plasmid pCpact5'mcherryEtact3' obtained with the decay wave electroporater Gene Pulser Xcell™. Scale bar length: 5 µm.

In order to knockout the CDPK1 gene, the reporter plasmid pCpact5'mcherryEtact3' was replaced by plasmid pSC-A-5'UTR_CpCDPK1-nptII-YFP-3'UTR_CpCDPK1 and the restriction enzyme Sap I was replaced by Nde I to linearize the plasmid in the subsequent electroporation. After incubation for 48 h post-infection, the culture was stained by DAPI and Sporo-glo. Untransfected *C. parvum* were detected meanwhile no transfected parasites could be spotted for any electroporation setup (Fig. 8).

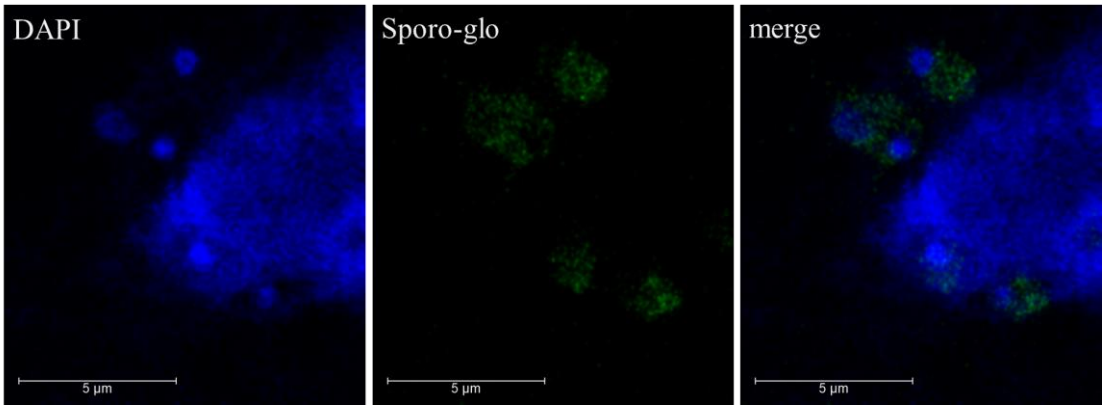

Figure 8. IFA of electroporation of *C. parvum* sporozoites with plasmid pSC-A-5'UTR_CpCDPK1-nptII-YFP-3'UTR_CpCDPK1. Scale bar length: 5 µm.

Because the use of REMI for the generation of CDPK1 K/O parasite line was unsuccessful I wondered whether this might be due to the method or reflect that CDPK1 gene was essential, making it impossible to generate a transgenic K/O line. I decided to attempt the knockout of CDPK1 using the more efficient and recently introduced CRISPR/Cas 9 technology (VINAYAK et al. 2015; PAWLOWIC et al. 2017).

4.2 CDPK1 knockout by CRISPR/Cas 9-mediated gene editing

In the CRISPR/Cas 9 based approach to silence CpCDPK1 the strategy starts with the cleavage of the CpCDPK1 gene in the *C. parvum*'s genome with the gRNA-oriented nuclease cas 9 to generate a double strand break (DSB). When DSB occurs, *C. parvum* will activate a repairing pathway to fix the DNA lesion, through homology directed repair (HDR). A cassette bearing sequences homologous to both ends of the CpCDPK1 gene was introduced into the cell through transfection to repair the DSB thereby disrupting the target gene and introducing a reporter that consists of a Nano luciferase gene and neomycin phosphotransferase gene (nptII). As nptII gene confers kanamycin, neomycin, geneticin, and paromomycin resistance to cells, successfully transfected parasites were selected by paromomycin (Fig. 9).

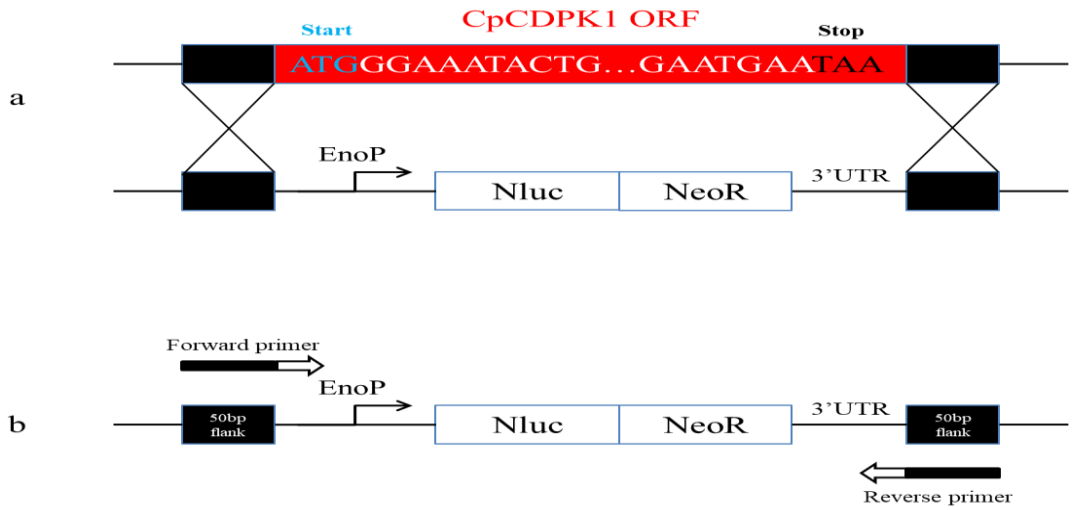

Figure 9. Genetic strategy to knock out CpCDPK1 using CRIPR/cas9 approach and the primers designing for repair cassette amplification. (a). Repair cassette containing enolase promoter (EnoP), nanoluciferase gene (Nluc) and neomycin resistance gene (NeoR) and supplemented at both ends with 50bp flanks (black) which are identical to the 5'UTR and 3'UTR of CpCDPK1. It was aimed to replace the CDPK1 open reading frame (CpCDPK1 ORF, red). (b) To amplify the repair cassette, the primers were designed with 22 bp long heads (arrowed bars) for the repair cassette and containing the 50 bp flanks (black).

4.2.1 Constructing CRISPR/Cas9_CpCDPK1_7 plasmid

A gRNA associated with CRISPR/cas 9 plasmid is essential in order to guide the enzyme function at the target gene locus. The gRNAs were designed using the online program EuPaGDT (http://grna.ctegd.uga.edu/). Out of 50 suggestions, 2 gRNAs (CpCDPK1_7 and CpCDPK1_181) with the length of 20 bp were selected for their high scores evaluated by the program based on multiple factors such as on-target efficiency, off-target rate, "GC" contents and so on. A manual "G" was added to the 5' end of the guides when it did not start with "G" for an appropriate transcription by the U6 promoter. Thus, two pairs of short oligonucleotides were designed. More specifically, they are forward primers with the same sequence of the guide and a reversed complement (Table 4). To the 5' end, an additional "GTTG" was added artificially to the forward primer and "AAAC" to the reverse primer to offer the gRNA compatibility to restriction enzyme site *Bbs*I which exists also in the plasmid. After annealing PCR, gRNAs were generated carrying *Bbs*I sticky overhangs at both ends.

In order to gain maximal HDR efficiency, the CpCDPK1_7 was used in further cloning because its targeting site on CDPK1 gene locates nearer to the start codon. Annealed gRNA (CpCDPK1_7) was inserted into plasmid p185 after restriction enzyme digestion and ligation. Colony PCR was applied with the gRNA screening primer and CpCDPK1_7 R. Since the binding loci of these two primers are 207 bp apart, bands on gel with the approximate size of 200 bp were considered positive and harvested for sequencing. The sequencing result confirmed that gRNA CpCDPK1_7 was inserted at the correct locus. Thus, plasmid CRISPR/cas 9 - CpCDPK1_7 was constructed (Fig. 10). This plasmid was ready to use in the subsequent transfection to disrupt the CpCDPK1 gene in the *C. parvum* genome.

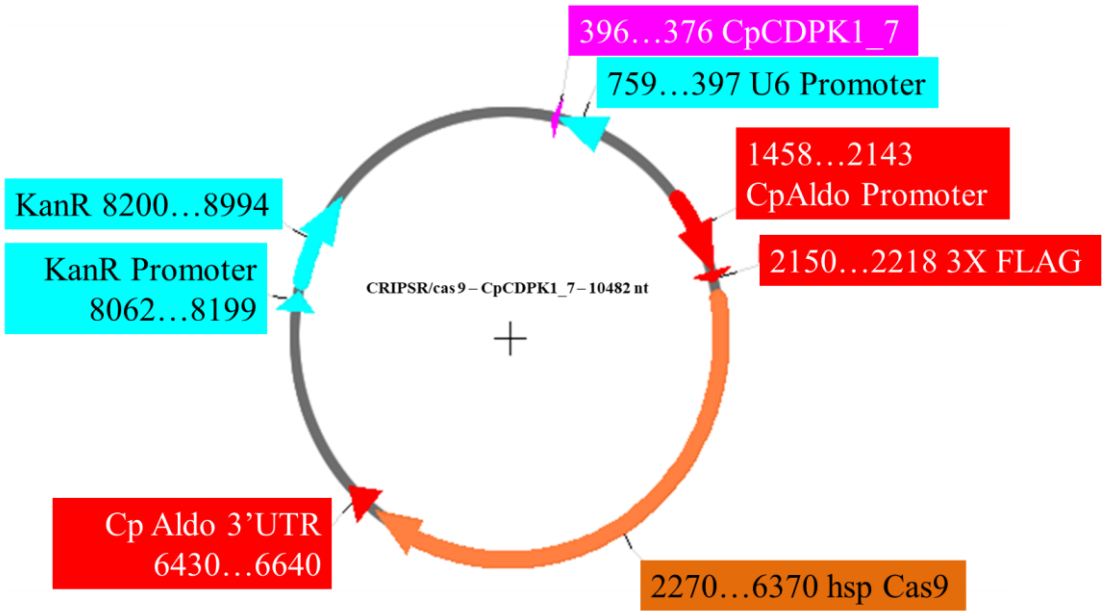

Figure 10. Schematic construction of plasmid CRIPSR/cas 9 – CpCDPK1_7. The restriction enzyme site BbsI was replaced by gRNA: CpCDPK1_7 through cloning.

4.2.2 Amplification of CDPK1 flanked repair cassette

The next step was to prepare the template for HDR which is the CDPK1 flanked repair cassette (Fig. 9). By TD PCR, the 1788 bp long repair cassette bearing 5'UTR_CDPK1, nanoluciferase, nptII and 3'UTR_CDPK1 was amplified and assessed by agarose gel electrophoresis (Fig. 11). Fragments were isolated from gel

and purified using GeneJET Gel Extraction Kit (Thermo Fisher Scientific, Waltham). The PCR product was verified by sequencing delivering identities of 100%. The repair cassette was then readily prepared in the flowing transfection step as an external repairing template to replace the endogenic CpCDPK1.

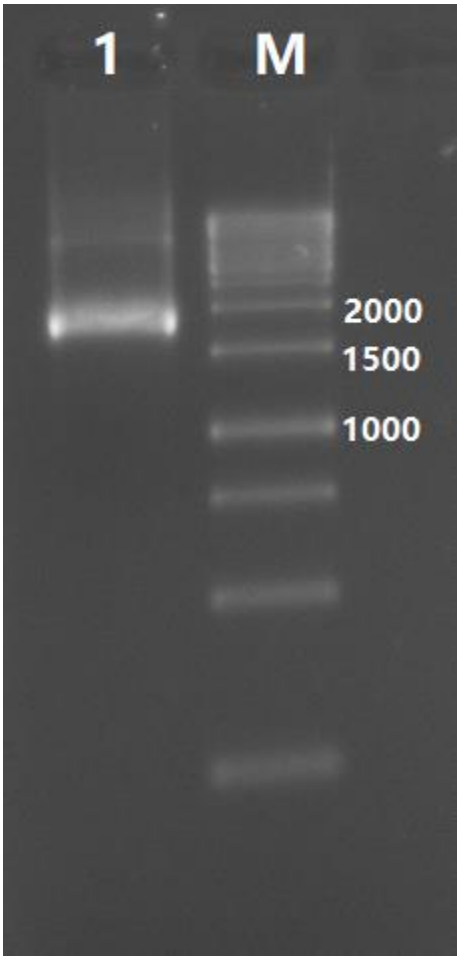

Figure 11. Gel electrophoresis of TD PCR products. 1: lane loaded with 5 µl of TD PCR products. M: lane loaded with GenerulerTM 1kb DNA Ladder (Thermo fischer, Waltham) as marker.

4.2.3 Knockout CDPK1 via CRISPR/cas 9

To understand the function of CpCDPK1, I tried to knockout this gene from the genome of *C. parvum* through two transfection methods, electroporation and CPP transfection.

4.2.3.1 Electroporation and *in vitro* analysis

Electroporation was performed using CRISPR/Cas9_CpCDPK1_7 plasmid and CDPK1 flanked repair cassette. The parameters of electroporation were applied almost the same as described previously (see 3.2.12.2) except the addition of

restriction enzyme. Transfected sporozoites were cultivated with HCT-8 cells and COLO-680 N cells for 24 h in presence of paromomycin. Through IFA, positive transfections including intracellular and extracellular parasites were detected in both cell lines (Fig. 12 and 13).

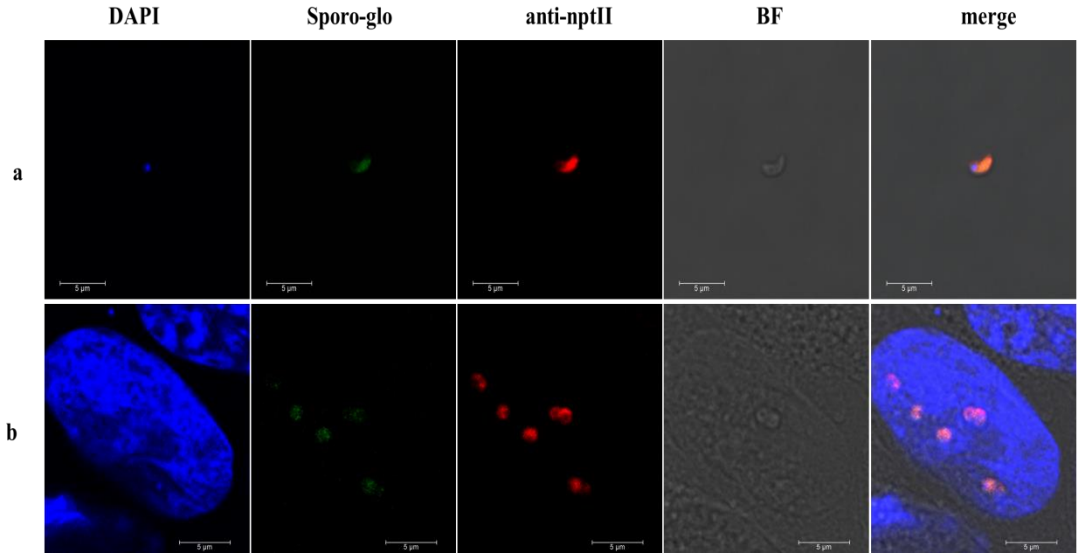

Figure 12. IFA of CpCDPK1 knockout *C. parvum* in HCT-8 cells by CRISPR/cas 9 and electroporation. Free sporozoites (a) and intra-cellular stages (b) were revealed. Sporo-glo was used for the detection of *C. parvum* and anti-nptII (Alex FluorTM 647) for the expression of nptII. Scale bar length: 5 µm.

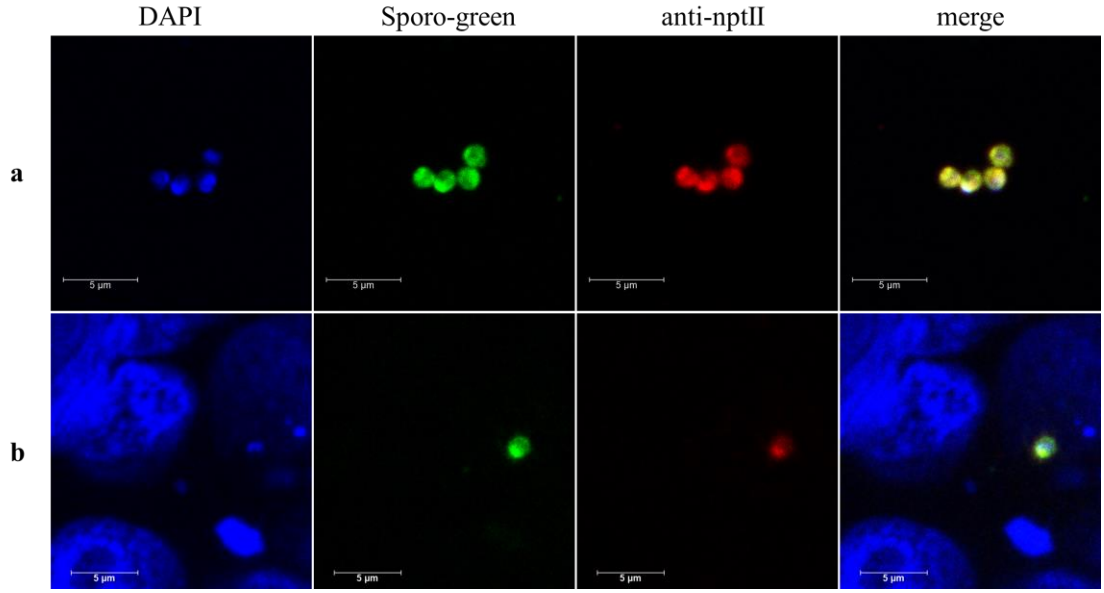

Figure 13. IFA of CpCDPK1 knockout *C. parvum* in COLO-680 N cells by CRISPR/cas 9 and electroporation. Free sporozoites (a) and intracellular stages (b) were revealed. Sporo-glo was used for the detection of *C. parvum* and

anti-nptII (Alex FluorTM 647) for the expression of nptII. Scale bar length: 5 µm.

4.2.3.2 CPP transfection and in vitro analysis

Due to the drawbacks of electroporation e.g. massive demands of DNA and unnecessary cell damage caused by electric pulses, cell-penetrating peptide (CPP) assisted-transfection served as an alternative without these disadvantages. CPPs are short positively charged peptides that were shown to be able to carry a wide range of cargoes including drugs, nucleic acids and proteins across nearly all known biological membranes (DERAKHSHANKHAH and JAFARI. 2018). The CPP applied in the present study was octaarginine. Like other CPPs, it is able to function as vector for intracellular delivery with limitied cytotoxicity and has been successfully applied in *Plasmodium* (SPARR et al. 2013).

CPP transfection was performed by using freshly excysted sporozoites and CPP complexed DNA as described in previous chapter (see 3.2.12.3). IFA results revealed that the transfection was successful (Fig. 14a), as well as in the electroporation control (Fig 13). The CPP transfected sporozoites were seeded into HCT-8 cells and incubated for 24 h prior to IFA. Positive transfection was detected (Fig. 15).

Since the COLO – 680 N cells were reported suitable to maintain *C .parvum* for long term and to allow the parasite to complete its lifecycle *in vitro*, the cells infected with transfected *C. parvum* were regarded as the 1^{st} generation of culture. Then, passage was applied every two weeks. IFA was performed for the $2^{nd,}$ $3^{rd,}$ 5^{th} and 6^{th} generation. Finally, immunostaining revealed that anti-nptII-positive parasites could be observed until generation 6 (Fig. 14b - e). These findings suggest that the transfection succeeded due to external paromomycin resistant gene was maintained over passages.

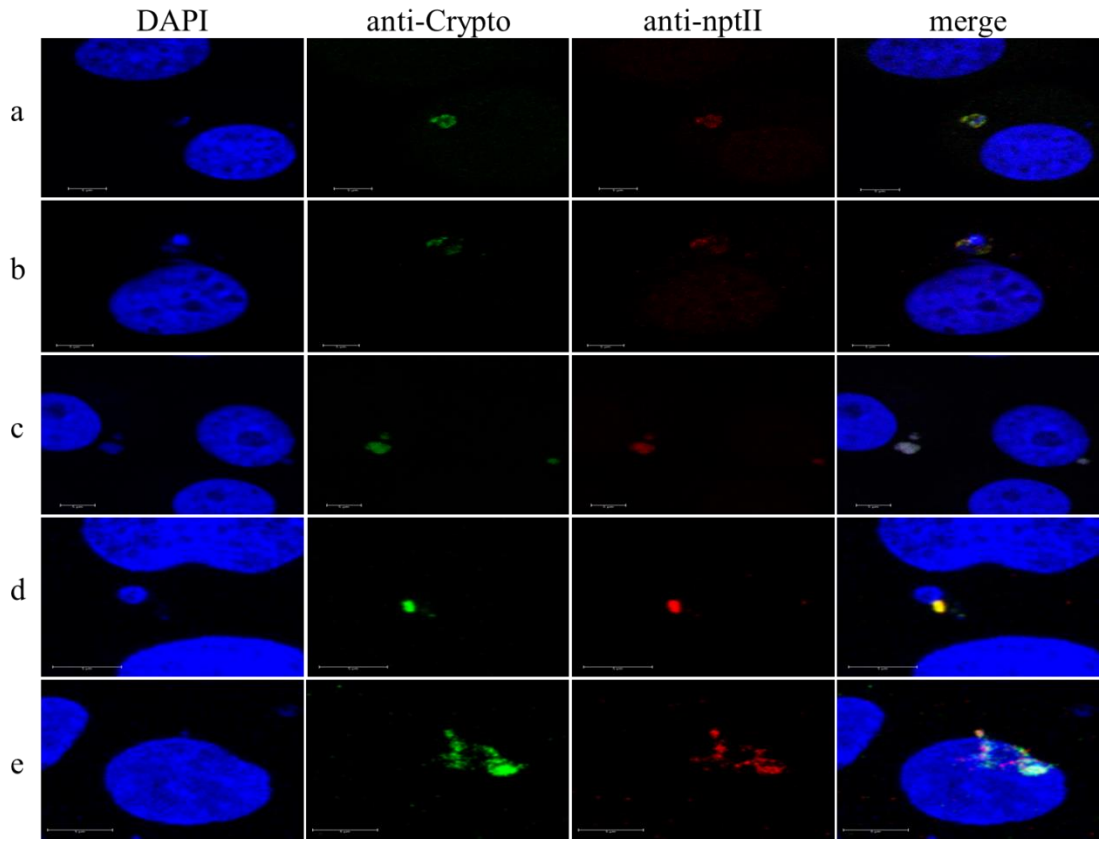

Figure 14. IFA of transfected *C. parvum* in COLO – 680 N cells by CPP transfection: generation 1 (a), 2 (b), 3 (c), 5 (d) and 6 (e). Anti-crypto (DylightTM 488) was used for the detection of *C. parvum* and anti-nptII (Alex FluorTM 647) for the expression of nptII. Scale bar length: 5 µm.

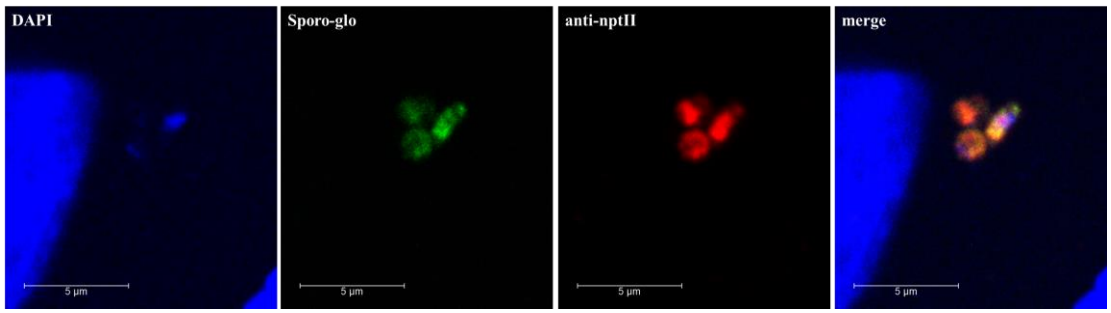

Figure 15. IFA of transfected *C. parvum* in HCT-8 cells by CRISPR/cas 9 and CPP transfection. Sporo-glo was used for the detection of *C. parvum* and anti-nptII (Alex FluorTM 647) for the expression of nptII. Scale bar length: 5 µm.

Despite the parasites could be detected after several passages, the population maintained at an extremely low level without any obvious change throughout the study.

4.2.3.3 Genetic assay of transfection

The transfection was also analyzed molecularly. HCT-8 cells were infected with 2 × 10^5 freshly excysted sporozoites of *C. parvum.* The culture medium was supplemented with 6 mg/ml paromomycin. The DNA was extracted from infected cells at various time points post-infection. Quantitative PCR revealed that transfected groups possessed nearly 4 fold more *C. parvum* DNA copies than the control infected with non-transfected parasites 24 h after infection. Moreover, the DNA copies of *C. parvum* in the transfection group kept increasing until day 3 and dropped slightly 2 days later (Fig. 16).

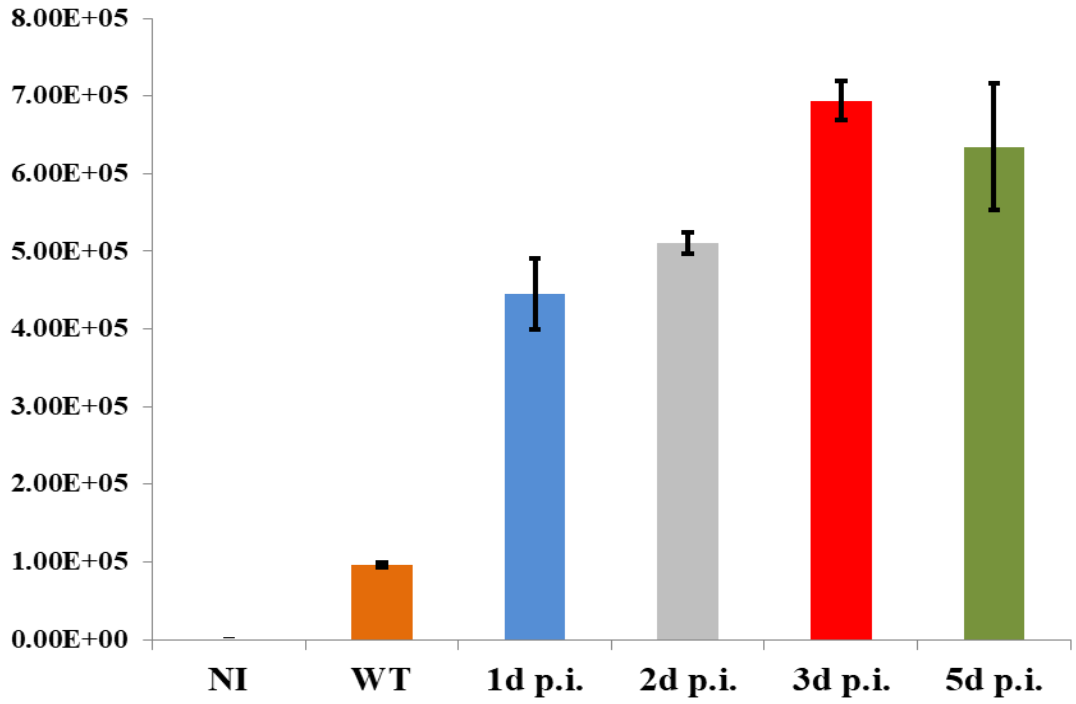

Figure 16. DNA copies of transfected *C. parvum* quantified by real time PCR at different time points after infection of HCT-8 cells. NI: non-infected cells; WT: Wild type (non-transfected) *C. parvum* (1d p.i.).

Conventional PCR was also performed to check the CDPK1 knockout. Several pairs of forward primers which bind with the 5'UTR of CDPK1 and the reverse primers bind with the Nluc-nptII repair cassette were designed. Attempts to amplify a fragment which overlaps the conjunction locus (genomic CDPK1 – repair cassette) with these primers and DNA extracted from cell cultures were made. However, no positive bands with expected size were detected on the agarose gel by electrophoresis.

4.3 *In vitro* and *in vivo* model for infection and propagation

Until now it has not been possible to develop an *in vitro* culture that enables a sexual reproduction of the parasite to generate large numbers of sporulated oocysts. So far, the only viable protocol to maintain transfected *C. parvum* requires the injection of freshly transfected sporozoites directly into the small intestine of a mouse. This is a very cumbersome and invasive procedure. Due to this problem the generation of transgenic parasites in order to study gene function remains a very challenging task.

For propagation of genetically modified organismns such as CDPK1 knockout *C. parvum in vitro* methods would be clearly preferable due to biosecurity and animal welfare issues. Thus I attempted to establish the COLO - 680 N cell line according to (MILLER et al. 2017) hoping that this might allow massive production of freshly sporulated (transfected) oocysts without using animal models.

4.3.1 *In vitro* model - *C. parvum* cultivation in COLO - 680 N cells

COLO - 680 N cell line was reported capable of effective propagation of *C. parvum in vitro*. Therefore, I infected the cells with *C. parvum* sporoziotes at the confluency of 70% - 80%. Parasites at intracellular stages were detected in the culture by IFA suggesting that the cell line is susceptible for *C. parvum* infection (Fig. 17).

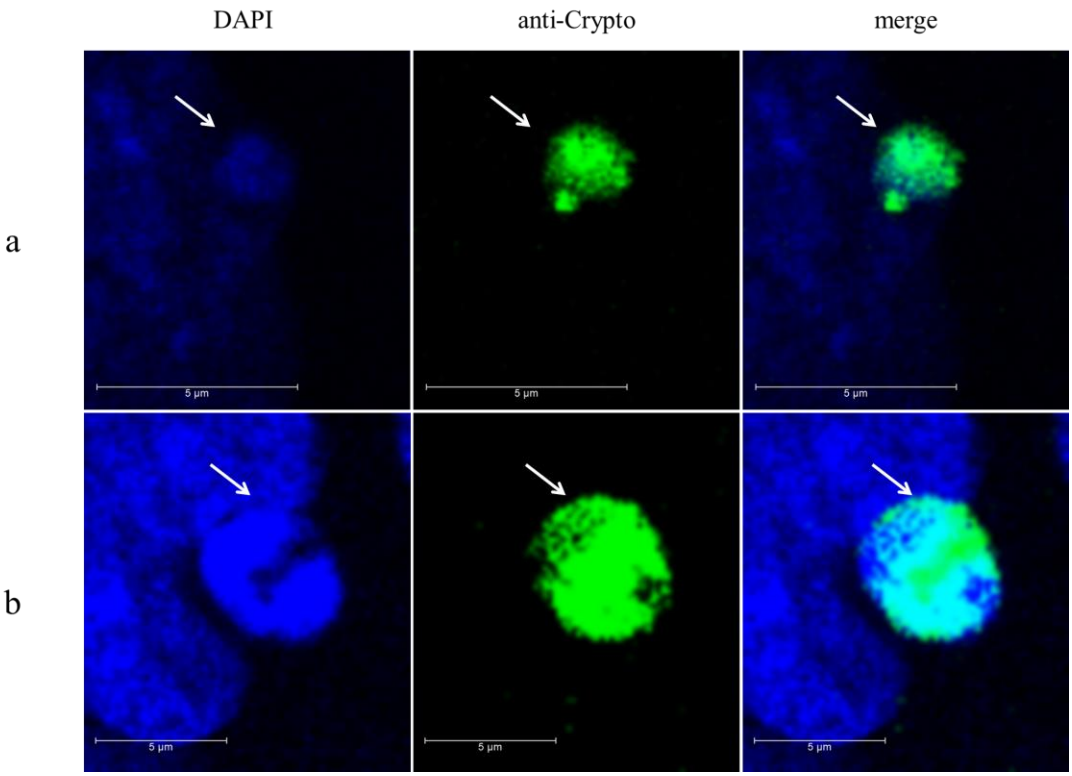

Figure 17. Intracellular stages of wild type *C. parvum* in COLO - 680 N cells. DAPI was used to stain the chromosome and anti-crypto (DylightTM 488) was used for the detection of *C. parvum*. Scale bar length: 5 µm.

The infected cells in 5 x T25 flasks were maintained for 8 weeks and the medium was changed once per week. Supernatant of all flasks were combined, however only 1 oocyst was observed. The harvested oocyst was stained by Crypto-a-glo (Waterbone, New Orleans) (Fig. 18). Moreover, no further oocysts were found in the other three repetitions. The poor efficiency and repeatability suggested the idea of continuous propagation of *C. parvum* in COLO – 680 N cell line was unrealistic.

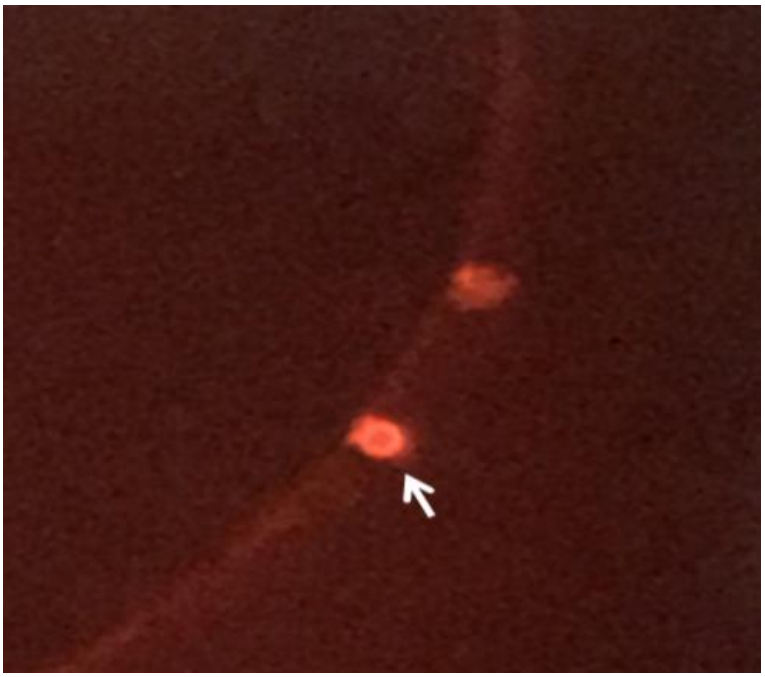

Figure 18. Oocyst harvested from supernatant of *C. parvum* infected COLO - 680 N cells. White arrow points at the oocyst. Magnification: 20 × 10.

4.3.2 *In vivo* model Infection pattern of *C. parvum* in RAGgc x IFN-g KO mice

As the COLO – 680 N cells could not serve as an *in vitro* model for the propagation of *C. parvum*, a trial in the RAGgc x IFN-g KO mouse was performed to evaluate its suitability for infection and propagation of *C. parvum*. Data of body weight, BSC and oocysts shedding were collected.

4.3.2.1 Clinical symptoms

As previously described in 3.2.11.2 and 3.2.14, experimental mice were orally infected with different doses of *C. parvum* oocysts and maintained until SD 21. Daily observation was performed to monitor the body weight and BCS.

Two mice in G2 displayed severe clinical symptoms of disease such as emaciation, rough fur and trembling. These mice died on SD 15 and SD 16, respectively. After SD 20, one mouse in G3 and three mice in G4 were found dead in the cage. Throughout the study, the survival percentage was 71.4 % (G2), 85.7 % (G3), 57.1 % (G4) and 100 % (G1) (Fig. 19).

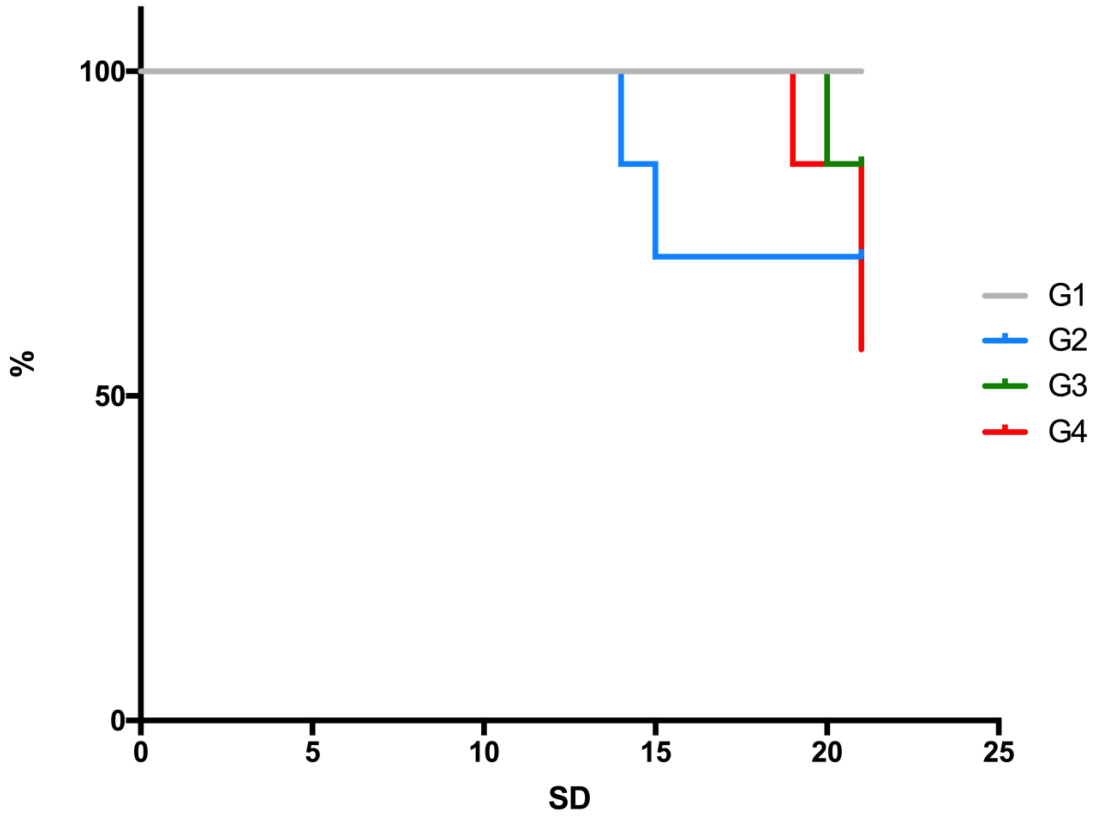

Figure 19. Survival percentage of crossbred KO mice (G2, G3, G4) and Balb/c (G1) orally infected with 500 (G2), 1000 (G3), or 5000 (G1, G4) oocysts of *C. parvum*.

Diminished responsiveness towards external stimulation was only observed in moribund mice within 24 h before death. Abnormal fur roughness was firstly recorded in three mice of G4 on SD 6, followed by three mice of G2 and four mice of G3 on SD 10. Until the termination of the experiment, abnormal fur roughness became successively obvious in all animals of the three groups of KO mice (G2, G3, and G4), whereas this was not seen in any of the infected BALB/c mice of G1.

The body weight of mice of G3 and G4 remained unaffected ($P \geq 0.05$) until SD 9, and for G2 until SD 10 ($P \geq 0.05$). Thereafter, rapid emaciation was observed in all KO groups (G2, G3, and G4). The decrease in body weight became statistically significant on SD 10 ($P < 0.05$) in groups G3 and G4 and on SD 11 in group G2 ($P < 0.05$). In groups G2 and G4, body weights appeared to increase again, at least temporarily, after SD 14 (G2) or SD 19 (G4). No such recovery was seen in group G3. In contrast, immunocompetent BALB/c mice (G1) did not experience any relevant

growth retardation and displayed a continuous increase in average body weight over the study period with only temporary fall-backs on SD 4 and SD 7. Moreover, the weight became significantly higher than the initial value first on SD 3 and thereafter from SD 5 onwards (Fig 20).

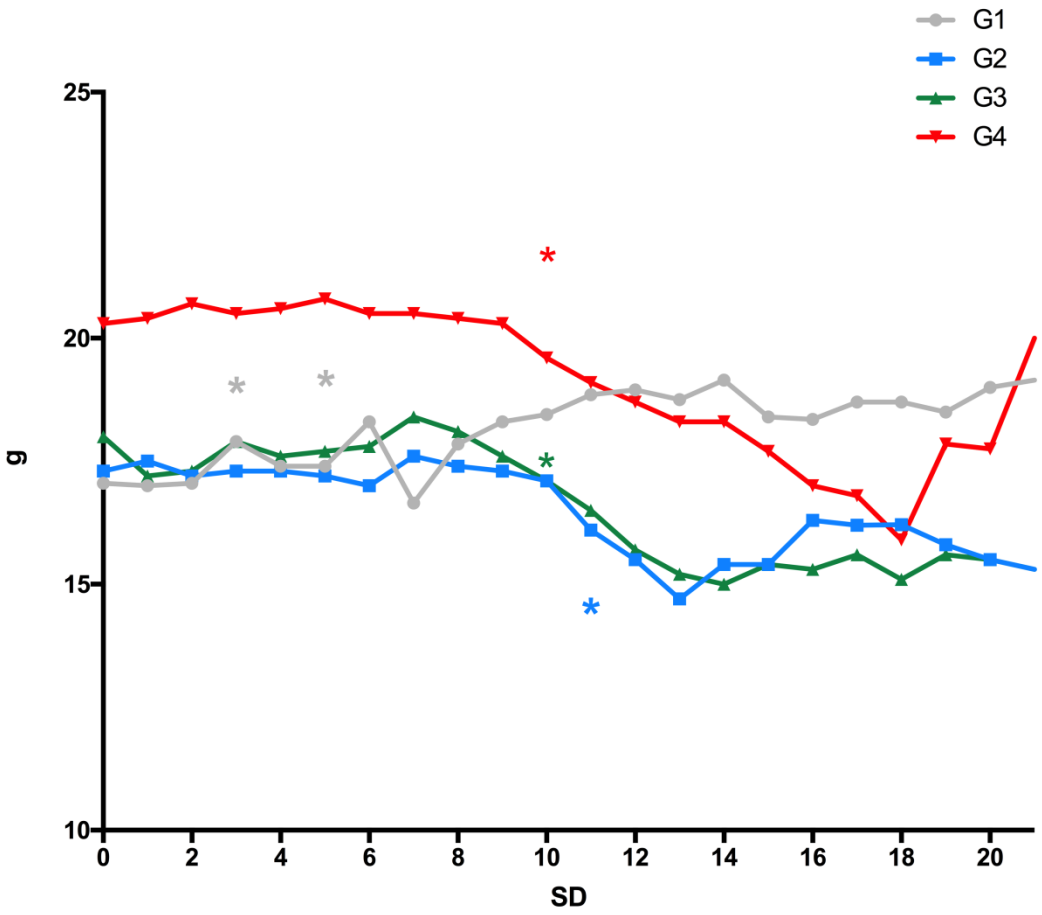

Figure 20. Mean body weights of crossbred KO mice (G2, G3, G4) and Balb/c mice (G1) following infection with 500 (G2), 1000 (G3), or 5000 (G1, G4) oocysts of *C. parvum*.* presents for the study day when statistical significance in body weight firstly showed.

Body temperature of G1 mice oscillated between 37.3 ℃ and 38.5 ℃, and no overall increase or decrease was observed. In contrast, body temperature tended to decrease in crossbred KO mice of groups G2, G3, and G4 and this trend became particularly obvious in comparison to G1 from SD 11 onwards. However, no statistically significant group difference was observed on any day over the study period (Fig. 21).

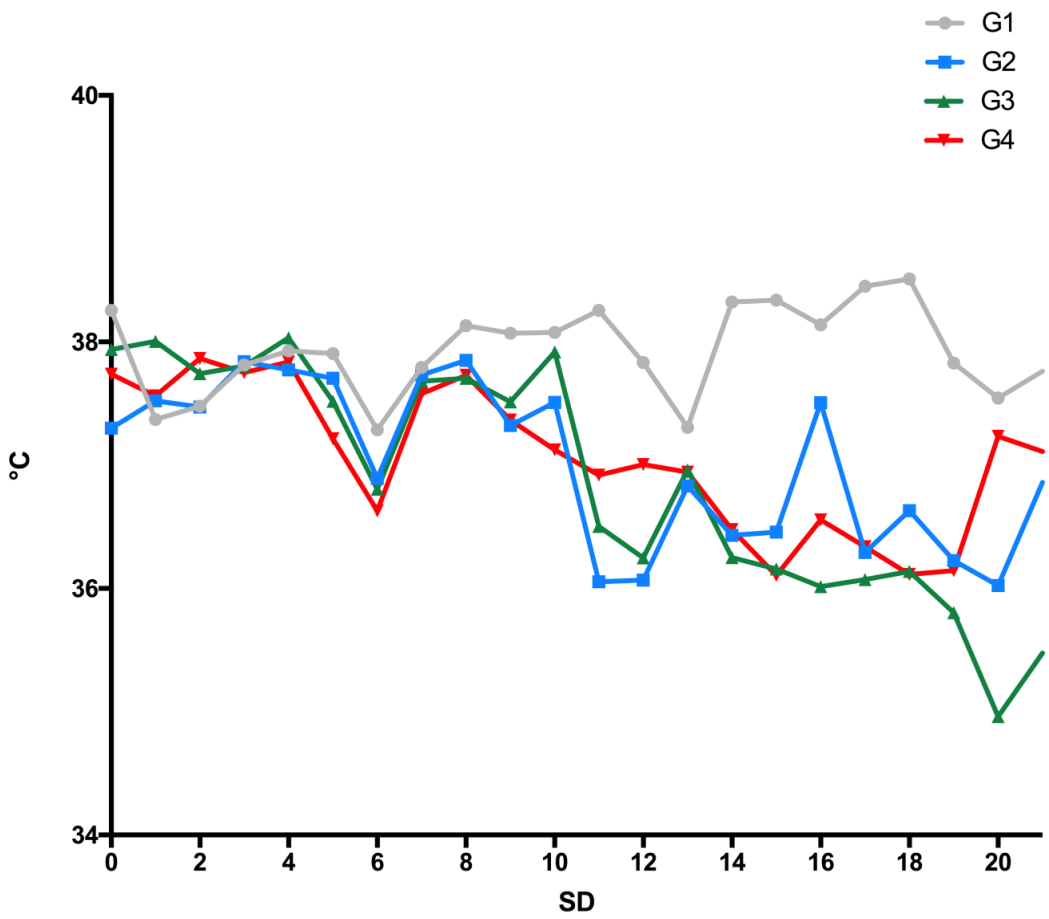

Figure 21. Average body temperature of crossbred KO mice (G2, G3, G4) and Balb/c mice (G1) over the study period (SD = study day) following infection with 500 (G2), 1000 (G3), or 5000 (G1, G4) oocysts of C. parvum on SD 0

4.3.2.2 Oocysts excretion

The oocysts excretion was investigated by qPCR and OPG was calculated as described in 3.2.16. In order to evaluate whether Cp_hsp 70 copy numbers obtained by qPCR can suitably reflect OPG, 10^2 - 10^7 of oocysts were used to spike mouse faeces and estimated by the same method. Mean OPG numbers calculated on this basis were above 90 % of expected values except for the samples spiked with 10^5 oocysts per 100 mg where detection efficacy was somewhat lower with 87.5% (Table 16). Regression analysis confirmed that calculated OPG numbers closely correlated to the expected OPG with R^2 = 99.83% (Fig. 22). Altogether, OPG determination from DNA copies appeared reasonably suited to assess excretion patterns of *C. parvum* infected mice.

Table 16. Evaluation of efficacy of quantification of oocysts in faecal samples by qPCR

Spiked OPG	Detected DNA copies	Calculated OPG (Mean)	Efficacy
1.00E+03	4.49E+01	1.12E+03	112.33%
1.00E+04	3.67E+02	9.18E+03	91.75%
1.00E+05	3.50E+03	8.75E+04	87.50%
1.00E+06	4.25E+04	1.06E+06	106.25%
1.00E+07	3.68E+05	9.20E+06	92.00%
1.00E+08	3.98E+06	9.95E+07	99.50%

100 mg faeces were spiked with *C. parvum* oocysts in a range of 10^2 - 10^7. Thus, spiked OPG ranged from 10^3 -10^8. DNA was extracted from the spiked samples and qPCR targeting Cp_hsp70 was performed. OPG were calculated from DNA copies of the Cp_hsp70 gene (formula: see 3.2.17); Efficacy = Calculated OPG ÷ Spiked OPG × 100%.

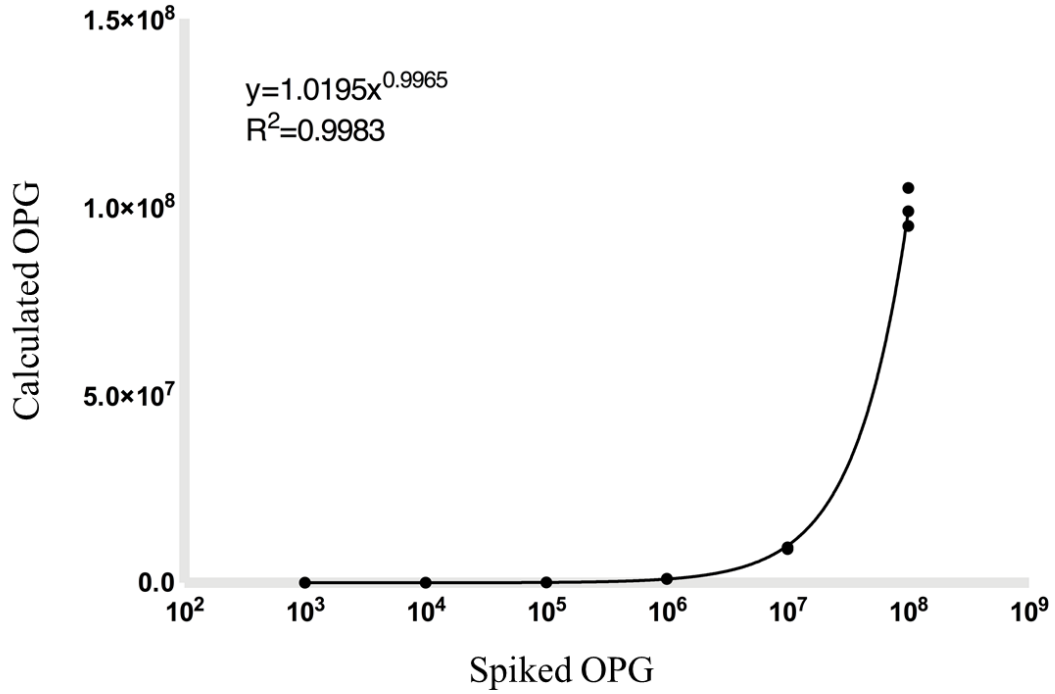

Figure 22. Correlation between OPG calculated from qPCR data and numbers of oocysts used to spike faecal samples. Power regression was applied to analyse the goodness-of-fit between Caculated OPG Spiked OPG, R2 indicates the coefficient of determination (X axis :logarithmic scale).

KO mice inoculated with 5000 *C. parvum* oocysts per mouse (G4) delivered positive PCR signals as early as SD 1 whereas those infected with 1000 (G3) or 500 (G2) oocysts became positive at SD 2 at the earliest (Fig. 23). OPG increased in all groups of KO mice (G2, G3, G4) rapidly and significantly compared to the amount during the first day of oocyst excretion ($P < 0.05$) and peak excretion was recorded on SD 10 (G2, G4) or SD 12 (G3). Oocyst shedding remained at a high level of $>10^8$ OPG afterwards with little variation. The three groups of KO mice (G2, G3, G4) did not differ remarkably in OPG over the whole experimental period and particularly after peak excretion ($P > 0.05$).

In the control group (G1), oocysts were detected in faecal samples at the earliest on SD 2. OPG increased slightly but steadily over the study period, however, values remained significantly lower than in the KO groups (G2, G3, G4; $P < 0.05$) from SD 6 onwards and always remained lower than 10^5 OPG.

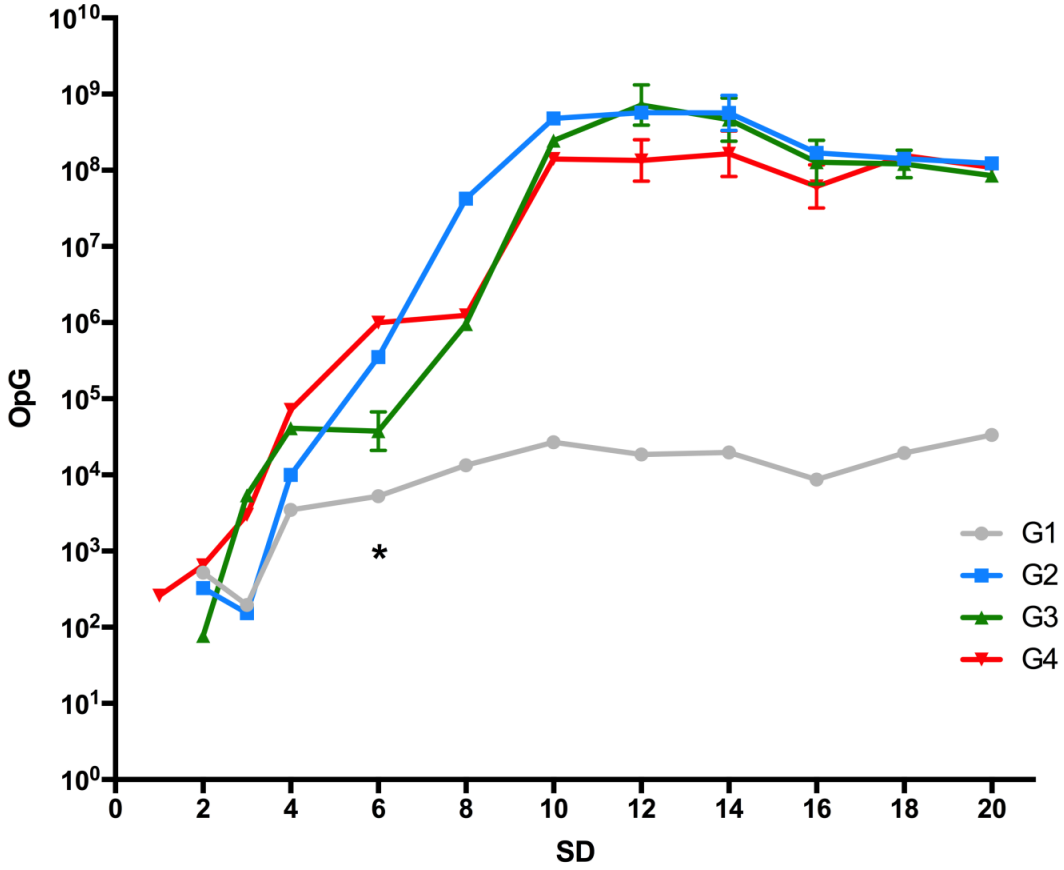

Figure 23. Average OPG of calculated from faeces based on qPCR data. Immunocompetent (BALB/c, G1) or immunodeficient KO mice (G2, G3, G4) infected with a dose of 500 (G2), 1000 (G3) or 5000 (G1, G4) oocysts of *C. parvum* at study day (SD) 0 (y axis: logarithmic scale). *

4.4 *In vitro* inhibition of CDPK1

As the generation of CpCDPK1 KO strain faced unforeseen difficulties, the functional study was reoriented from using genetic modification to chemical inhibition.

To understand the role that CDPK1 gene plays in the invasion processes, I decided to investigate its influence on host actin remodeling. MDBK cells were applied because these cells assemble as monolayer in culture in a way that makes them superior to HCT-8 cells when being observed by microscopy. First, MDBK cells were transfected with plasmid pCAG-mGFP-Actin by electroporation as described in 3.2.12.1. Then, the cells were infected by *C.parvum* treated or non-treated with CDPK1 inhibitor. The host cell actin remodeling was analyzed by immunofluorescent microscopy.

4.4.1 Generating bAct-GFP-MDBK cells

The optimal electroporation conditions for MDBK cells were determined. At least 55 μg pCAG-mGFP-Actin plasmid were applied to 5×10^6 suspended MDBK cells in the complete cytomix buffer with the total volume of 500 μl. Five pulses were applied by ECM 830 square wave electroporator (BTX, Holliston), with the voltage of 900 V and the duration of 990 μs. Efficiency of transfection reached approximately 20%, which turned out to be the highest among all trials. The MDBK cells started to express GFP 24 h post electroporation (Fig. 24a). However, the percentage of GFP positive MDBK cells decreased during cultivation due to the overgrowth by untransfected cells. Therefore, the transfected cells were isolated with a micropipette and seeded into a new petri dish. Geneticin (G418) was added as selection drug with the working concentration of 250 μg/ml. After 10 days cultivation, the percentage of GFP-MDBK cells gradually achieved 100% (Fig. 24b and 24c). Once the cells reached confluency, they were trypsinized and sorted by FACS according to fluorescent intensity. Cells that strongly expressed GFP were seeded in a separate petri dish and confocal fluorescent microscopy was applied. Beta-actin filaments could be clearly observed (Figure 25).

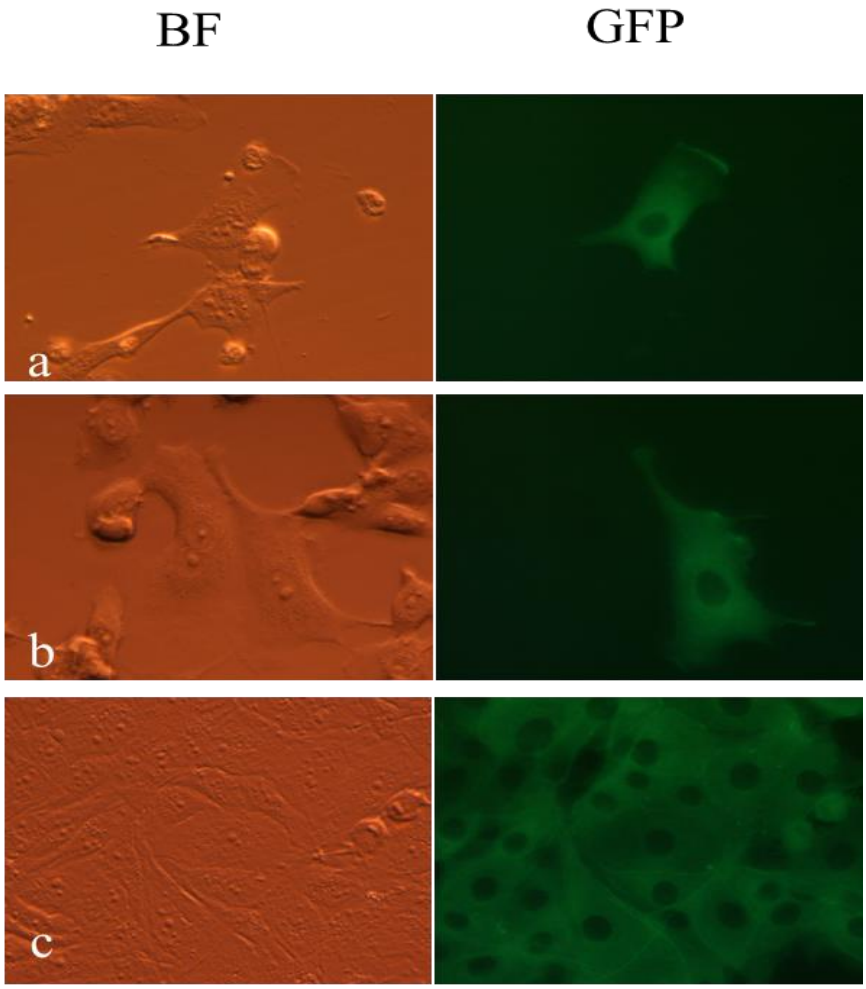

Figure 24. Transfected bAct-GFP-MDBK cells. All images were taken with the magnification of 400 times. BF: Bright field. GFP: Fluorescence microscope with FITC filter to detect GFP expression. a: 24 h after electroporation; b: 24 h after passage; c: 10 days after passage. Magnification: 10 × 40.

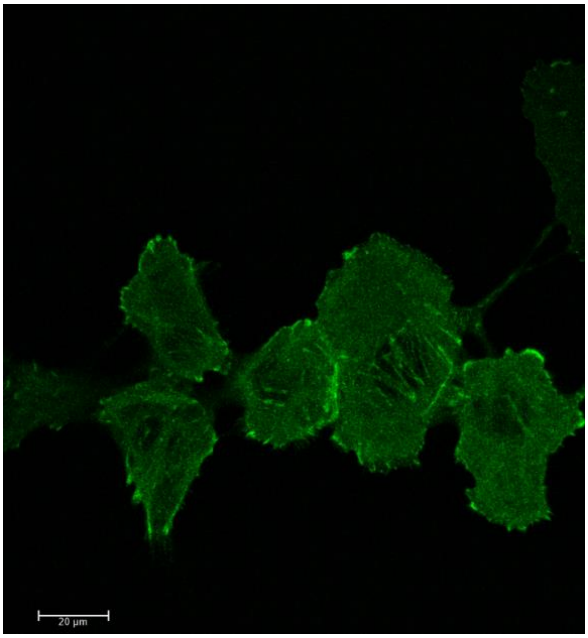

Figure 25. CLSM of bAct-GFP-MDBK cells at 24 h after sorting through FACS. GFP expressed in the actin filaments was detected by photomultiplier (PMT) detector. Scale bar length: 20 µm.

Next, the purified bAct-GFP-MDBK cells were harvested and stored in 2 ml Cryo-vials tube (Carl Roth, Karsruhe) containing 50% DMSO-growth medium in liquid nitrogen. After 4 weeks, the cells were recovered from cryopreservation and cultivated in growth medium for 10 days. The cells were confirmed to be able to express GFP after cryopreservation and recovery for at least 4 weeks (Fig. 26).

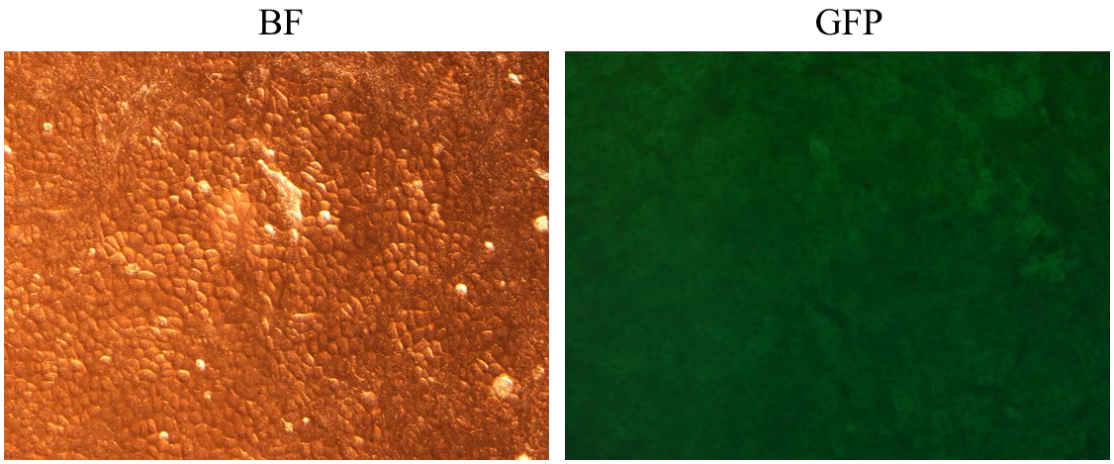

Figure 26. The bAct-GFP-MDBK cells recoverd after cryopreservation. Confluence of 100% was achieved after 10 d. BF: bright filed. GFP: Fluorescence microscope with FITC filter to detect GFP expression. Magnification: 10 × 10.

4.4.2 Influence of CDPK1 inhibition on infection

The bumped kinase inhibitor of CDPK1, compound 1294, was added to growth medium of MDBK cell cultures (0.1 µM). IFA was applied at 24, 48 and 72 h p.i.. Increased intensity of GFP signals indicating accumulation of host cell actin was found at the location of parasites of intracellular stages (Fig 27). This is an essential phenomenon at the early stage of PV formation (ELLIOTT and CLARK 2000). However, such features did not display in cultures supplemented with 500 nM 1294 at 24 h p.i. and 48 h p.i. (Fig 28a and 28b). Accumulation of host actin was observed at 72 h, but not typically shaped as displayed in the controls (Fig 28c). Moreover, free sporoziotes were found localized apart from the host cells 24 h after infection (Fig. 29). In addition, a meront which was localized beneath the monolayer of host cells was firstly detected at 72 h p.i. indicating the impairing of development and translocation (Fig 30).

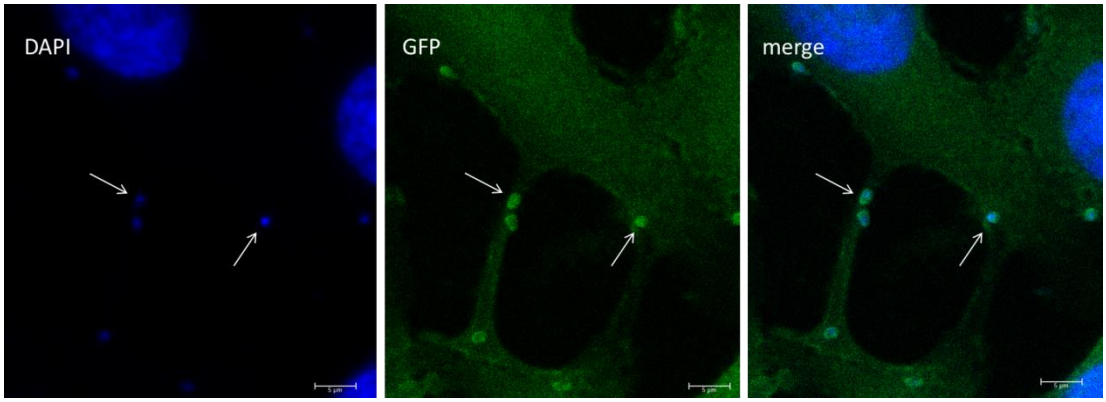

Figure 27. bAct-GFP-MDBK cells infected with untreated *C. parvum* 12 h after infection. The white arrows point at the parasites Host cell actin was accumulated at the site of parasite-host cell interfaces. Scale bar length: 5 µm.

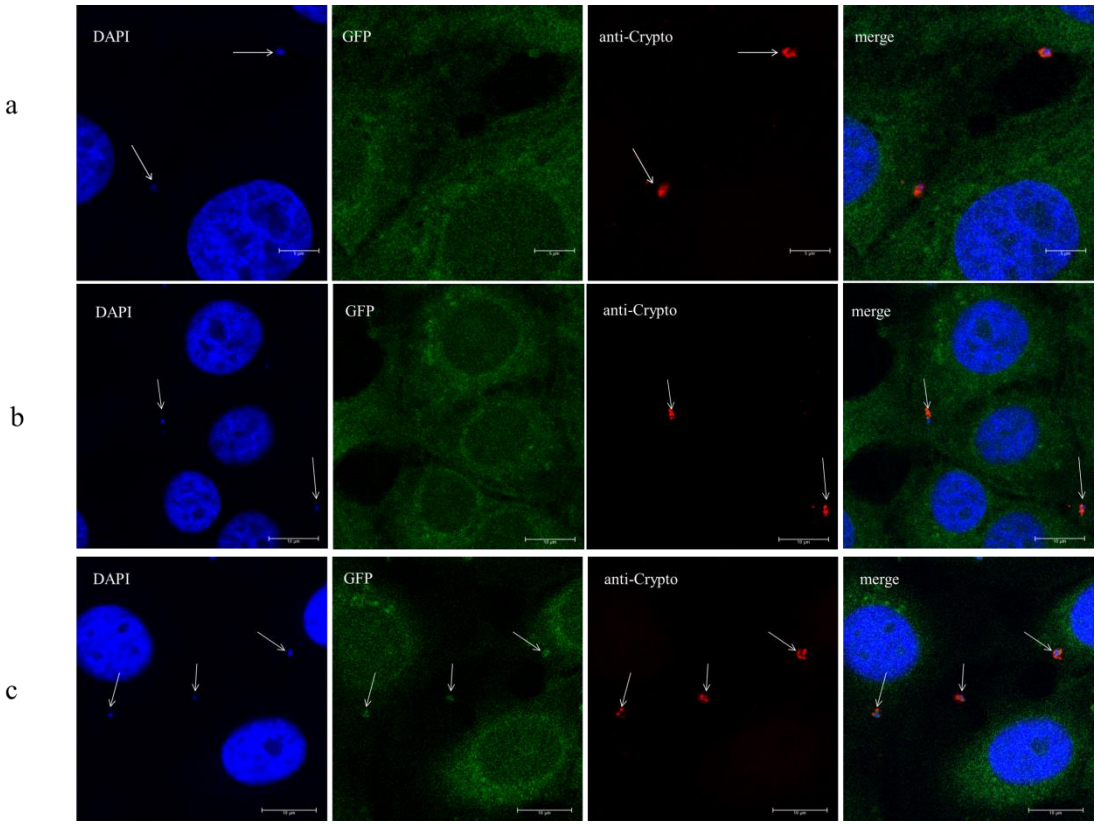

Figure 28. bAct-GFP-MDBK cells infected with 1294 treated *C. parvum* at 24 h (a), 48 h (b) and 72 h (c) p.i.. Anti-crypto (Dylight 647) with red fluorescent signal was used to specifically detect *C. parvum*. White arrows point at the parasites. Scale bar length: 5 µm.

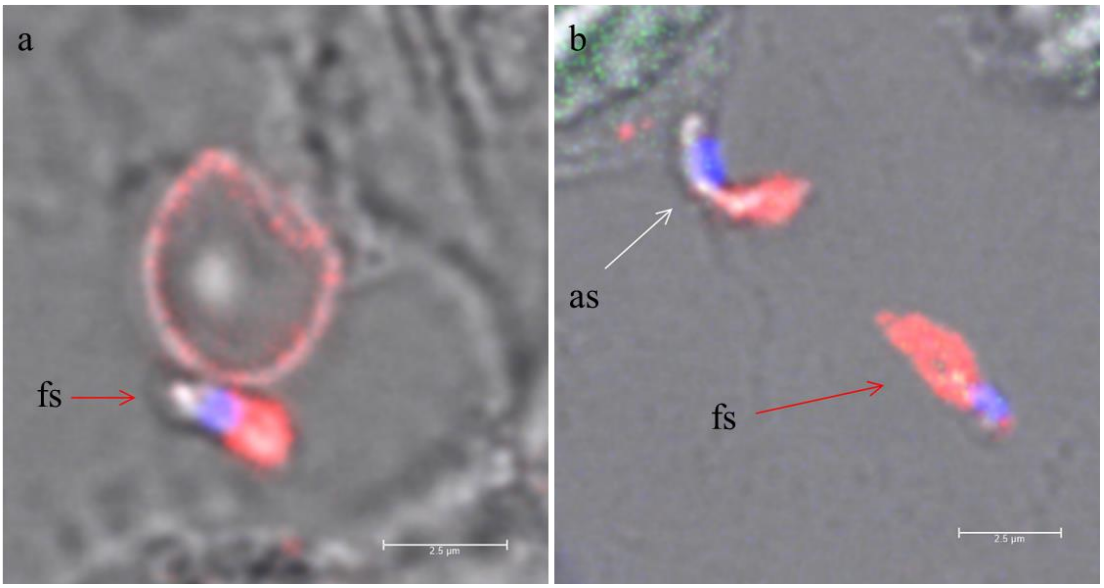

Figure 29. Free *C. parvm* sporozoites in the culture complemented with 1294 at 24 h p.i.. Phase contrast channel was applied along with DAPI, GFP and Dylight 647 merged. fs: free sporozoites; as: attached sporozoites. Scale bar length: 2.5 µm.

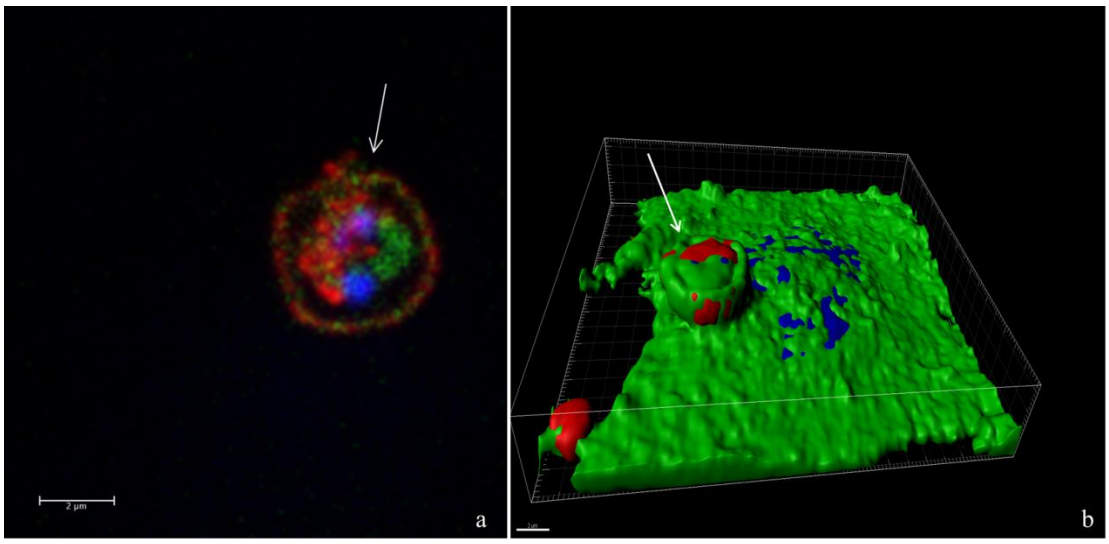

Figure 30. *C. parvum* meront localized beneath the host cell in the culture supplemented with 1294 at 72 h p.i.. (a) Single layer image of meront with merged fluorescent channels including blue (DAPI), green (GFP) and red (Dylight 647). (b) 3D model constructed by Imaris (Bitplane, Zurich). White arrows point at the meront. Scale bar length: 2 µm.

5. Discussion

5.1 Sub-cloning

As demonstrated in the current study, successful construction of recombinant plasmid pSC-A-5'UTR_CpCDPK1-nptII-YFP-3'UTR_CpCDPK1 which could be used to develop *C. parvum* CDPK1 knockouts was achieved. The four gene fragments were sequentially cloned in a mutual vector by using restriction enzymes and T4 ligase. This stepwise strategy mediated by specific double restriction endonucleases ensured the correct site and orientation of inserts. Moreover, since the chosen five enzymes generate sticky ends, the ligation is much more efficient than in case of blunt ends. The sub-cloning method was similar to the one applied by JANG et al. (2015) except for one step. I isolated the linearized DNA from the uncut plasmids by gel electrophoresis after each digestion. Self-ligation could thereby be avoided. Thus the risk of false positive transformation was decreased. However, an intrinsic drawback exists in the present strategy. During several repetitions of gel purification, the risk of DNA mutation may rise due to the exposure to UV light (GOODSELL 2001; PFEIFER et al. 2005). Therefore, the integrity of nucleotide sequence should be considered in further studies, and the cloning strategy may be modified to increase the efficiency and accuracy by using less time-consuming methods such as chain reaction cloning (CRC), hot fusion or One-Step Cloning (PACHUK et al. 2000; LIU et al. 2012; FU et al. 2014).

5.2 Inhibition of CpCDPK1 delays the host cell actin accumulation *in vitro*

The effect of CpCDPK1 on host cell actin accumulation during the invasion process was elucidated. For this purpose, I established the GFP-MDBK cells. To the best of my current knowledge, beta actin was targeted by GFP expression in MDBK cells for the first time. This model provides an easy and powerful tool to study morphological

changes of host cells related to actin remodeling. It was proven in the current study that GFP could be continuously expressed for more than two weeks without any signs of fading. The expression remained stable through passage and cryopreservation. Unlike conventional studies into actin, no specific fluorescent dye is needed due to the expression of GFP by the transfected cells which makes the assay more reliable and less prone to alteration related to additional staining procedures (ELLIOTT and CLARK 2000).

CDPK1 has been proposed as a promising drug target in apicomplexan parasites such as *Toxoplasma gondii*, *Neospora caninum*, *Theileria equi* and also, *C. parvum* (MURPHY et al. 2010; OJO et al. 2014; GIMENEZ et al. 2018). Inhibition of CpCDPK1 was reported to prevent both invasion and growth of *C. parvum in vitro* (CASTELLANOS-GONZALEZ et al. 2013; HUANG et al. 2017). However, KUHLENSCHIMDT et al. (2016) disagreed. They reported they tried to inhibit CpCDPK1 *in vitro* using various compounds. As a consequence, they found no correlation between the potent inhibition of CpCDPK1 and growth and cell invasion by *C. parvum*. *In vivo*, treatment with inhibitors appeared to be suited for control of cryptosporidiosis in calves (CASTELLANOS-GONZALEZ et al. 2013; LENDNER et al. 2015).

In the present study, the CpCDPK1 inhibitor compound 1294 was found to profoundly depress host cell actin accumulation *in vitro*. As the accumulation is an essential and characteristic process in *C. parvum* invasion (ELLIOTT and CLARK 2000; ELLIOTT et al. 2001), the invasion was also depressed. Cell invasion by *C. parvum* was fully completed in 24 h in the control group, and no free sporozoites were observed after this incubation period. In fact, the parasite might have finished the invasion much sooner, since it was reported that sporozoites may invade host cells within 30 s (FORNEY et al. 1999). The finding of free and invading sporozoites in inhibitor treated cell cultures at 24 h p.i. suggested that the invasion was rather delayed than completely prevented by supplementation of 1294.

Moreover, one meront was detected at 72 h after inoculation in the inhibitor treated cultures. This indicates that although the invasion and growth of *C. parvum* was impaired, development was not completely prevented. These findings are in contrast to the those of HUANG et al (2017).They conclude that the CDPK1 inhibitor can prevent the growth and proliferation of *C. parvum in vitro*.

Interestingly, the meront I found was initially regarded to be located extracellularly. Because its vertical location differed from the layer that most cells and other parasites were at with a distance larger than 5 μm. Extracellular development of *C. parvum* was reported in previous studies, however, in axenic cultures (HIJJAWI et al. 2004; ALDEYARBI and KARANIS 2016). When the respective picture was further processed by the 3D image analysis, this meront was also found embraced by host cell actin. Therefore, in the present experiment host cell actin was indeed utilized by *C. parvum* to form PV which is consistent to the results of previous studies (ELLIOTT and CLARK 2000; ELLIOTT et al. 2001; O'HARA et al. 2004). It remains an open question that needed to be investigated in further studies whether the inhibition of CpCDPK1 leads to the observed untypical translocation of the meront? If this is the case, does the translocation alter the activity or virulence of *C. parvum*?

Altogether, inhibition of host cell actin remodeling by the CpCDPK1 inhibitor 1294 did not completely block the invasion and growth of the parasite. However, invasion was reduced and consequently development of further parasitic stages was impaired. Genotypic variation between strains may also affect drug sensitivity (WIDMER 1998). Drug sensitivity of *Cryptosporidium spp.* is related to the particular parasitic site, the unique structure of the PV, and the parasite's ability to block drug influx. All of these features are determined by the genome (WIDMER et al. 1998; MEAD 2002). It appears possible that 1294 is well suited to impair invasion and development of particular strains such as the one used in my experiments (in house strain LE-08-Cp-08, GP60 subtype IIa A15G2RI) whereas other strains may react less

sensitive, like e.g. the Iowa strain (CASTELLANOS-GONZALEZ et al. 2013). Future study is needed evaluate this consideration.

5.3 RAGgc x IFN-gamma KO mice for *C. parvum* propagation

Although *in vitro* culture is applied to study *C. parvum* in many laboratories worldwide, oocyst formation is generally lacking or low in *in vitro* systems and thus propagation of *C. parvum* still depends on infected animals (RYAN and HIJJAWI 2015). Laboratory mice were found to be basically susceptible to *C. parvum* infection, however, reproduction is generally insufficient in immunocompetent adult mice. Neonatal mice were suggested to be better suited than adults due to the undeveloped immune system (MCDONALD et al. 2004; FILATOVA et al. 2018), however, they are difficult to handle and rather unsuitable for clinical studies. Several groups attempted to make adult mice more susceptible to *C. parvum* by various strategies including malnutrition or pharmacological induction of immunodeficiency (COSTA et al. 2012; GORLA et al. 2014; MEAD et al. 1991). Genetically induced immunodeficiency, particularly knock out of IFN gamma (GKO), appears to be a promising strategy to promote acute infection and increase oocyst production in laboratory rodents. However, prolonged watery diarrhea may not be seen in such models either (GRIFFITHS et al. 1998b). In general, immunodepressed mice display only moderate sensitivity to cryptosporidiosis while, GKO mice appear to be a more sensitive model due to the low infection dose needed to induce successful infection and massive production of oocysts.

Diarrhea as a typical symptom of cryptosporidiosis in the natural host is not observed in any mice model whereas other clinical signs and even mortality were recorded in our GKO model. The ideal laboratory infection model should fulfil the following demands: (1) high morbidity (2) low to moderate mortality (3) short prepatency (4) high oocyst yield (5) low infection dose. We evaluated crossbreds of two

immunodeficient parent mouse lines for fulfilment of these criteria under strictly controlled laboratory conditions.

Interleukin-2 receptor gamma chain KO (common gamma chain (gc) deficient) mice lack functional receptors for various cytokines. Consequently, the numbers of lymphocytes are greatly reduced. 350-fold reduction of NK cells and nearly 10-fold reduction of B and T cells were reported (DISANTO et al. 1995). Differentiation of B and T lymphocytes demands so-called V (D) J recombination which includes a series of complex reactions. RAG1 and RAG2 collaborate in events that are essential for initiation of V (D) J recombination (ROTH and CRAIG 1998; CHEN et al. 1993). Hence, the genetically induced deficiency in RAG2 reinforces the negative effect of gc deletion on lymphocyte differentiation as observed in RAGgc KO mice (MAZURIER et al. 2004).

NK cells and IFN-gamma play important roles in innate immunity against *C. parvum* as observed in experimentally infected RAG2 KO and RAGgc KO mice (MCDONALD et al. 2013). Severe clinical symptoms including weight loss, fur roughness, listlessness and mortality showed up in RAGgc KO mice. Similar patterns of chronic infection were seen in these two mouse strains for up to 91 days (BARAKAT et al. 2009). In our RAGgc x IFN-gamma KO crossbreds cryptosporidiosis appeared to be a more acute disease thus rather simulating the situation in the natural host. Mortality was seen from SD 15 onwards, and up to 6 of 21 mice died or had to be sacrificed. This is consistent to the report of GRIFFTHS et al. (1998) and may reflect that various types of lymphocytes and cytokines are involved in host defence, IFN-gamma plays the most pivotal role. In RAGgc x IFN-gamma KO mice no correlation was found between the infection dose and the course of the disease within the chosen range of oocysts applied. We therefore propose that even a dose as low as 500 oocysts per mice is sufficient and appropriate for production of large numbers of oocysts and to induce clinical signs of disease in this animal model.

NOVAK and STERLLING (1991) reported that wildtype mice older than 26 days were not susceptible to infection by *C. parvum*. McDONALD et al. (2013) inoculated BALB/c mice at the age of 8 to 12 weeks with 2×10^7 oocysts which resulted in an oocyst excretion peak 18 to 20 days after infection and full recovery in the following days. In our hands KO mice were very susceptible to infection even at an age of 6 weeks. The peaks of oocysts shedding showed up much sooner and remained high for nearly 10 days with limited shifting until the end of the study.

Positive PCR signals were recorded as early as SD1 or SD2. Since *C. parvum* is known to have a prepatent period of 4-5 days in mice, this may be explained by excretion of parasites that failed to infect intestinal cells or by detection of merozoite/meront DNA. We did not analyse this assumption, however, in the context of the study this aspect is not very relevant because the current studies were focused on the suitability of the crossbred KO model to yield high numbers of oocysts and observation of clinical symptoms and mortality in clinical studies. From the reported pattern and level of oocyst excretion and clinical observations we conclude that this KO animal model is very suited for laboratory scale studies and probably superior to previously reported mouse models.

The level of oocyst shedding as calculated from qPCR data and the pattern of excretion were rather uniform irrespective of the infection dose in the RAGgc x IFN-gamma KO groups. OPG remained at a constantly high level for almost 10 days once peak OPG were achieved. Probably this level of continuing high level parasite excretion is mainly due to permanent endogenous autoinfection by thin walled oocysts. In immunocompetent mice (G1) OPG were likewise recorded over the whole study period, albeit on a much lower level, confirming the relevance of an intact immune system and particularly of IFN to limit intestinal replication of the parasite.

GRIFFITHS et al. (1998) reported a peak of oocyst excretion that was 10^2 - 10^3 fold higher in GKO mice than in immunocompetent controls. In present study, the deletion of both RAGgc and IFN-gamma resulted in an even higher increase of parasite replication by > 10^4 fold as compared to Balb/C mice showing that combination of KO of at least two factors that contribute to intestinal immunity is a feasible strategy to optimise laboratory rodent models for cryptosporidiosis.

The crossbred KO mice used in the present study were clearly more susceptible to *C. parvum* than Balb/C both in terms of parasite replication and clinical disease, however, diarrhoea which is a typical symptom of *C. parvum* infection in e.g. neonate ruminants, was not observed. In immunocompetent adult mice *C. parvum* infection is generally not related to clinical symptoms at all while the crossbred KO mice displayed clinical signs of disease such as fur roughness and increased mortality.

In conclusion, this is to the best of my current knowledge the first report on RAGgc x IFN-gamma KO mice as a laboratory animal model for *C. parvum*. The model is well suited to propagate the parasite and to induce clinical disease accordingly. The lowest dose applied in this study of 500 oocysts per mouse appeared to exert the same effects as the tenfold dose and possibly even lower doses will result in sufficient multiplication of the parasite. This may be of interest not only for drug screening or pathogenesis research in general but particularly for scenarios where only a limited amount of oocysts is available for propagation, e.g. studies into field isolates or sub-genotypes or where research in the animal host is related to difficulties, e.g. studies into genetically modified *C. parvum*.

5.4 CpCDPK1 knockout by CRISPR/cas 9

Here, I demonstrated a method to knockout CpCDPK1 gene by using the technology of CRISPR/cas 9. Genomic modification of *C. parvum* by CRISPR/cas 9 has been firstly achieved by VINAYAK et al. (2015). This offered a powerful tool to overcome

hurdles in gene targeting or production of knockout organisms. Electroporation and surgical procedure were applied in their study. Different to their original protocol, I applied CPP for transfection and a COLO-680 N cell for propagation.

Instead of conventional PCR, TD-PCR was applied to overcome problems related to amplification of CpCDPK1 flanked repair cassette caused by the long tailed primers. This method was firstly reported by DON et al. (1991), and then became a popular solution to enhance the efficacy and sensitivity of the method. Through gradually decreasing the annealing temperature, it is possible to abrogate false binding and unspecific amplification (KORBIE and MATTICK 2008). In the current experiment, the primers were constructed with a short complementary region plus a long non-complementary tail. With the Tm higher than the projected melting point, only very specific base pairs between primers and template. Therefore, TD PCR enhanced the specificity of the initial primer-template duplex formation in the first 10 cycles which are the most critical phase of amplification in PCR. With subsequent shifting to lower Tm, more permissive binding occurred yielding more of the desired products (HECKER and ROUX 1996). Hence, mispriming or stochastic amplification in the later stage was effectively reduced due to the presence of specifically produced templates.

Electroporation is the most commonly used method for *Cryptosporidium* spp. transfection. Due to the impulse of high voltage to introduce external DNA into cells, it causes a considerable ratio of sporoziote lethality (SUAREZ et al. 2017; TETENS et al. 2017; POTTER and HELLER 2018). Meanwhile CPPs have gained much attention for their ability to translocate large molecules through plasma membrane with low cytotoxicity (MADANI et al. 2011).

Octaarginine was reported able to carry plasmid into NIH/3T3 cells (KHALIL et al. 2004) as well as to deliver chemotherapeutic agents into *Plasmodium* and *Mycobacterium* (SPARR et al. 2013). In the present study, I tested its ability to

transport plasmid and linearized DNA into sporozoites of *C. parvum*. PEI was added to the CPP-DNA complex to increase efficiency of gene delivery into sporozoites (JIANG et al. 2011).

Since no apparent difference in positive transfection efficiency was observed as compared with electroporation, it appears that octaarginine could be used as an alternative to electroporation, especially if no appropriate electroporation device is at hand. The presence of CpCDPK1 KO parasites in all subsequent passages supports the results found in the inhibition study. Elimination of CpCDPK1 activity impairs, however, does not completely block cell invasion and development.

It is remarkable that the amount of external DNA necessary for transfection by CPP is extremely lower than that needed for electroporation. As little as 5 μg DNA was able to initiate the transfection whereas at least 50 μg DNA was needed for electroporation which is only slightly higher than the amount of 10-30 μg reported in previous papers (VINAYAK et al. 2015; PAWLOWIC et al. 2017) and distinctly lower than the range of 100-200 μg reported by others (LI et al. 2009; TETENS et al. 2017). Thus, in consideration of DNA consumption, transfection mediated by octaarginine is clearly superior to electroporation.

It was proven by IFA that the transfection succeeded. In contrast, no PCR product of the genomic CDPK1 – repair cassette fragment was achieved in the following genetic assay. These might be due to the limited numbers of CDPK1 KO parasites. Because the nptII gene can also be expressed in the case of transient transfection caused by off-targets effect which is common in CRISPR/cas 9, the finding of paromomycin selected parasites does not guarantee successful knockout. Even though I tried to minimize the chance of off – target effect while designing gRNA, it appears not completely avoidable. Up to date, this side effect can only be controlled by the new technology, genome-wide CRISPR screening which needs to be carried out in further studies.

5.5 COLO-680 N cells are not suited to propagate *C. parvum in vitro*

Irrespective of the mode of inoculation efficient propagation of *C. parvum* relies on suitable animal models. In order to avoid the negative effect of stomach passage on sporozoites islolated from oocysts (FAYER et al. 1991), surgical inoculation of transfected sporoziotes was applied by VINAYAK et al. (2015). However, experimental infection of animals in general and highly invasive techniques such as surgery is in conflict with animal welfare considerations. Unfortunately, all attempts to continuously culture *C. parvum* in cell cultures, oraganoids or under axenic conditions have yielded only limited or no success in terms of permanent and reliable delivery of oocysts (YANG et al. 2015; VARUGHESE et al. 2014; PAZIEWSKA-HARRIS et al. 2016). COLO-680 N cells were reported to be a suitable tool for sustainable *in vitro* generation of oocysts (MILLER et al. 2018). In the current study, *C. parvum* were observed capable of developing into various stages in these cells suggesting that the cell line might support infection and development. Besides, in most of the previous studies the growth of *Cryptosporidium in vitro* was recorded to peak at 48-72 h after infection and then to gradually decline (FAYER and XIAO 2008). In contrast, COLO-680 N cells were able to maintain infection as long as 8 weeks without further sub-infection and intensive care. This observation suggests COLO-680 N might be a suitable cell platform to be used not only for infection, but also for transfection studies as well.

As shown in the results, the repair cassette was expressed from the first generation of the transfected *C. parvum* to the end of the study. However, the population of transfected parasites did not increase as rapid as the non-transfected ones. This might be attributed to the combined action of two factors, drug selection and silencing of CpCDPK1. The transfected parasites obtained drug resistance which supported them to survive the selection, however displayed reduced activities regarding cell invasion and further development in host cells. The relative low population of transfected

parasites suggests that the inhibition of CDPK1 impairs the invasion and growth of *C. parvum* on the other side.

Wild type sporozoites were inoculated into at least five T25 flasks seeded with COLO-680 N cells when the confluency of 70 - 80% was reached, and cultivated for 8 weeks. Supernatant of all flasks were collected every week to increase the probability of detection of oocysts that might have been produced in these cultures. Harvesting was performed exactly as described by MILLER et al. (2018). In only one out of four parallel experiments oocysts (6.5×10^4) were detected in the present study. In contrast, MILLER et al. (2018) reported that in their study oocysts were observed every week and they calculated a 50-fold increase of oocysts at 10 days p.i. and a 120-fold increase at 60 days p.i. (MILLER et al. 2018). Considering the initial inoculation dose of 4×10^5 sporozoites per flask, no multiplication could be observed in my experiments. Therefore, a high yield of infectious oocysts appears not to be possible by the applied method in terms of reliability and repeatability. At least for the in-house strain used in the present investigation (GP60 subtype IIa A15G2RI of *C. parvum*) *in vitro* reproduction of the whole life cycle in COLO-680 N cells was not achieved on a satisfactory level.

It cannot be excluded that differences between strains of *C. parvum* could be a factor that influences the success of *in vitro* production of oocysts. A *C. parvum* cattle genotype (Swiss cattle C26) was reported to complete its life cycle and yield infectious oocysts in both HCT-8 cell and axenic cultures (HIJJAWI et al. 2001; HIJJAWI et al. 2004). However, the method was rated not appliable to *C. parvum* Moredun or IOWA strains or the *C. hominis* strain TU502 (GIROUARD et al. 2006). Unfortunately, transfected oocysts were not found in the current *in vitro* experiments. To the best of my current knowledge no continuous axenic production of oocysts has been established anywhere, however, would be ideal to fulfill the 3R principle or for studies with genetically modified *C. parvum*. In the foreseen near future, the propagation of genetically modified *C. parvum* still has to rely on animal

models. Whatsoever, efforts need to be paid on developing less harmful method than surgical inoculation of *C. parvum* into mice.

The present study demonstrates the knockout of CDPK1 gene in *C. parvum* through CRISPR/cas 9 for the first time and the trials of propagate *C. parvum* both *in vitro* and *in vivo*. The animal model RAGgc x IFN-gamma KO mice is suited to serve the aim of propagation whereas the *in vitro* model, COLO - 680 N cell appears unsuited. The CpCDPK1 is proven very important but not absolutely essential to the invasion process *in vitro*, thus influence development into further phase of *C. parvum* by the CDPK1 inhibition assay. Due to the gene's importance in the life cycle, a low percentage of transfected *C. parvum* survived the *in vitro* transfection. Therefore, strategies to stabilize the generation of CDPK1KO *C. parvum* solutions remain to be developed to increase the rate of survivors in further studies. One option is RAGgc x IFN-gamma KO mice that might allow the propagation of CDPK1KO *C. parvum* as this model only requires low number of parasites to produce high yields of oocysts. The other possibility is to search a new transfection method which can overcome barrier of occyst wall, thereby the transfected sporozoites can be well protected until the invasion process initiates. For the currently available transfection protocols the rigidity of oocyst walls are a relevant obstacle. Methods that allow large molecules to penetrate the oocyst wall without altering sporozoites vitality would be most welcome, however, are not available so far.

6. Summary

Wanpeng Zheng

Calcium dependent protein kinase 1 in *Cryptosporidium parvum* (CpCDPK1): attempts to produce knockout parasites and functional studies

Institute of Parasitology, Faculty of Veterinary Medicine, Leipzig University

Submitted in September 2019

88 pages, 30 figures, 16 tables, 213 references

Keywords: *Cryptosporidium parvum*, CDPK1, host cell actin, transfection, propagation

Introduction: *Cryptosporidium parvum* is a protozoan parasite that causes diarrhoea in many host species worldwide. CpCDPK1 appears to be essential for invasion and a promising drug target.

Aim of the study: The aims of this study were to expand the knowledge of CpCDPK1. To achieve that, attempts were made to inhibit this gene by BKI-1294 *in vitro* and generate CpCDPK1 KO *C. parvum*. To maintain the genetically modified parasites, I studied the suitability of infection and propagation in a new animal model RAGgc × IFN-gamma mouse and *in vitro* model COLO - 680 N cell line.

Animals, materials and methods: 4×10^6 freshly excysted *C. parvum* sporozoites were seeded into transfected GFP-MDBK cultures at the confluency of 70 – 80 % and simultaneously exposed to 500 nM of BKI-1294. IFA was applied to observe the invasion and host cell actin accumulation. Guide RNA (gRNA) for CRISPR-mediated transfection was designed and the Nluc-neoR repair cassette was flanked with 50 bp long 5'- and 3'UTR of CpCDPK1 by PCR. Transfection was performed by octaarginine transportation and compared to electroporation. COLO - 680 N cells with the confluency of 70 – 80% were infected with 4×10^6 non-transfected and transfected sporozoites of *C. parvum*. To establish a laboratory animal model for propagation of *C. parvum* and drug screening RAGgc × IFN-gamma mice were infected with 500 (G2), 1000 (G3) and 5000

(G4) of oocysts. BALB/c WT mice were inoculated with 5000 (G1) oocysts as control. Faeces were sampled for *C. parvum* DNA extraction. Real time PCR was applied to calculate the oocyst yield.

Results: In the presence of 500 nM BKI-1294, parasite-induced host cell actin accumulation was not observed at 24 and 48 h after inoculation *in vitro* pointing at altered infectivity of CDPK inhibited sporozoites. Extracellular noninvasive sporozoites were found at 24 h p.i., only one meront was observed in a host cell at 72 h p.i. CRISPR-mediated gene editing was applied to *C. parvum* to knock out CDPK1. Transfected *C. parvum* were found in COLO-680 N cells through 6 passages. However, no newly generated oocysts were harvested. RAGgc × IFN-gamma mice were tested suitable as an animal model for *C. parvum* infection studies and oocyst propagation. These crossbred mice are very sensitive to infection at doses as low as 500 oocysts. They displayed emaciation, rough fur and trembling. The survival percentage was 71.4 % (G2), 85.7 % (G3), 57.1 % (G4) and 100 % (G1) at the end of study. Oocyst yield of 10^8 OPG was calculated in the crossbred mice whereas only 10^4 OPG were counted in Balb/C mice. Yields did not differ significantly ($P > 0.05$) in crossbred mice infected with different oocysts doses.

Conclusions: 1.The function of CpCDPK1 is obviously important to the invasion process including attachment and utilization of host cell actin to form PV. This assumption was confirmed by CDPK inhibition and genetic KO. However, methods that increase the transfection efficiency are needed to enhance the generation of KO *C. parvum*. 2. The transfection method mediated by octargninine is superior to electroporation in consideration of DNA consumption and requirement of device. 3. Due to the low required infection dose and clinical manifestation RAGgc × IFN-gamma mice appear very well suited to serve as an *in vivo* laboratory model of *C. parvum* infection and for propagation of particularly transgenic *C. parvum* strains. 4. COLO – 680 N cells appear suited to be an *in vitro* model for *C. parvum* infection and transfection study, however, not qualified for propagation.

7. Zusammenfassung

Wanpeng Zheng

Knockout Calciumabhängiger Proteinkinase 1 (CpCDPK1) in *Cryptosporidium parvum* und Funktionsstudien

Institut für Parasitologie, Veterinärmedizinische Fakultät, Universität Leipzig

Eingereicht im September 2019

88 Seiten, 30 Abbildungen, 16 Tabellen, 213 Literaturangaben

Schlüsselwörter: *Cryptosporidium parvum*, CpCDPK1, Wirtszellaktin, Transfektion, Mausmodell

Einleitung: *Cryptosporidium parvum* ist ein parasitärer Protozoe, der bei vielen Wirtsarten Durchfall verursacht. CpCDPK1 scheint für die Invasion essentiell und ein vielversprechendes therapeutisches Ziel zu sein.

Ziele der Untersuchungen: Der CDPK-Inhibitor BKI-1294 wurde auf seine Wirkung auf *C. parvum in vitro* untersucht. Ferner sollte versucht werden eine Knock-out-Mutante des CDPK1 kodierenden Gens (CpCDPK1KO) herzustellen. Ein Mausmodell sowie eine Zelllinie wurden auf ihre Eignung zur Oozystenproduktion getestet.

Tiere, Material und Methoden: 4×10^6 frisch exzystierte *C. parvum*-Sporozoiten wurden in MDBK-Kulturen ausgesät und gleichzeitig 500 nM des CDPK-Inhibitors BKI-1294 ausgesetzt. Mittels IFA wurden die Invasion und die Akkumulation von Wirtszell-Aktin dargestellt. GuideRNA (gRNA) wurde für die CRISPR-vermittelte Transfektion entworfen und in das Plasmid 185 integriert. Die Nluc-neoR-Reparaturkassette wurde mit 50 bp langen 5'- und 3'-UTRs des CpCDPK1-Gens flankiert. Die Transfektion wurde mittels Octaarginin durchgeführt und mit der Elektroporation verglichen. Konfluente COLO - 680 N-Zellen wurden mit 4×10^6 transfizierten und nicht transfizierten Sporozoiten infiziert und für 8 Wochen kultiviert und anschließend auf Oozystenproduktion untersucht. 7 Immundefiziente RAGgc × IFN-Gamma-Mäuse wurden mit 500 (G2), 1000 (G3) oder 5000 (G4) Oozysten infiziert. 6 BALB/c WT-Mäuse wurden mit 5000 (G1) Oocysten als Kontrolle inokuliert. Mittels PCR wurde die Oozystenausbeute bestimmt.

Ergebnisse: In Gegenwart von 500 nM BKI-1294 wurde 24 und 48 h *post infectionem* (p.i.) *in vitro* keine Aktinakkumulation in Wirtszellen beobachtet, was auf eine reduzierte Infektiosität von CDPK-inhibierten Sporozoiten hinweist. Extrazelluläre nicht-invasive Sporozoiten wurden 24 h p.i. gefunden, 72 h p.i. wurde ein Meront festgestellt. CRISPR-vermittelte Geneditierung wurde angewendet, um CpCDPK1 mittels guideRNA auszuschalten. Mittels Octaarginin wurden die jeweilige gRNA und die amplifizierte Reparaturkassette in die Zielzelle transportiert. So transfizierte *C. parvum* wurden in COLO-680 N-Zellen über 6 Wirtszellpassagen gefunden. Es wurden jedoch keine neu erzeugten Oozysten gefunden. RAGgc × IFN-Gamma-Mäuse erwiesen sich schon bei Dosen von nur 500 Oozysten als sehr anfällig für *C. parvum*. Mäuse zeigten Abmagerung, raues Fell und Zittern, die Überlebensrate betrug am Ende der Studie 71,4% (G2), 85,7% (G3), 57,1% (G4), BalbC-Mäuse überlebten dagegen zu 100% (G1). Eine Oozystenausbeute von bis zu 10^8 OPG wurde für die Gruppen G2, G3 und G4 berechnet ($P > 0,05$), wohingegen Balb/C-Mäuse nur 10^4 OPG ausschieden.

Schlussfolgerungen: 1. CpCDPK1 ist wichtig für den Invasionsprozess, einschließlich der Mobilisierung von Wirtszell-Aktin zur Bildung der parasitophoren Vakuole. Dies konnte durch Anwendung des Inhibitors BKI-1294 und Knock-out-Studien gezeigt werden. Es werden jedoch Verfahren benötigt, die die Transfektionseffizienz erhöhen. 2. Die durch Octaarginin vermittelte Transfektion ist der Elektroporation überlegen. 3. RAGgc × IFN-Gamma-Mäuse sind sehr gut als Labornagermodell geeignet. 4. COLO - 680 N - Zellen scheinen als In-vitro-Modell für Infektions- und Transfektionsstudien geeignet zu sein, ermöglichen jedoch nicht eine Vermehrung des Parasiten.

8. References

Abrahamsen M S, Templeton T J, Enomoto S, Abrahante J E, Zhu G, Lancto C A et al. Complete genome sequence of the apicomplexan, *Cryptosporidium parvum*. Science. 2004;304(5669):441–445.

Ajonina C, Buzie C, Ajonina I U, Basner A, Reinhardt H, Gulyas H et al. Occurrence of *Cryptosporidium* in a wastewater treatment plant in North Germany. J Toxicol Environ Health. A 2012;75(22-23):1351–1358.

Aldeyarbi H M, Karanis P. Electron microscopic observation of the early stages of *Cryptosporidium parvum* asexual multiplication and development in in vitro axenic culture. Eur J Protistol. 2016;52:36–44.

Alvarez-Pellitero P, Sitj à-Bobadilla A. *Cryptosporidium molnari* n. sp. (Apicomplexa. Cryptosporidiidae) infecting two marine fish species, *Sparus aurata* L. and Dicentrarchus labrax L. Int J Parasitol. 2002;32(8):1007–1021.

Amadi B, Mwiya M, Sianongo S, Payne L, Watuka A, Katubulushi M et al. High dose prolonged treatment with nitazoxanide is not effective for cryptosporidiosis in HIV positive Zambian children: a randomised controlled trial. BMC Infect Dis. 2009;9:p. 195.

Barakat F M, McDonald V, Di Santo J P, Korbel D S. Roles for NK cells and an NK cell-independent source of intestinal gamma interferon for innate immunity to *Cryptosporidium parvum* infection. Infect Immun. 2009;77(11):5044–5049.

Billker O, Dechamps S, Tewari R, Wenig G, Franke-Fayard B, Brinkmann V. Calcium and a calcium-dependent protein kinase regulate gamete formation and mosquito transmission in a malaria parasite. Cell. 2004;117(4):503–514.

Billker O, Lourido S, Sibley L D. Calcium-dependent signaling and kinases in apicomplexan parasites. Cell Host Microbe. 2009;5(6):612–622.

Borowski H, Clode P L, Thompson R C A. Active invasion and/or encapsulation? A reappraisal of host-cell parasitism by *Cryptosporidium*. Trends Parasitol. 2008;24(11):509–516.

Broglia A, Reckinger S, Caccio S M, Nockler K. Distribution of *Cryptosporidium parvum* subtypes in calves in Germany. Vet Parasitol. 2008;154(1-2):8–13.

Cai X, Woods K M, Upton S J, Zhu G. Application of quantitative real-time reverse transcription-PCR in assessing drug efficacy against the intracellular pathogen *Cryptosporidium parvum in vitro*. Antimicrob Agents Chemother. 2005;49(11):4437–4442.

Carruthers V B, Giddings O K, Sibley L D. Secretion of micronemal proteins is associated with toxoplasma invasion of host cells. Cell Microbiol. 1999;1(3):225–235.

Carruthers V B, Sibley L D. Mobilization of intracellular calcium stimulates microneme discharge in *Toxoplasma gondii*. Mol Microbiol. 1999;31(2):421–428.

Castellanos-Gonzalez A, White A CJR, Ojo K K, Vidadala R S R, Zhang Z, Reid M C et al. A novel calcium-dependent protein kinase inhibitor as a lead compound for treating cryptosporidiosis. J Infect Dis. 2013;208(8):1342–1348.

Castro-Hermida J A, Pors I, Méndez-Hermida F, Ares-Mazás E, Chartier C. Evaluation of two commercial disinfectants on the viability and infectivity of *Cryptosporidium parvum* oocysts. Vet J. 2006;171(2):340–345.

Cavalier-Smith T. Gregarine site-heterogeneous 18S rDNA trees, revision of gregarine higher classification, and the evolutionary diversification of Sporozoa. Eur J Protistol. 2014;50(5):472–495.

Chalmers R M, Campbell B M, Crouch N, Charlett A, Davies A P. Comparison of diagnostic sensitivity and specificity of seven *Cryptosporidium* assays used in the UK. J Med Microbiol. 2011;60(Pt 11):1598–1604.

Chalmers R M, Katzer F. Looking for *Cryptosporidium*. The application of advances in detection and diagnosis. Trends Parasitol. 2013;29(5):237–251.

Chalmers R M, Robinson G, Elwin K, Hadfield S J, Xiao L, Ryan U, Modha D, Mallaghan C. *Cryptosporidium* sp. rabbit genotype, a newly identified human pathogen. Emerging Infect Dis. 2009;15(5):829–830.

Checkley W, White A C, Jaganath D, Arrowood M J, Chalmers R M, Chen X-M et al. A review of the global burden, novel diagnostics, therapeutics, and vaccine targets for cryptosporidium. Lancet Infect Dis. 2015;15(1):85–94.

Chen J, Lansford R, Stewart V, Young F, Alt F W. RAG-2-deficient blastocyst complementation. An assay of gene function in lymphocyte development. Proc Natl Acad Sci U S A. 1993;90(10):4528–4532.

Chen X-M, LaRusso N F. Mechanisms of attachment and internalization of *Cryptosporidium parvum* to biliary and intestinal epithelial cells. Gastroenterology. 2000;118(2):368–379.

Chen X-M, O'Hara S P, Huang B Q, Nelson J B, Lin J J-C, Zhu G et al. Apical organelle discharge by *Cryptosporidium parvum* is temperature, cytoskeleton, and intracellular calcium dependent and required for host cell invasion. Infect Immun. 2004;72(12):6806–6816.

Chen X-M, O'Hara S P, Huang B Q, Splinter P L, Nelson J B, LaRusso N F. Localized glucose and water influx facilitates *Cryptosporidium parvum* cellular invasion by means of modulation of host-cell membrane protrusion. Proc Natl Acad Sci U S A. 2005;102(18):6338–6343.

Clancy J L, Marshall M M, Hargy T M, Korich D G. Susceptibility of five strains of "*Cryptosporidium parvum*" oocysts to UV light. J Am Water Works Assoc. 2004;96(3):84–93.

Clavel A, Arnal A C, Sánchez E C, Varea M, Castillo F J, Ramírez de Ocáriz I et al. Evaluation of the optimal number of faecal specimens in the diagnosis of cryptosporidiosis in AIDS and immunocompetent patients. Eur J Clin Microbiol Infect Dis. 1995;14(1):46–49.

Costa L B, JohnBull E A, Reeves J T, Sevilleja J E, Freire R S, Hoffman P S et al. *Cryptosporidium*-malnutrition interactions: mucosal disruption, cytokines, and TLR signaling in a weaned murine model. J Parasitol. 2011;97(6):1113–1120.

Costa L B, Noronha F J, Roche J K, Sevilleja J E, Warren C A, Oria R et al. Novel *in vitro* and *in vivo* models and potential new therapeutics to break the vicious cycle of *Cryptosporidium* infection and malnutrition. J Infect Dis. 2012;205(9):1464–1471.

Delling C, Holzhausen I, Daugschies A, Lendner M. Inactivation of *Cryptosporidium parvum* under laboratory conditions. Parasitol Res. 2016;115(2):863–866.

Díaz P, Quílez J, Robinson G, Chalmers R M, Díez-Baños P, Morrondo P. Identification of *Cryptosporidium xiaoi* in diarrhoeic goat kids (Capra hircus) in Spain. Vet Parasitol. 2010;172(1-2):132–134.

DiSanto J P, Muller W, Guy-Grand D, Fischer A, Rajewsky K. Lymphoid development in mice with a targeted deletion of the interleukin 2 receptor gamma chain. Proc Natl Acad Sci U S A. 1995;92(2):377–381.

Don R H, Cox P T, Wainwright B J, Baker K, Mattick J S. 'Touchdown' PCR to circumvent spurious priming during gene amplification 1991. Nucleic Acids. Res;19(14):p. 4008.

Elliott D A, Clark D P. *Cryptosporidium parvum* induces host cell actin accumulation at the host-parasite interface. Infect Immun. 2000;68(4):2315–2322.

Elliott D A, Coleman D J, Lane M A, May R C, Machesky L M, Clark D P. *Cryptosporidium parvum* Infection Requires Host Cell Actin Polymerization. Infect Immun. 2001;69(9):5940–5942.

El-Shafei R A, Eladl A H, Hamed H R, El-Amaiem W E A. Competency of commercially available medicaments on treatment of chicken cryptosporidiosis. Int J Innov Appl Stud. 2014;6(4):758–767.

Enemark H L, Bille-Hansen V, Lind P, Heegaard P M H, Vigre H, Ahrens P, Thamsborg S M. Pathogenicity of *Cryptosporidium parvum*--evaluation of an animal infection model. Vet Parasitol. 2003;113(1):35–57.

Etzold M, Lendner M, Daugschies A, Dyachenko V. CDPKs of *Cryptosporidium parvum*--stage-specific expression *in vitro*. Parasitol Res. 2014;113(7):2525–2533.

Ezzaty Mirhashemi M, Zintl A, Grant T, Lucy F E, Mulcahy G, Waal T de. Comparison of diagnostic techniques for the detection of *Cryptosporidium* oocysts in animal samples. Exp Parasitol. 2015;151-152:14–20.

Fayer R, Dubey J P, Lindsay D S. Zoonotic protozoa: from land to sea. Trends Parasitol. 2004;20(11):531–536.

Fayer R, Nerad T, Rall W, Lindsay D S, Blagburn B L. Studies on Cryopreservation of *Cryptosporidium parvum*. J Parasitol. 1991;77(3):p. 357.

Fayer R, Sant ń M, Macarisin D. *Cryptosporidium ubiquitum* n. sp. in animals and humans. Vet Parasitol. 2010;172(1-2):23–32.

Fayer R, Xiao L. *Cryptosporidium* and cryptosporidiosis. 2. ed. London: CRC Press; 2008.

Ferrari C. HBV and the immune response. Liver Int. 2015;35:121–128.

Filatova N A, Knyazev N A, Skarlato S O, Anatskaya O V, Vinogradov A E. Natural killer cell activity irreversibly decreases after *Cryptosporidium* gastroenteritis in neonatal mice. Parasite Immunol. 2018;40(5):e12524.

Forney JR, DeWald DB, Yang S, Speer CA, Healey MC. A role for host phosphoinositide 3-kinase and cytoskeletal remodeling during *Cryptosporidium parvum* infection. Infect Immun. 1999;67(2):844–852.

Fournet N, Deege M P, Urbanus A T, Nichols G, Rosner B, Chalmers R M et al. Simultaneous increase of *Cryptosporidium* infections in the Netherlands, the United Kingdom and Germany in late summer season, 2012. Euro Surveill. 2013;18(2). pii: 20348.

Fritzler J M, Millership J J, Zhu G. *Cryptosporidium parvum* long-chain fatty acid elongase. Eukaryot Cell. 2007;6(11):2018–2028.

Fu C, Donovan W P, Shikapwashya-Hasser O, Ye X, Cole R H. Hot Fusion. An efficient method to clone multiple DNA fragments as well as inverted repeats without ligase. PLoS One. 2014;9(12):e115318.

Garcia LS, Shimizu RY. Evaluation of nine immunoassay kits (enzyme immunoassay and direct fluorescence) for detection of *Giardia lamblia* and *Cryptosporidium parvum* in human fecal specimens. J Clin Microbiol. 1997;1(6):1526–1529.

Gelfand M S, Cleveland K O. Oral serum-derived bovine immunoglobulin for management of infectious diarrhea due to norovirus and cryptosporidiosis in solid organ transplant patients. Infect Dis Clin Pract 2017;25(4):218–220.

Geurden T, Thomas P, Casaert S, Vercruysse J, Claerebout E. Prevalence and molecular characterisation of *Cryptosporidium* and *Giardia* in lambs and goat kids in Belgium. Vet Parasitol. 2008;155(1-2):142–145.

Gimenez F, Hines S A, Evanoff R, Ojo K K, van Voorhis W C, Maly D J et al. *In vitro* growth inhibition of *Theileria equi* by bumped kinase inhibitors. Vet Parasitol. 2018;251:90–94.

Girouard D, Gallant J, Akiyoshi D E, Nunnari J, Tzipori S. Failure to propagate *Cryptosporidium* spp. in cell-free culture. J Parasitol. 2006;92(2):399–400.

Goodsell D S. The Molecular Perspective. Ultraviolet Light and Pyrimidine Dimers. Oncologist. 2001;6(3):298–299.

Gorla S K, McNair N N, Yang G, Gao S, Hu M, Jala V R et al. Validation of IMP dehydrogenase inhibitors in a mouse model of cryptosporidiosis. Antimicrob Agents Chemother. 2014;58(3):1603–1614.

Widmer G. Genetic heterogeneity and PCR detection of *Cryptosporidium parvum*. Adv Parasitol. 1998;40:p. 223.

Griffiths J K, Balakrishnan R, Widmer G, Tzipori G. Paromomycin and geneticin inhibit intracellular *Cryptosporidium parvum* without trafficking through the host cell cytoplasm: implications for drug delivery. Infect Immun. 1998;66(8):3874–3883.

Griffiths J K, Theodos C, Paris M, Tzipori S. The gamma interferon gene knockout mouse: a highly sensitive model for evaluation of therapeutic agents against *Cryptosporidium parvum*. J Clin Microbiol. 1998;36(9):2503–2508.

Guitard J, Menotti J, Desveaux A, Alimardani P, Porcher R, Derouin F et al. Experimental study of the effects of probiotics on *Cryptosporidium parvu*m infection in neonatal rats. Parasitol Res. 2006;99(5):522–527.

Hallier-Soulier S, Guillot E. Detection of cryptosporidia and *Cryptosporidium parvum* oocysts in environmental water samples by immunomagnetic separation-polymerase chain reaction. J Appl Microbiol. 2000;89(1):5–10.

Harmon A C, Gribskov M, Harper J F. CDPKs - a kinase for every Ca^{2+} signal? Trends Plant Sci. 2000;5(4):154–159.

Harper J F, Breton G, Harmon A. Decoding Ca^{2+} signals through plant protein kinases. Annu Rev Plant Biol. 2004;55:263–288.

Harper J F, Harmon A. Plants, symbiosis and parasites: a calcium signalling connection. Nat Rev Mol Cell Biol. 2005;6(7):555–566.

Harris J R, Adrian M, Petry F. Amylopectin. A major component of the residual body in *Cryptosporidium parvum* oocysts. Parasitology. 1999;128(3):269–282.

Hecker K H, Roux K H. High and low annealing temperatures increase both specificity and yield in touchdown and stepdown PCR. BioTechniques. 1996;20(3):478–485.

Helmy Y A, Samson-Himmelstjerna G von, Nockler K, Zessin K-H. Frequencies and spatial distributions of *Cryptosporidium* in livestock animals and children in the Ismailia province of Egypt. Epidemiol Infect. 2015;143(6):1208–1218.

Hijjawi N S, Meloni B P, Ng'anzo M, Ryan U M, Olson M E, Cox P T et al. Complete development of *Cryptosporidium parvum* in host cell-free culture. Int J Parasitol. 2004;34(7):769–777.

Hijjawi N S, Meloni B P, Morgan U M, Thompson R CA. Complete development and long-term maintenance of *Cryptosporidium parvum human* and cattle genotypes in cell culture. Int J Parasitol. 2001;31(10):1048–1055.

Hoblet K H, Charles T P, Howard R R. Evaluation of lasalocid and decoquinate against coccidiosis resulting from natural exposure in weaned dairy calves. Am J Vet Res. 1989;50(7):1060–1063.

Hong S, Kim K, Yoon S, Park W-Y, Sim S, Yu J-R. Detection of *Cryptosporidium parvum* in environmental soil and vegetables. J Korean Med Sci. 2014;29(10):1367–1371.

Huang W, Choi R, Hulverson M A, Zhang Z, McCloskey M C, Schaefer D A et al. 5-Aminopyrazole-4-Carboxamide-Based Compounds Prevent the Growth of *Cryptosporidium parvum*. Antimicrob Agents Chemother. 2017;61(8) e00020-17..

Hunt E, Fu Q, Armstrong M U, Rennix D K, Webster D W, Galanko J A et al. Oral bovine serum concentrate improves cryptosporidial enteritis in calves. Pediatr Res. 2002;51(3):370–376.

Ishino T, Orito Y, Chinzei Y, Yuda M. A calcium-dependent protein kinase regulates *Plasmodium* ookinete access to the midgut epithelial cell. Mol Microbiol. 2006;59(4):1175–1184.

Jacob P, Henry A, Meheut G, Charni-Ben-Tabassi N, Ingrand V, Helmi K. Health risk assessment related to waterborne pathogens from the river to the tap. Int J Environ Res Public Health. 2015;12(3):2967–2983.

Jang M S, Song W C, Shin S W, Park K S, Kim J, Kim D-I et al. A novel multigene cloning method for the production of a motile ATPase. J Biotechnol. 2015;207:1–7.

Jarvie B D, Trotz-Williams L A, McKnight D R, Leslie K E, Wallace M M, Todd C G et al. Effect of halofuginone lactate on the occurrence of *Cryptosporidium parvum* and growth of neonatal dairy calves. J Dairy Sci. 2005;88(5):1801–1806.

Jiang Q Y, Lai L H, Shen J, Wang Q Q, Xu F J, Tang G P. Gene delivery to tumor cells by cationic polymeric nanovectors coupled to folic acid and the cell-penetrating peptide octaarginine. Biomaterials. 2011;32(29):7253–7262.

Jirku M, Valigurová A, Koudela B, Krížek J, Modrý D. New species of *Cryptosporidium Tyzzer*, 1907 (Apicomplexa) from amphibian host: morphology, biology and phylogeny. Folia Parasitologica. 2008;55(2):81–94.

Joachim A, Krull T, Schwarzkopf J, Daugschies A. Prevalence and control of bovine cryptosporidiosis in German dairy herds. Vet Parasitol. 2003;112(4):277–288.

Johnston S P, Ballard M M, Beach M J, Causer L, Wilkins P P. Evaluation of three commercial assays for detection of *Giardia* and *Cryptosporidium* organisms in fecal specimens. J Clin Microbiol. 2003;41(2):623–626.

Karanis P, Schoenen D, Seitz H. Distribution and removal of in water supplies in germany. Water Sci Technol. 1998;37(2):9–18.

Kaushik K, Khurana S, Wanchu A, Malla N. Evaluation of staining techniques, antigen detection and nested PCR for the diagnosis of cryptosporidiosis in HIV seropositive and seronegative patients. Acta Trop. 2008;107(1):1–7.

Keidel J, Daugschies A. Integration of halofuginone lactate treatment and disinfection with p-chloro-m-cresol to control natural cryptosporidiosis in calves. Vet Parasitol. 2013;196(3-4):321–326.

Keithly J S, Zhu G, Upton S J, Woods K M, Martinez M P, Yarlett N. Polyamine biosynthesis in Cryptosporidium parvum and its implications for chemotherapy. Mol Biochem Parasitol. 1997;88(1-2):35–42.

Khalil I A, Futaki S, Niwa M, Baba Y, Kaji N, Kamiya H et al. Mechanism of improved gene transfer by the N-terminal stearylation of octaarginine: enhanced cellular association by hydrophobic core formation. Gene Ther. 2004;11(7):636–644.

King B J, Monis P T. Critical processes affecting *Cryptosporidium* oocyst survival in the environment. Parasitology. 2007;134(Pt 3):309–323.

Koh W, Clode P L, Monis P, Thompson R C A. Multiplication of the waterborne pathogen *Cryptosporidium parvum* in an aquatic biofilm system. Parasit Vectors. 2013;6:p. 270.

Korbie D J, Mattick J S. Touchdown PCR for increased specificity and sensitivity in PCR amplification. Nat Protoc. 2008;3(9):1452–1456.

Kotloff K L, Nataro J P, Blackwelder W C, Nasrin D, Farag T H, Panchalingam S et al. Burden and aetiology of diarrhoeal disease in infants and young children in developing countries (the Global Enteric Multicenter Study, GEMS): a prospective, case-control study. Lancet. 2013;382(9888):209–222.

Kuhlenschmidt T B, Rutaganira F U, Long S, Tang K, Shokat K M, Kuhlenschmidt M S et al. Inhibition of calcium-dependent protein kinase 1 (CDPK1) i*n vitro* by pyrazolopyrimidine derivatives does not correlate with sensitivity of *Cryptosporidium parvum* growth in cell culture. Antimicrob Agents Chemother. 2016;60(1):570–579.

Lacroix S, Mancassola R, Naciri M, Laurent F. *Cryptosporidium parvum*-specific mucosal immune response in C57BL/6 neonatal and gamma interferon-deficient mice: role of tumor necrosis factor alpha in protection. Infect Immun 2001;69(3):1635–1642.

Lalibert éJ, Carruthers V B. Host cell manipulation by the human pathogen *Toxoplasma gondii*. Cell Mol Life Sci. 2008;65(12):1900–1915.

Lallemand M, Villeneuve A, Belda J, Dubreuil P. Field study of the efficacy of halofuginone and decoquinate in the treatment of cryptosporidiosis in veal calves. Vet Rec. 2006;159(20):672–676.

Lee J Y, Yoo B C, Harmon A C. Kinetic and calcium-binding properties of three calcium-dependent protein kinase isoenzymes from soybean. Biochemistry. 1998;37(19):6801–6809.

Lefay D, Naciri M, Poirier P, Chermette R. Efficacy of halofuginone lactate in the prevention of cryptosporidiosis in suckling calves. Vet Rec. 2001;148(4):108–112.

Lendner M, Böttcher D, Delling C, Ojo K K, van Voorhis W C, Daugschies A. A novel CDPK1 inhibitor--a potential treatment for cryptosporidiosis in calves? Parasitol Res. 2015;114(1):335–336.

Lendner M, Daugschies A. *Cryptosporidium* infections: molecular advances. Parasitology. 2014;141(11):1511–1532.

Lim D C, Cooke B M, Doerig C, Saeij J P J. *Toxoplasma* and *Plasmodium* protein kinases: roles in invasion and host cell remodelling. Int J Parasitol. 2012;42(1):21–32.

Liu Y, Li S, Zhang H, Wan Z, Zhang X, Du R. A one-step cloning method for the construction of somatic cell gene targeting vectors. Application to production of human knockout cell lines. BMC Biotechnol. 2012;12:p. 71.

Love M S, Beasley F C, Jumani R S, Wright T M, Chatterjee A K, Huston C D et al. A high-throughput phenotypic screen identifies clofazimine as a potential treatment for cryptosporidiosis. PLoS Negl Trop Dis. 2017;11(2):e0005373.

Lucio-Forster A, Griffiths J K, Cama V A, Xiao L, Bowman D D. Minimal zoonotic risk of cryptosporidiosis from pet dogs and cats. Trends Parasitol. 2010;26(4):174–179.

MacKenzie W R, Schell W L, Blair K A, Addiss D G, Peterson D E, Hoxie N J et al. Massive outbreak of waterborne cryptosporidium infection in Milwaukee, Wisconsin: recurrence of illness and risk of secondary transmission. Clin Infect Dis. 1995;21(1):57–62.

Madani F, Lindberg S, Langel U, Futaki S, Gräslund A. Mechanisms of cellular uptake of cell-penetrating peptides. J Biophys. 2011;2011:p. 414729.

Geisler M, Venema K. Transporters and pumps in plant signaling. 1. ed. New York and Berlin: Springer; 2011.

Mazurier F, Fontanellas A, Salesse S, Taine L, Landriau S, Moreau-Gaudry F et al. A novel immunodeficient mouse model--RAG2 x common cytokine receptor gamma chain double mutants--requiring exogenous cytokine administration for human hematopoietic stem cell engraftment. J Interferon Cytokine Res. 2004;19(5):533–541.

McDonald S A C, O'Grady J E, Bajaj-Elliott M, Notley C A, Alexander J, Brombacher F et al. Protection against the early acute phase of *Cryptosporidium parvum* infection conferred by interleukin-4-induced expression of T helper 1 cytokines. J Infect Dis. 2004;190(5):1019–1025.

McDonald V, Korbel D S, Barakat F M, Choudhry N, Petry F. Innate immune responses against *Cryptosporidium parvum* infection. Parasite Immunol. 2013;35(2):55–64.

Mead J R. Cryptosporidiosis and the challenges of chemotherapy. Drug Resist Updat. 2002;5(1):47–57.

Mead J R. Challenges and prospects for a *Cryptosporidium* vaccine. Future Microbiol. 2010;5(3):335–337.

Mead J R. Prospects for immunotherapy and vaccines against *Cryptosporidium*. Hum Vaccin Immunother. 2014;10(6):1505–1513.

Mead J R, Arrowood M J, Sidwell R W, Healey M C. Chronic *Cryptosporidium parvum* infections in congenitally immunodeficient SCID and nude mice. J Infect Dis. 1991;163(6):1297–1304.

Meamar A-R, Rezaian M, Rezaie S, Mohraz M, Kia E B, Houpt E R et al. *Cryptosporidium parvum* bovine genotype oocysts in the respiratory samples of an AIDS patient: efficacy of treatment with a combination of azithromycin and paromomycin. Parasitol Res. 2006;98(6):593–595.

Miller C N, Joss é L, Brown I, Blakeman B, Povey J, Yiangou L et al. A cell culture platform for *Cryptosporidium* that enables long-term cultivation and new tools for the systematic investigation of its biology. Int J Parasitol. 2018;48(3-4):197–201.

Molbak K, Andersen M, Aaby P, Hojlyng N, Jakobsen M, Sodemann M et al. *Cryptosporidium* infection in infancy as a cause of malnutrition: a community study from Guinea-Bissau, west Africa. Am J Clin Nutr. 1997;65(1):149–152.

Molloy S F, Smith H V, Kirwan P, Nichols R A B, Asaolu S O, Connelly L et al. Identification of a high diversity of *Cryptosporidium* species genotypes and subtypes in a pediatric population in Nigeria. Am J Trop Med Hyg. 2010;82(4):608–613.

Mondal D, Haque R, Sack R B, Kirkpatrick B D, Petri W AJR. Attribution of malnutrition to cause-specific diarrheal illness: evidence from a prospective study of preschool children in Mirpur, Dhaka, Bangladesh. Am J Trop Med Hyg. 2009;80(5):824–826.

Moore D A, Atwill E R, Kirk J H, Brahmbhatt D, Alonso L H, Hou L et al. Prophylactic use of decoquinate for infections with *Cryptosporidium parvum* in experimentally challenged neonatal calves. J Am Vet Med Assoc. 2003;223(6):839–845.

Moriarty E M, Duffy G, McEvoy J M, Caccio S, Sheridan J J, McDowell D et al. The effect of thermal treatments on the viability and infectivity of *Cryptosporidium parvum* on beef surfaces. J Appl Microbiol. 2005;98(3):618–623.

Mosier D A, Oberst R D. Cryptosporidiosis: a Global Challenge. Ann N Y Acad Sci. 2000;916(1):102–111.

Murphy R C, Ojo K K, Larson E T, Castellanos-Gonzalez A, Perera B G K, Keyloun K R et al. Discovery of potent and selective inhibitors of calcium-dependent protein kinase 1 (CDPK1) from *C. parvum* and *T. gondii.* ACS Med Chem Lett. 2010;1(7):331–335.

Naciri M, Mancassola R, Fort G, Danneels B, Verhaeghe J. Efficacy of amine-based disinfectant KENO™COX on the infectivity of *Cryptosporidium parvum* oocysts. Vet Parasitol. 2011;179(1-3):43–49.

Naciri M, Mancassola R, Répérant J M, Canivez O, Quinque B, Yvoré P. Treatment of experimental ovine cryptosporidiosis with ovine or bovine hyperimmune colostrum. Vet Parasitol. 1994;53(3-4):173–190.

Najdrowski M, Heckeroth A R, Wackwitz C, Gawlowska S, Mackenstedt U, Kliemt D et al. Development and validation of a cell culture based assay for *in vitro* assessment of anticryptosporidial compounds. Parasitol Res. 2007;101(1):161–167.

Ndao M, Nath-Chowdhury M, Sajid M, Marcus V, Mashiyama S T, Sakanari J et al. A cysteine protease inhibitor rescues mice from a lethal *Cryptosporidium parvum* infection. Antimicrob Agents Chemother. 2013;57(12):6063–6073.

Němejc K, Sak B, Květoňová D, Kernerová N, Rost M, Cama V A et al. Occurrence of *Cryptosporidium suis* and *Cryptosporidium scrofarum* on commercial swine farms in the Czech Republic and its associations with age and husbandry practices. Parasitol Res. 2013;112(3):1143–1154.

Nord J, Ma P, DiJohn D, Tzipori S, Tacket C O. Treatment with bovine hyperimmune colostrum of cryptosporidial diarrhea in AIDS patients. AIDS. 1990;4(6):581–584.

Novak S M, Sterling C R. Susceptibility dynamics in neonatal BALB/c mice infected with *Cryptosporidium parvum*. J Protozool. 1991;38(6):103S–104S.

Nydam D V, Wade S E, Schaaf S L, Mohammed H O. Number of *Cryptosporidium parvum* oocysts or *Giardia* spp. cysts shed by dairy calves after natural infection. Am J Vet Res. 2001;62(10):1612–1615.

O'Hara S P, Yu J-R, Lin J J-C. A novel *Cryptosporidium parvum* antigen, CP2, preferentially associates with membranous structures. Parasitol Res. 2004;92(4):317–327.

Ojo K K, Reid M C, Kallur Siddaramaiah L, Müller J, Winzer P, Zhang Z et al. *Neospora caninum* calcium-dependent protein kinase 1 is an effective drug target for neosporosis therapy. PLoS One. 2014;9(3):e92929.

Ono T, Cabrita-Santos L, Leitao R, Bettiol E, Purcell L A, Diaz-Pulido O et al. Adenylyl cyclase alpha and cAMP signaling mediate *Plasmodium* sporozoite apical regulated exocytosis and hepatocyte infection. PLoS Pathog. 2008;4(2):e1000008.

Operario D J, Bristol L S, Liotta J, Nydam D V, Houpt E R. Correlation between diarrhea severity and oocyst count via quantitative PCR or fluorescence microscopy in experimental cryptosporidiosis in calves. Am J Trop Med Hyg. 2015;92(1):45–49.

Pachuk C J, Samuel M, Zurawski J A, Snyder L, Phillips P, Satishchandran C. Chain reaction cloning: a one-step method for directional ligation of multiple DNA fragments. Gene. 2000;243(1-2):19–25.

Palmer C S, Traub R J, Robertson I D, Devlin G, Rees R, Thompson R C A. Determining the zoonotic significance of *Giardia* and *Cryptosporidium* in Australian dogs and cats. Vet Parasitol. 2008;154(1-2):142–147.

Pantenburg B, Dann S M, Wang H-C, Robinson P, Castellanos-Gonzalez A, Lewis D E. Intestinal immune response to human *Cryptosporidium* sp. infection. Infect Immun. 2008;76(1):23–29.

Paraud C, Pors I, Journal J P, Besnier P, Reisdorffer L, Chartier C. Control of cryptosporidiosis in neonatal goat kids. Efficacy of a product containing activated charcoal and wood vinegar liquid (Obionekk®) in field conditions. Vet Parasitol. 2011;180(3-4):354–357.

Pawlowic M C, Vinayak S, Sateriale A, Brooks C F, Striepen B. Generating and maintaining transgenic *Cryptosporidium parvum* parasites. Curr Protoc Microbiol. 2017;46:20B.2.1-20B.2.32.

Paziewska-Harris A, Singer M, Schoone G, Schallig H. Quantitative analysis of *Cryptosporidium* growth in in vitro culture--the impact of parasite density on the success of infection. Parasitol Res. 2016;115(1):329–337.

Pfeifer G P, You Y-H, Besaratinia A. Mutations induced by ultraviolet light. Mutat Res. 2005;571(1-2):19–31.

Plutzer J, Karanis P. Genetic polymorphism in *Cryptosporidium* species: an update. Vet Parasitol. 2009;165(3-4):187–199.

Potter H, Heller R. Transfection by electroporation. Curr Protoc Mol Biol. 2018;121:9.3.1-9.3.13.

Potters I, van Esbroeck M. Negative staining technique of Heine for the detection of *Cryptosporidium* spp: a fast and simple screening technique. Open Parasitol J. 2010;4(1):1–4.

Preidis G A, Wang H-C, Lewis D E, Castellanos-Gonzalez A, Rogers K A, Graviss E A et al. Seropositive human subjects produce interferon gamma after stimulation with recombinant *Cryptosporidium hominis* gp15. Am J Trop Med Hyg. 2007;77(3):583–585.

Rengifo-Herrera C, Ortega-Mora L M, Gómez-Bautista M, García-Moreno F T, García-Párraga D, Castro-Urda J et al. Detection and characterization of a *Cryptosporidium* isolate from a southern elephant seal (*Mirounga leonina*) from the antarctic peninsula. Appl Environ Microbiol. 2011;77(4):1524–1527.

Rider S D, Zhu G. *Cryptosporidium*: genomic and biochemical features. Exp Parasitol. 2010;124(1):2–9.

Robertson L J. *Giardia* and *Cryptosporidium* infections in sheep and goats: a review of the potential for transmission to humans via environmental contamination. Epidemiol Infect. 2009;137(7):913–921.

Robertson L J, Campbell A T, Smith H V. Survival of *Cryptosporidium parvum* oocysts under various environmental pressures. Appl. Environ Microbiol. 1992;58(11):3494–3500.

Robertson L J, Gjerde B K. Effects of the Norwegian winter environment on *Giardia* cysts and *Cryptosporidium* Oocysts. Microbial Ecology. 2004;47(4):359–365.

Robinson G, Elwin K, Chalmers R M. Unusual *Cryptosporidium* genotypes in human cases of diarrhea. Emerging Infect Dis. 2008;14(11):1800–1802.

Roth D B, Craig N L. VDJ Recombination. Cell. 1998;94(4):411–414.

Ryan U, Fayer R, XIAO L. *Cryptosporidium* species in humans and animals: current understanding and research needs. Parasitology. 2014;141(13):1667–1685.

Ryan U, Hijjawi N. New developments in *Cryptosporidium* research. Int J Parasitol. 2015;45(6):367–373.

Sanderson S J, Xia D, Prieto H, Yates J, Heiges M, Kissinger J C et al. Determining the protein repertoire of *Cryptosporidium parvum* sporozoites. Proteomics. 2008;8(7):1398–1414.

Sant ń M, Dixon B R, Fayert R. Genetic characterization of *Cryptosporidium* isolates from ringed seals (*Phoca hispida*) in Northern Quebec, Canada. J Parasitol. 2005;91(3):712–716.

Schnyder M, Kohler L, Hemphill A, Deplazes P. Prophylactic and therapeutic efficacy of nitazoxanide against *Cryptosporidium parvum* in experimentally challenged neonatal calves. Vet Parasitol. 2009;160(1-2):149–154.

Scholtyseck E. Fine structure of parasitic protozoa: an atlas of micrographs, drawings and diagrams. 5. ed. New York and Berlin: Springer; 2012.

Scorza A V, Lappin. Co-infection of *Cryptosporidium* and *Giardia* in naturally infected cats, in diagnosis and treatment of cryptosporidiosis and giardiasis in cats and dogs in the United States. Clinical Sciences. 2007 Colorado State University.

Shahiduzzaman M, Daugschies A. Therapy and prevention of cryptosporidiosis in animals. Vet Parasitol. 2012;188(3-4):203–214.

Shahiduzzaman M, Dyachenko V, Keidel J, Schm äschke R, Daugschies A. Combination of cell culture and quantitative PCR (cc-qPCR) to assess disinfectants efficacy on *Cryptosporidium* oocysts under standardized conditions. Vet Parasitol. 2010;167(1):43–49.

Sharma P, Chitnis C E. Key molecular events during host cell invasion by Apicomplexan pathogens. Curr Opin Microbiol. 2013;16(4):432–437.

Sheoran A, Wiffin A, Widmer G, Singh P, Tzipori S. Infection with *Cryptosporidium hominis* provides incomplete protection of the host against *Cryptosporidium parvum*. J Infect Dis. 2012;205(6):1019–1023.

Sibley L D. Invasion strategies of intracellular parasites. Science. 2004;305(5668):248–253.

Sibley L D. How apicomplexan parasites move in and out of cells. Curr Opin Biotechnol. 2010;21(5):592–598.

Sparr C, Purkayastha N, Kolesinska B, Gengenbacher M, Amulic B, Matuschewski K et al. Improved efficacy of fosmidomycin against *Plasmodium* and *Mycobacterium* species by combination with the cell-penetrating peptide octaarginine. Antimicrob Agents Chemother. 2013;57(10):4689–4698.

Staggs S E, Keely S P, Ware M W, Schable N, See M J, Gregorio D et al. The development and implementation of a method using blue mussels (*Mytilus* spp.) as biosentinels of *Cryptosporidium* spp. and *Toxoplasma gondii* contamination in marine aquatic environments. Parasitol Res. 2015;114(12):4655–4667.

Stark D, Barratt J L N, van Hal S, Marriott D, Harkness J, Ellis J T. Clinical significance of enteric protozoa in the immunosuppressed human population. Clin Microbiol Rev. 2009;22(4):634–650.

Stinear T, Matusan A, Hines K, Sandery M. Detection of a single viable *Cryptosporidium parvum* oocyst in environmental water concentrates by reverse transcription-PCR. Appl Environ Microbiol. 1996;62(9):3385–3390.

Striepen B. Parasitic infections: time to tackle cryptosporidiosis. Nature. 2013;503(7475):189–191.

Suarez C E, Bishop R P, Alzan H F, Poole W A, Cooke B M. Advances in the application of genetic manipulation methods to apicomplexan parasites. Int J Parasitol. 2017;47(12):701–710.

Sugi T, Kato K, Kobayashi K, Watanabe S, Kurokawa H, Gong H et al. Use of the kinase inhibitor analog 1NM-PP1 reveals a role for *Toxoplasma gondii* CDPK1 in the invasion step. Eukaryot Cell. 2010;9(4):667–670.

Tetens A-K, Hanig S, Kurth M, Greif G, Entzeroth R. Transient transfection of *Cryptosporidium baileyi*. Parasitol Int. 2017;66(6):813–816.

Thompson RCA, Olson M E, Zhu G, Enomoto S, Abrahamsen M S, Hijjawi N S. *Cryptosporidium* and Cryptosporidiosis. Adv Parasitol. 2005;59:77-158.

Topouchian A, Huneau J F, Barbot L, Rome S, Gobert J G, Tom éD et al. Evidence for the absence of an intestinal adaptive mechanism to compensate for *C. parvum*-induced amino acid malabsorption in suckling rats. Parasitol Res. 2003;91(3):197–203.

Topouchian A, Kapel N, Huneau J F, Barbot L, Magne D, Tom éD et al. Impairment of amino-acid absorption in suckling rats infected with *Cryptosporidium parvum*. Parasitol Res. 2001;87(11):891–896.

Traversa D. Evidence for a new species of *Cryptosporidium* infecting tortoises: *Cryptosporidium ducismarci*. Parasit Vectors. 2010;3:p. 21.

Traversa D, Giangaspero A, Molini U, Iorio R, Paoletti B, Otranto D et al. Genotyping of *Cryptosporidium* isolates from *Chamelea gallina* clams in Italy. Appl Environ Microbiol. 2004;70(7):4367–4370.

Trotz-Williams L A, Jarvie B D, Peregrine A S, Duffield T F, Leslie K E. Efficacy of halofuginone lactate in the prevention of cryptosporidiosis in dairy calves. Vet Rec. 2011;168(19):p. 509.

Tyzzer E E. A sporozoan found in the peptic glands of the common mouse. Exp Biol Med.1907;5(1):12–13.

Tzipori S, Rand W, Griffiths J, Widmer G, Crabb J. Evaluation of an animal model system for cryptosporidiosis: therapeutic efficacy of paromomycin and hyperimmune bovine colostrum-immunoglobulin. Clin Diagn Lab Immunol. 1994;1(4):450–463.

Umemiya R, Fukuda M, Fujisaki K, Matsui T. Electron microscopic observation of the invasion process of *Cryptosporidium parvum* in severe combined immunodeficiency mice. J Parasitol. 2005;91(5):1034–1039.

Upton S J, Tilley M, Brillhart D B. Comparative development of *Cryptosporidium parvum* (Apicomplexa) in 11 continuous host cell lines. FEMS Microbiol Lett. 1994;118(3):233–236.

Vaid A, Thomas D C, Sharma P. Role of Ca^{2+}/calmodulin-PfPKB signaling pathway in erythrocyte invasion by *Plasmodium falciparum*. J Biol Chem. 2008;283(9):5589–5597.

Valigurova A, Hofmannova L, Koudela B, Vavra J. An ultrastructural comparison of the attachment sites between *Gregarina steini* and *Cryptosporidium muris*. J Eukaryot Microbiol. 2007;54(6):495–510.

Valigurova A, Jirku M, Koudela B, Gelnar M, Modry D, Slapeta J. Cryptosporidia: epicellular parasites embraced by the host cell membrane. Int J Parasitol. 2008;38(8-9):913–922.

van Zeeland Y R A, Schoemaker N J, Kik M J L, van der Giessend J W B. Upper respiratory tract infection caused by *Cryptosporidium baileyi* in three mixed-bred falcons (*Falco rusticolus* x *Falco cherrug*). Avian Dis. 2008;52(2):357–363.

Varughese E A, Bennett-Stamper C L, Wymer L J, Yadav J S. A new *in vitro* model using small intestinal epithelial cells to enhance infection of *Cryptosporidium parvum*. J Microbiol Methods. 2014;106:47–54.

Vinayak S, Pawlowic M C, Sateriale A, Brooks C F, Studstill C J, Bar-Peled Y et al. Genetic modification of the diarrhoeal pathogen *Cryptosporidium parvum*. Nature. 2015;523(7561):477–480.

Viu M, Quílez J, Sánchez-Acedo C, del Cacho E, López-Bernad F. Field trial on the therapeutic efficacy of paromomycin on natural *Cryptosporidium parvum* infections in lambs. Vet Parasitol. 2000;90(3):163–170.

Ware M W, Villegas E N. Improved *Cryptosporidium parvum* oocyst propagation using dexamethasone suppressed CF-1 mice. Vet Parasitol. 2010;168(3-4):329–331.

Watarai S, Tana, Koiwa M. Feeding activated charcoal from bark containing wood vinegar liquid (nekka-rich) is effective as treatment for cryptosporidiosis in calves. J Dairy Sci. 2008;91(4):1458–1463.

Weir S C, Pokorny N J, Carreno R A, Trevors J T, Lee H. Efficacy of common laboratory disinfectants on the infectivity of *Cryptosporidium parvum* oocysts in cell culture. Appl Environ Microbiol. 2002;68(5):2576–2579.

Wetzel D M, Schmidt J, Kuhlenschmidt M S, Dubey J P, Sibley L D. Gliding motility leads to active cellular invasion by *Cryptosporidium parvum* sporozoites. Infect Immun. 2005;73(9):5379–5387.

Widerström M, Schönning C, Lilja M, Lebbad M, Ljung T, Allestam G et al. Large outbreak of *Cryptosporidium hominis* infection transmitted through the public water supply, Sweden. Emerging Infect Dis. 2014;20(4):581–589.

Widmer G, Tzipori S, Fichtenbaum C J, Griffiths J K. Genotypic and phenotypic characterization of *Cryptosporidium parvum* isolates from people with AIDS. J Infect Dis. 1998;178(3):834–840.

Xiao L, Ryan U M, Graczyk T K, Limor J, Li L, Kombert M et al. Genetic diversity of *Cryptosporidium* spp. in captive reptiles. Appl Environ Microbiol. 2004;70(2):891–899.

Xiao L. Molecular epidemiology of cryptosporidiosis: an update. Exp Parasitol. 2010;124(1):80–89.

Xiao L, Feng Y. Zoonotic cryptosporidiosis. FEMS Immunol Med Microbiol. 2008;52(3):309–323.

Yamagishi J, Wakaguri H, Sugano S, Kawano S, Fujisaki K, Sugimoto C et al. Construction and analysis of full-length cDNA library of *Cryptosporidium parvum*. Parasitol Int. 2011;60(2):199–202.

Yang R, Elankumaran Y, Hijjawi N, Ryan U. Validation of cell-free culture using scanning electron microscopy (SEM) and gene expression studies. Exp Parasitol. 2015;153:55–62.

Yang Y, Zhou Y-B, XIAO P-L, Shi Y, Chen Y, Liang S et al. Prevalence of and risk factors associated with *Cryptosporidium* infection in an underdeveloped rural community of southwest China. Infect Dis Poverty. 2017;6(1):p. 2.

Yin J, Shen Y, Yuan Z, Lu W, Xu Y, Cao J. Prevalence of the *Cryptosporidium* pig genotype II in pigs from the Yangtze River Delta, China. PLoS One. 2011;6(6):e20738.

Youn S, Kabir M, Haque R, Petri W A. Evaluation of a screening test for detection of *Giardia* and *Cryptosporidium* parasites. J Clin Microbiol. 2009;47(2):451–452.

Yui T, Nakajima T, Yamamoto N, Kon M, Abe N, Matsubayashi M. Age-related detection and molecular characterization of *Cryptosporidium suis* and

Cryptosporidium scrofarum in pre- and post-weaned piglets and adult pigs in Japan. Parasitol Res. 2014;113(1):359–365.

Zahedi A, Paparini A, Jian F, Robertson I, Ryan U. Public health significance of zoonotic *Cryptosporidium* species in wildlife: critical insights into better drinking water management. Int J Parasitol Parasites Wildl. 2016;5(1):88–109.

Zambrano L D, Levy K, Menezes N P, Freeman M C. Human diarrhea infections associated with domestic animal husbandry: a systematic review and meta-analysis. Trans R Soc Trop Med Hyg. 2014;108(6):313–325.

Zeng B, Cai X, Zhu G. Functional characterization of a fatty acyl-CoA-binding protein (ACBP) from the apicomplexan *Cryptosporidium parvum*. Microbiology. 2006;152(Pt 8):2355–2363.

Zeng B, Zhu G. Two distinct oxysterol binding protein-related proteins in the parasitic protist *Cryptosporidium parvum* (Apicomplexa). Biochem Biophys Res Commun. 2006;346(2):591–599.

Zhang W, Yang F, Liu A, Wang R, Zhang L, Shen Y et al. Prevalence and genetic characterizations of *Cryptosporidium* spp. in pre-weaned and post-weaned piglets in Heilongjiang Province, China. PLoS One. 2013;8(7):e67564.

Zhu G. Current progress in the fatty acid metabolism in *Cryptosporidium parvum*. J Eukaryot Microbiol. 2004;51(4):381–388.

Zhu G, Li Y, Cai X, Millership J J, Marchewka M J, Keithly J S. Expression and functional characterization of a giant Type I fatty acid synthase (CpFAS1) gene from *Cryptosporidium parvum*. Mol Biochem Parasitol. 2004;134(1):127–135.

Acknowledgements

First of all, I would like to express my heartfelt thanks to my honorable supervisor, **Prof. Dr. Arwid Daugschies** for his constant scholastic guidance and advisement in setting up the theme, performing the experiments and preparing the thesis.

I would like to thank **Dr. Matthias Lendner** and **Dr. Faustin Kamena** for their professional suggestions which greatly helped me tackle technical difficulties throughout my study.

Also, I would like to express special thanks to **Sandra Gawlowska** for her experimental assistance and **Janet Reichenbach** for her help in formatting of my dissertation. Equally, thanks to all of my colleagues in the Institute of Parasitology.

I sincerely acknowledge the scholarship provided by China Scholarship Council (CSC) supported me completing my doctoral study in Germany.

At last, I want to send my special gratitude to my wife and my family who always stand by me. None of these would be accomplished without their love and belief.